WADC TECHNICAL REPORT 54-101

STUDIES OF PHASE RELATIONSHIPS AND TRANSFORMATION PROCESSES OF TITANIUM-ALLOY SYSTEMS

DONALD J. McPHERSON
WILLIAM ROSTOKER

ARMOUR RESEARCH FOUNDATION
ILLINOIS INSTITUTE OF TECHNOLOGY

OCTOBER 1954

MATERIALS LABORATORY
CONTRACT No. AF 33(038)-8708
PROJECT No. 7351
TASK No. 73510

WRIGHT AIR DEVELOPMENT CENTER
AIR RESEARCH AND DEVELOPMENT COMMAND
UNITED STATES AIR FORCE
WRIGHT-PATTERSON AIR FORCE BASE, OHIO

Carpenter Litho & Prtg. Co., Springfield, O.
300 - 2 March 1955

FOREWORD

This report was prepared by the Armour Research Foundation of the Illinois Institute of Technology under USAF Contract No. AF 33(038)-8708. The contract was initiated under Project No. 7351, Metallic Materials, Task No. 73510, Titanium Metal and Alloys, formerly RDO No. 615-11, and was administered under the direction of the Materials Laboratory, Directorate of Research, Wright Air Development Center, with Major R. J. Kotfila and Lt G. Hahn acting as project engineers.

ABSTRACT

Time-temperature-transformation charts have been determined for the following titanium-base alloys, which are of interest for high temperature application: 8% Al-6% Mo, 8% Al-4% Mo, 6% Al-6% Fe, 6% Al-6% Mn and 8% Al-4% Cr.

Alloys in the titanium-rich corner of the Ti-Mo-V system were investigated. The locus of minimum total compositions for the complete retention of beta phase on quenching was determined. Aging studies showed that none of the alloys investigated are permanently β stable. The alloys are evaluated from the standpoint of probable ability to retain ductility under elevated temperature service conditions.

Because of the promising behavior of Ti-Al-V alloys at elevated temperatures, the phase relationships in the titanium-rich corner of this system were determined. The investigation covered the space bounded by Ti-22% Al, Ti-11% V, and 600° to 1200°C. Seven isothermal sections and three selected vertical sections are presented and the phase relationships are discussed.

Phase relationships in the titanium-rich corner of the Ti-Al-Si system were studied for similar reasons. The space bounded by Ti-8% Al, Ti-2% Si and 600° to 1200°C was covered. The diagram is represented by six isothermal and four selected vertical sections.

As a prerequisite for the study of possible age hardening titanium-base systems, the solubility limits of silicon, boron, beryllium and carbon in the base compositions Ti-4% V, Ti-3% Mo and Ti-2% Cr were investigated. The carbon-containing alloys were not completed. Information on the other systems is presented in the form of nine partial vertical sections. From this information, selection of the amounts of third component additions and solution treatment temperatures for aging studies will be made.

The formation of two separate and reproducible martensites (both based on a hexagonal lattice) upon quenching binary alloys containing 7 and 9% molybdenum was discovered. No such dual martensitic phases were produced upon similar treatment of Ti-Cr and Ti-Mn alloys.

The method of integrated x-ray diffraction line intensities was proved to be unsuitable for determining the relative amounts of β and α' phases in titanium alloys.

ABSTRACT (CONT'D)

It was possible by careful techniques to follow progressively the tempering of selected needles of α' in a titanium-molybdenum binary alloy. It was demonstrated that two mechanisms exist: (1) development of a finely dispersed precipitate (inferred to be a) within the needle, and (2) development of a duplex structure possessing a midrib (β) and two side bands (α). The duplex tempered structure occurred only at 700° and 750° C, while the fine internal precipitate was observed at all temperatures employed.

PUBLICATION REVIEW

This report has been reviewed and is approved.

FOR THE COMMANDER:

M. R. WHITMORE
Technical Director
Materials Laboratory
Directorate of Research

TABLE OF CONTENTS

LIST OF TABLES

LIST OF ILLUSTRATIONS

LIST OF ILLUSTRATIONS (CONT'D)

LIST OF ILLUSTRATIONS (CONT'D)

LIST OF ILLUSTRATIONS (CONT'D)

LIST OF ILLUSTRATIONS (CONT'D)

LIST OF ILLUSTRATIONS (CONT'D)

STUDIES OF PHASE RELATIONSHIPS

AND TRANSFORMATION PROCESSES OF TITANIUM ALLOY SYSTEMS

I. INTRODUCTION

This is a summary report of the fourth year's work on Contract No. AF 33(038)-8708 covering the period January 8, 1953 to January 8, 1954. Work under this contract was confined principally to phase diagrams of titanium-base alloys during the first three years of its existence. For the year being reported the project title was "Studies of Phase Relationships and Transformation Processes of Titanium Alloy Systems." The main aim of the program was to provide fundamental studies, such as partial ternary phase diagrams, TTT charts and aging studies in support of Contract No. AF 33(038)-22806, entitled "Titanium Alloys for Elevated Temperature Application." This information is necessary to an intelligent attack on the latter contract but could not be supported directly by it without a reduction in the scope of alloy development.

This summary report is divided into self-consistent sections; purpose, procedures, results and discussions are included for each separate research topic. Authorship of the succeeding report sections is assigned to the responsible engineers in the Nonferrous Metals and Physical Metallurgy Sections of the Metals Research Department.

II. MATERIALS AND PREPARATION OF ALLOYS

Information relating to the form, source, purity and principal impurities of the various materials used in the researches reported herein are presented in Table I.

Alloys were prepared by arc melting in water cooled spun copper crucibles. Two melting procedures were used: (1) non-consumable electrode arc melting with a tungsten tipped electrode and (2) double melting, which consisted of non-consumable electrode arc melting, followed by forging of the ingot thus produced to rod and remelting this rod as a consumable electrode in a separate arc furnace. Details of these melting procedures have been described elsewhere (1,2).

The first procedure, non-consumable electrode arc melting, was used for producing ingots of 200 grams or less. The ingots were melted and remelted three or more times; the number of remelts was designed to insure homogeneity in each case. All ingots used in the work reported herein except those used in Section III were made by this procedure.

TABLE I

MATERIALS

Element	Form	Source	Purity	Impurities, %	Phase of Work* in which used
Aluminum	Granulated Shot	Aluminum Company of America	99.71	0.19 Fe, 0.09 Si, 0.01 each Cr, Cu, Mg, Mn, Zn	III, V, VI
Boron	Pellets	Cooper Metallurgical Associates	99.1	0.47 Fe, 0.38 C	VII
Beryllium	Shot	Brush Beryllium Corp.	99.0	0.89 Fe, 0.10 Si	VII
Chromium	Electrolytic Plates	Bureau of Mines	99.3	0.60 (0), 0.10 Fe, 0.02 S	III, VII, VIII
Iron	Chips	National Research Corp.	99.9+	0.013 S, 0.012 Ni, 0.011 C, 0.009 Si, 0.002 P	III
Manganese	Electrolytic Plates	Bureau of Mines	99.9+	0.018 S, 0.0035 Fe, 0.001 Cu, 0.001 Pb, 0.0005 As	III, VIII
Molybdenum	Powder	Fansteel Metallurgical Corp.	99.9+	0.045 (0), 0.02 Co + Ni, 0.015 C, 0.005 Fe	III, VIII, X
Molybdenum	Sheet	Fansteel Metallurgical Corp.			IV, VII, XI
Silicon	Powder	Electro Metallurgical Div. Union Carbon & Carbide Co.	99.8-99.9	0.03-0.08 (0), 0.02-0.04 C, 0.02-0.03 Al, 0.005-0.015 Fe, 0.005-0.010 Pb, Trace - 0.010 Ca	VI, VII

TABLE I (Continued)

Element	Form	Source	Purity	Impurities, %	Phase of Work* in which used
Tantalum	Strip	Fansteel Metallurgical Corp.	99.9	0.03 C, 0.03 Fe	IX
Titanium	Sponge "B"	DuPont de Nemours & Co.	140 BHN (160 DPH)	0.033 Fe, 0.015 N, 0.035 C, 0.018 Si	III
Titanium	Sponge "J"	Titanium Metals Corp.	140 BHN (160 DPH)	0.043 N, 0.03 Fe, 0.027 C, 0.003 Si	VIII, X
Titanium	Sponge "N"	DuPont de Nemours & Co.	124 BHN	0.068 Fe, 0.03 C, 0.018 N, <0.005 Si	VIII, IX
Titanium	Sponge "K"	Bureau of Mines	103 BHN (125 DPH)	<0.03 Fe, 0.026 C, 0.018 N, 0.005 Si	IV, V, VI, VII
Titanium	Iodide Bar	Foote Mineral Co.	98 DPH		XI
Vanadium	Chips	Electro Metallurgical Div. Union Carbon & Carbide Co.	99.7	0.11 (O), 0.09 N, 0.08 C, 0.001 H	IV, V, VII

* Numerals refer to section numbers.

III. TIME-TEMPERATURE-TRANSFORMATION STUDIES

by F. A. Crossley and W. F. Carew

A. Introduction

Time-temperature-transformation studies were made of several ternary titanium-base alloys to provide basic information needed to develop heat treatments for alloys being investigated under Contract No. AF 33(038)-22806 ("Titanium Alloys for Elevated Temperature Application"). Alloys selected were 8% Al-6% Mo, 8% Al-4% Mo, 6% Al-6% Fe, 6% Al-6% Mn, 8% Al-4% Cr. Originally, an 8% Al-6% Cr alloy was included but was later dropped as it was no longer of interest to the alloy development program.

B. Procedure

With the exception of 8% Al-4% Mo alloy, TTT curves were determined by the following procedure. Specimens were cut from forged double-melted stock. To avoid contamination, the samples were vacuum sealed in Vycor bulbs, annealed in the β phase field for 1/2 hour, then isothermally quenched into lead at temperatures ranging from 400° to 700°C. All specimens were water quenched upon removal from the lead bath. The bulbs were broken mechanically immediately upon immersion in the water.

The above procedure failed to give satisfactory results for the 8% Al-4% Mo alloy. It was especially difficult to determine completion of transformation. Consequently, a second determination was made by a method developed by Levinson (3). Briefly, this method consisted of following isothermal transformation by means of changes in electrical resistivity. Wyatt (4) found that there is considerable difference in electrical conductivity between α and β titanium. Also, there is sufficient difference between the conductivities of α' and equilibrium isothermal α that resistivity measurements can be used to follow the progress of transformation. The results of the Levinson and McPherson TTT determination on a series of titanium-manganese alloys indicated perfect correlation between resistivity measurements and microstructures of specimens heat treated at 700°C. The 700°C temperature was selected as it is one at which the transformation may easily be followed micrographically.

A single specimen was used for the time series at a given temperature in order to eliminate specimen to specimen variation as much as possible. The resistivity specimens were centerless ground to approximately 1/4 in. diameter from forged, doubled melted stock and were 2-1/2 in. in length. Prior to quenching in the lead bath, the specimens were solution treated at 1050°C in a protective atmosphere of helium. (In this procedure, specimens were not enclosed in Vycor bulbs as in the metallographic procedure described above, which was used for all alloys other than Ti-8% Al-4% Mo.) The resistivities were determined by the usual

current-potential method employing a series standard resistance. The potentials were taken at pure copper knife edges and were reproducible to approximately one part in 500. The potentials were measured at room temperature with a Leeds and Northrup Model 8657 potentiometer. Typical resistivity versus time curves are shown in Figure 1. A few specimens were taken for micrographic checks on the resistivity data. These micrographic specimens confirmed the resistivity data in every case.

C. Results and Discussion

The TTT diagrams determined are shown in Figures 2 to 5. In the determination of the diagrams represented in Figures 2 to 4, the specimens were in Vycor capsules when quenched into the lead baths. Some lag in transformation results from this practice as compared with the data obtained by quenching specimens in the conventional manner into lead baths. However, the error is not significant for our purpose.

Considering the three eutectoid type alloys, 6% Al-6% Fe, 8% Al-4% Cr and 6% Al-6% Mn, the 6% Al-6% Fe alloy is the least sluggish in rate of eutectoid decomposition and the 6% Al-6% Mn alloy is the most reluctant to decompose. The $\beta \rightarrow \alpha + \beta$ transformation, however, proceeds much more rapidly in the 6% Al-6% Mn alloy than in the 6% Al-6% Fe alloy. Eutectoid decomposition products of Ti-6% Al-6% Fe appear after approximately 2-1/2 hours at 550°C and of the Ti-8% Al-4% Cr alloy after 20 hours at 550°C. Eutectoid decomposition products of Ti-6% Al-6% Mn were not evident after 96 hours at temperatures between 400° and 800°C.

Quenching from the β field appears to give the softest condition in these alloys. Hardening is associated with the isothermal transformation, β to $\alpha + \beta$. Hardening was most pronounced in the 6% Al-6% Fe alloy. An increase of about 150 DPH took place in about 5 minutes at 500°C in this alloy. Very little additional hardening was associated with the appearance of eutectoid decomposition products in the 6% Al-6% Fe and 8% Al-4% Cr alloys. However, the hardness increase observed in Ti-6% Al-6% Mn in 24 hours (1440 minutes) at 400°C may be indicative of the beginning of eutectoid decomposition.

The TTT diagram for Ti-8% Al-4% Cr is very similar to that reported for Ti-6% Al-4% Cr by Kessler and Hansen (5). There are differences in the curve indicating approximately 95% completion of the β to $\alpha + \beta$ transformation and the temperatures at which the nose occurs in the transformation curves. However, the difference in the curve indicating approximately 95% completion is perhaps more a reflection of the experimental accuracy inherent in transformation studies of titanium-base alloys by metallographic means than a real difference. The nose of the curve indicating the beginning of the β to $\alpha + \beta$ transformation occurs at 700°C and about 0.2 minute in the Ti-6% Al-4% Cr diagram and at about 450°C and about 0.1 minute in the Ti-8% Al-4% Cr diagram. The nose of the curve showing the beginning of eutectoid decomposition occurs at about 600°C and 24 hours (1440 minutes) in the Ti-6% Al-4% Cr diagram and at about 500°C and 24 hours (1440 minutes) in the Ti-8% Al-4% Cr diagram.

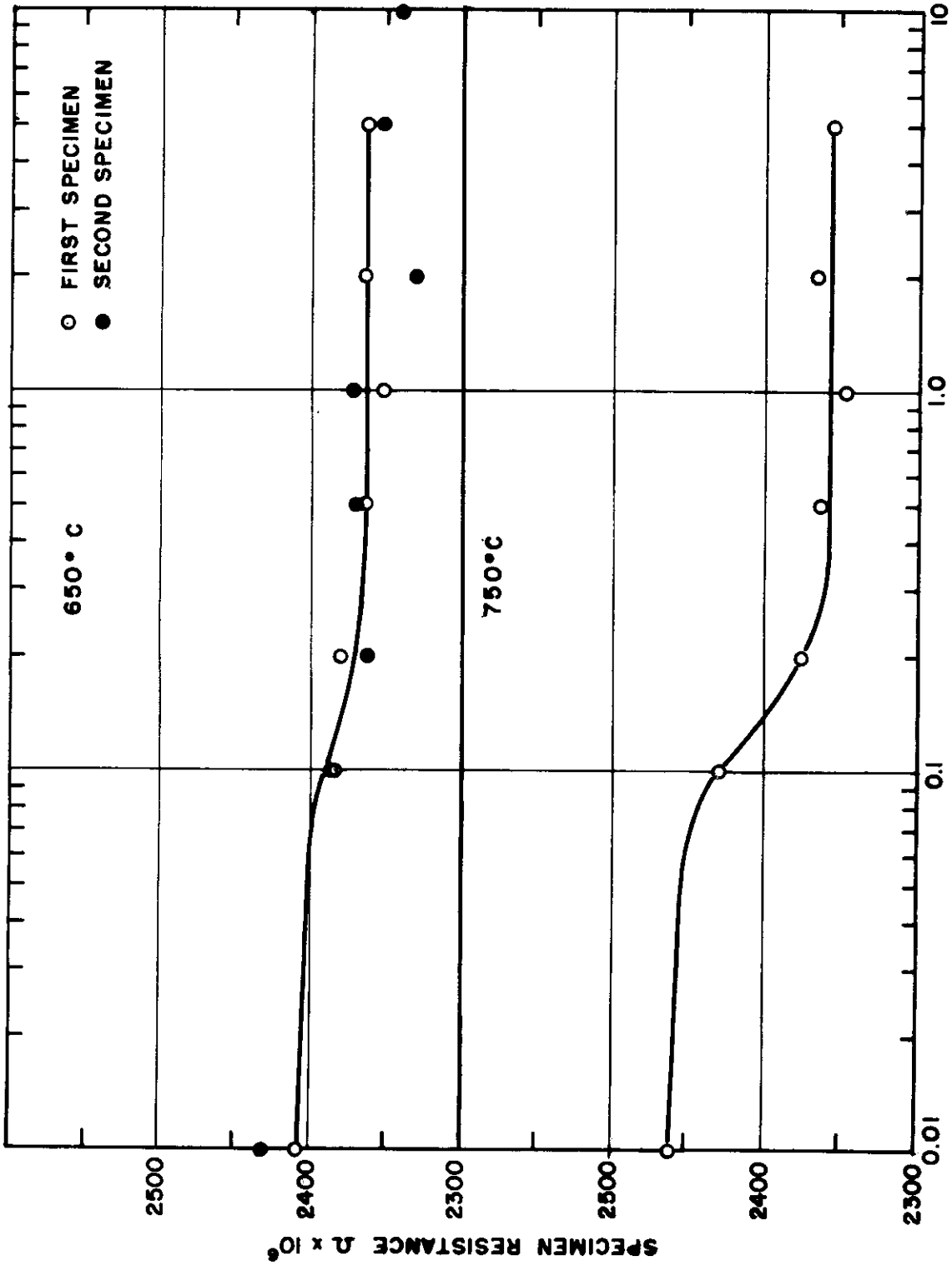

FIG. 1 - TITANIUM - 8% ALUMINUM - 4% MOLYBDENUM TRANSFORMED AT 650°C AND 750°C AFTER 20 MINUTES AT 1050°C.

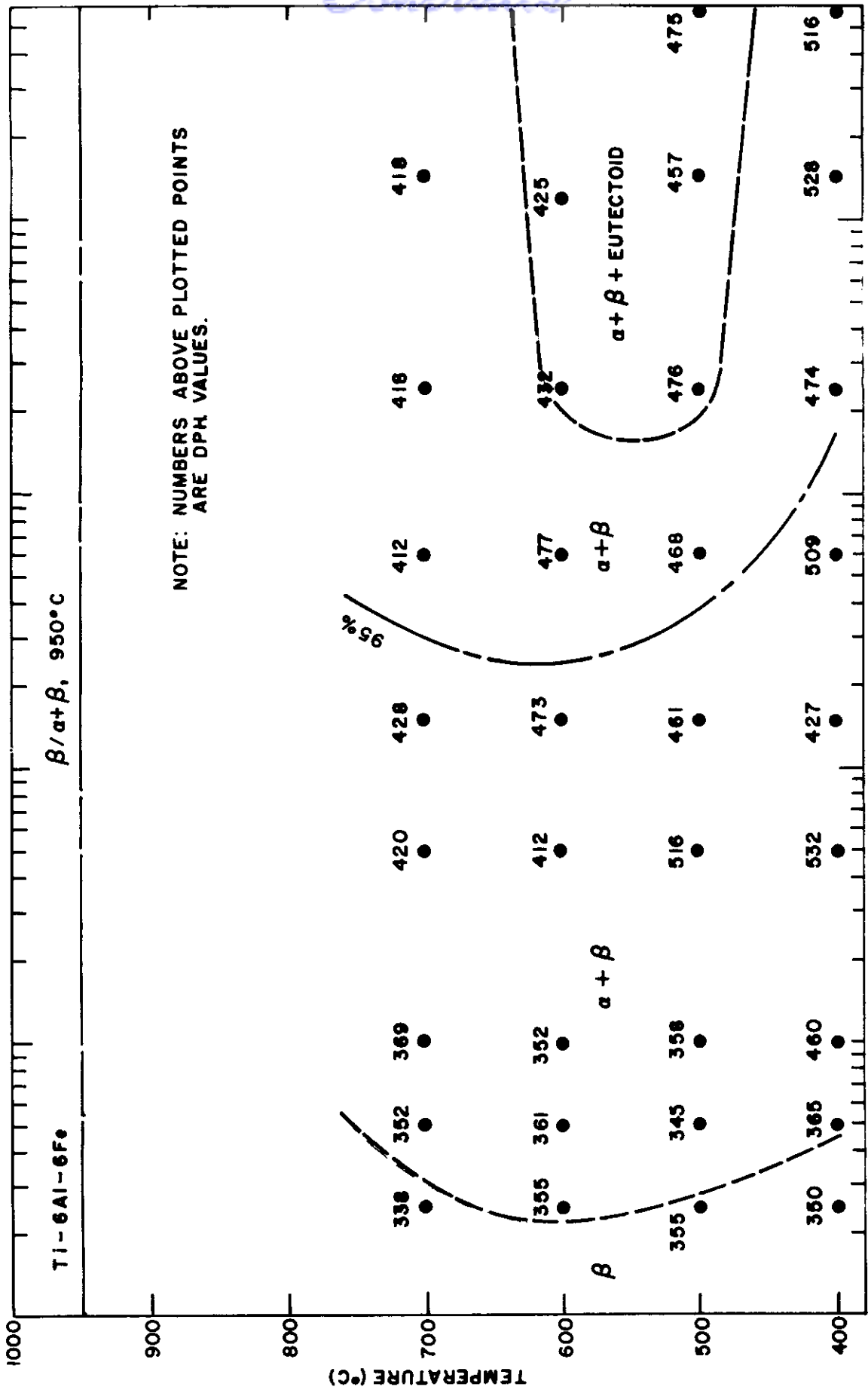

FIG. 2 – TTT CURVES FOR A TITANIUM – 6% ALUMINUM – 6% IRON ALLOY.

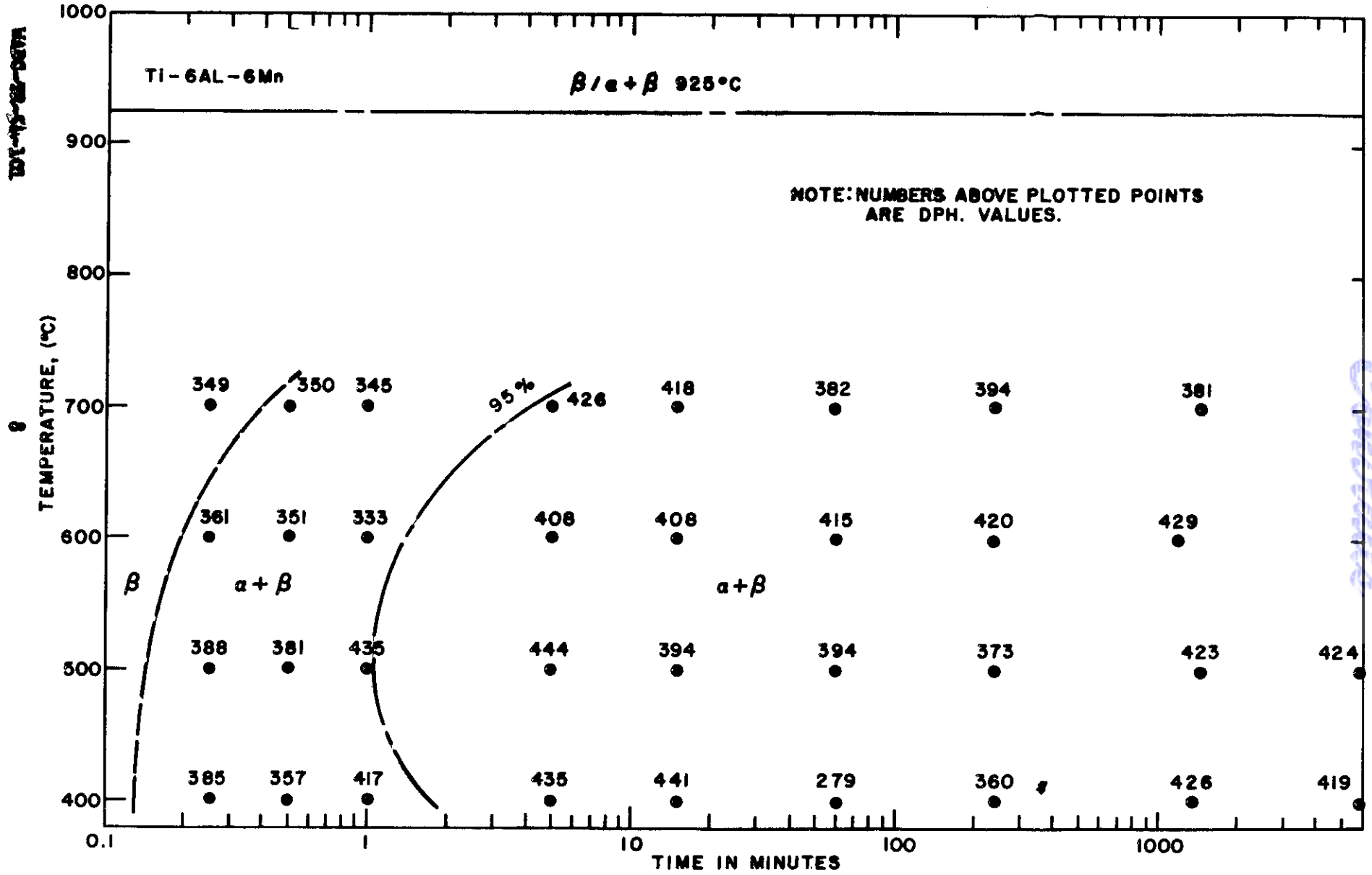

FIG. 3 — TTT CURVES FOR A TITANIUM - 6 % ALUMINUM - 6 % MANGANESE ALLOY.

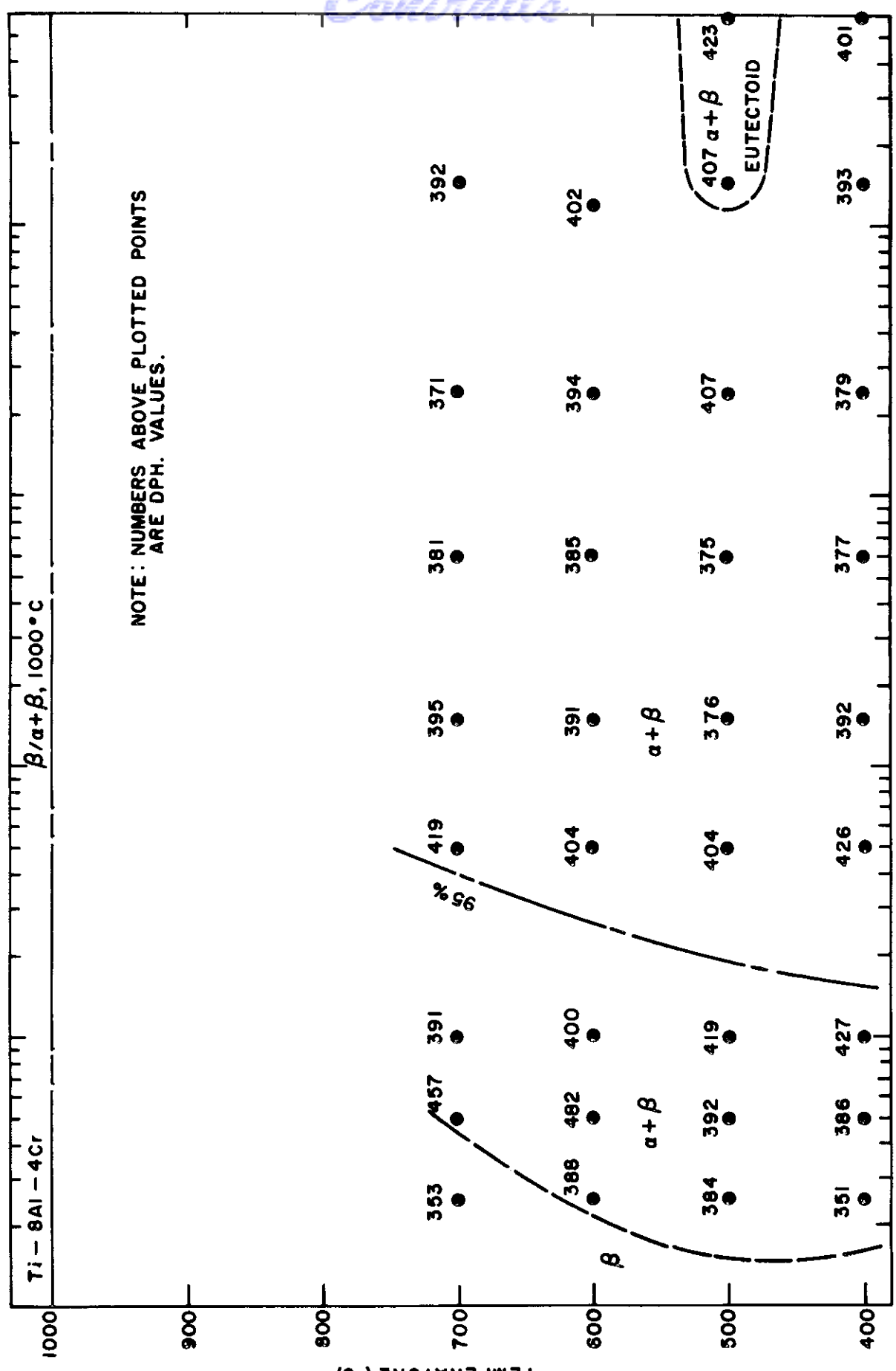

FIG. 4 – TTT CURVES FOR A TITANIUM-8% ALUMINUM-4% CHROMIUM ALLOY.

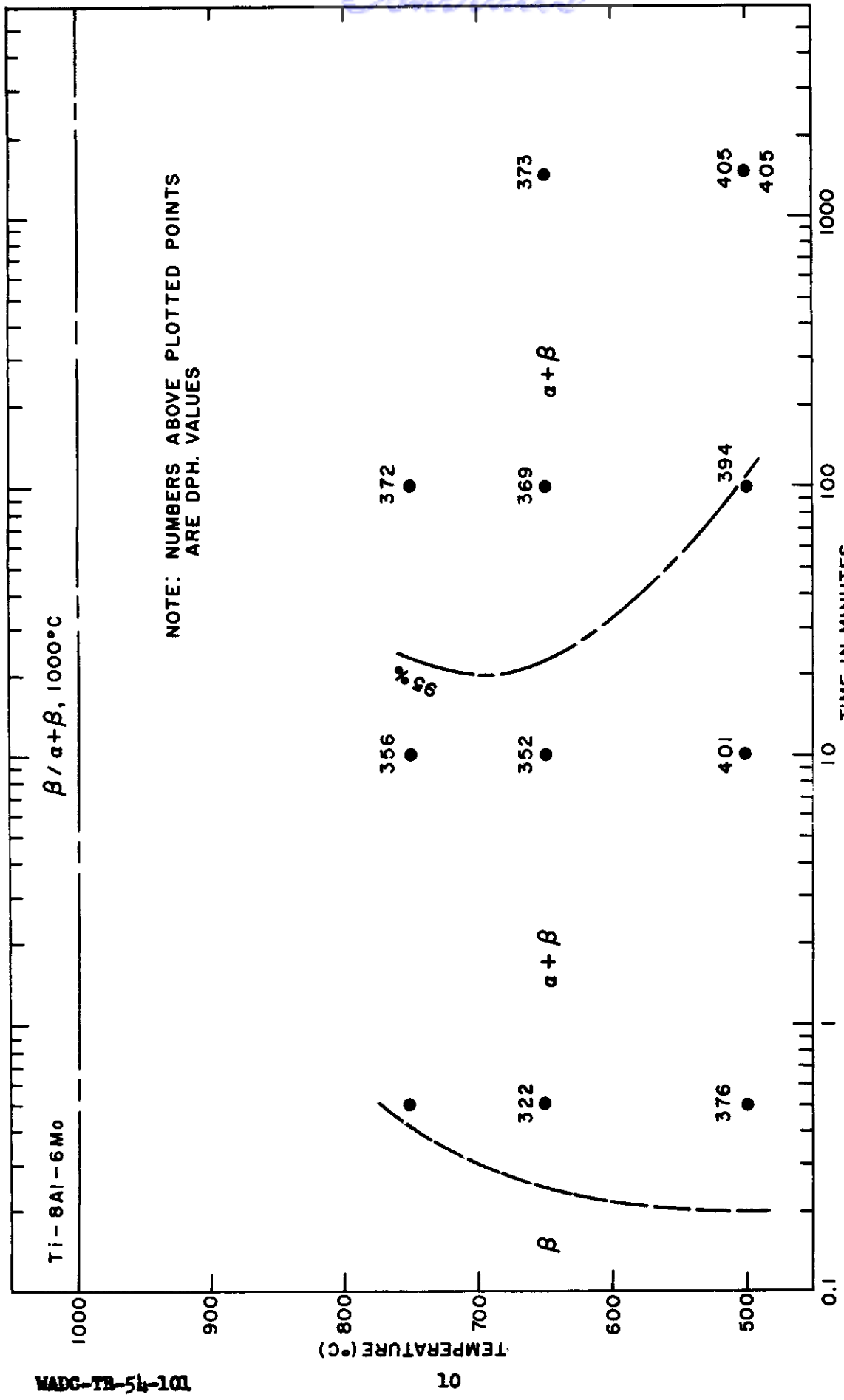

FIG. 5 - TTT CURVES FOR A TITANIUM-8% ALUMINUM-6% MOLYBDENUM ALLOY.

The TTT diagram for the 8% Al-6% Mo alloy is very similar to that for the 6% Al-6% Mo alloy reported by Kessler and Hansen (6). The slight differences in the two diagrams may be attributable to the fact that in the work referred to, the specimens were not capsulated during the isothermal quench and anneal for annealing times of 1 minute or less.

Specimens for the determination of the diagram for Ti-8% Al-6% Mo were capsulated during the isothermal quench and anneal. It is probable that the two diagrams would have even greater similarity were it not for this difference in procedure.

Figure 6 shows the TTT diagram for Ti-8% Al-4% Mo. Transformation appears to occur considerably faster in this alloy than in the others, even after allowing for the difference in quenching procedures explained above. At the nose of the curve, 550°C, transformation appears to be complete in about 0.2 minute. The difference in times for completion of transformation for the 8% Al-6% Mo and 8% Al-4% Mo (Figures 2 and 6) may be, to a certain extent, a reflection of the difficulty in determining the completion or 95% completion of transformation in titanium alloys by metallographic means.

Upon water quenching from the β field, β is completely retained in the following alloys: 6% Al-6% Fe, 6% Al-6% Mn, 6% Al-6% Mo. The alloys 8% Al-4% Cr and 8% Al-4% Mo have structures of $\alpha' + \beta$ as water quenched from the β field.

IV. THE TITANIUM-RICH CORNER OF THE Ti-Mo-V SYSTEM

by W. F. Carew and F. A. Crossley

A. Introduction and Theoretical Considerations

In March, 1953, an investigation into the titanium-rich corner of the Ti-Mo-V system was initiated to supply information towards the development of a creep-resistant, weldable alloy, with minimum alloying additions, for use in the 425°-550°C range. The primary objective was the development of a stable β alloy with somewhat less total alloying additions than is found in Ti-30% Mo. When this program was begun it was believed that the 30% Mo alloy consisted of effectively stable β; that is, no matter what heat treatment the alloy was subjected to, it would remain completely β. This statement is pertinent, since it later developed that Ti-30% Mo undergoes transformation when subjected to stress at elevated temperatures (7,8). A secondary objective was the development of a creep-resistant, weldable α-β alloy for use at lower temperatures in the 300°C range. Molybdenum was selected as the primary additive on the basis of an investigation conducted at the Armour Research Foundation, which showed Ti-30% Mo to have promising tensile strength at elevated temperatures (9). Also, aging studies (9) showed

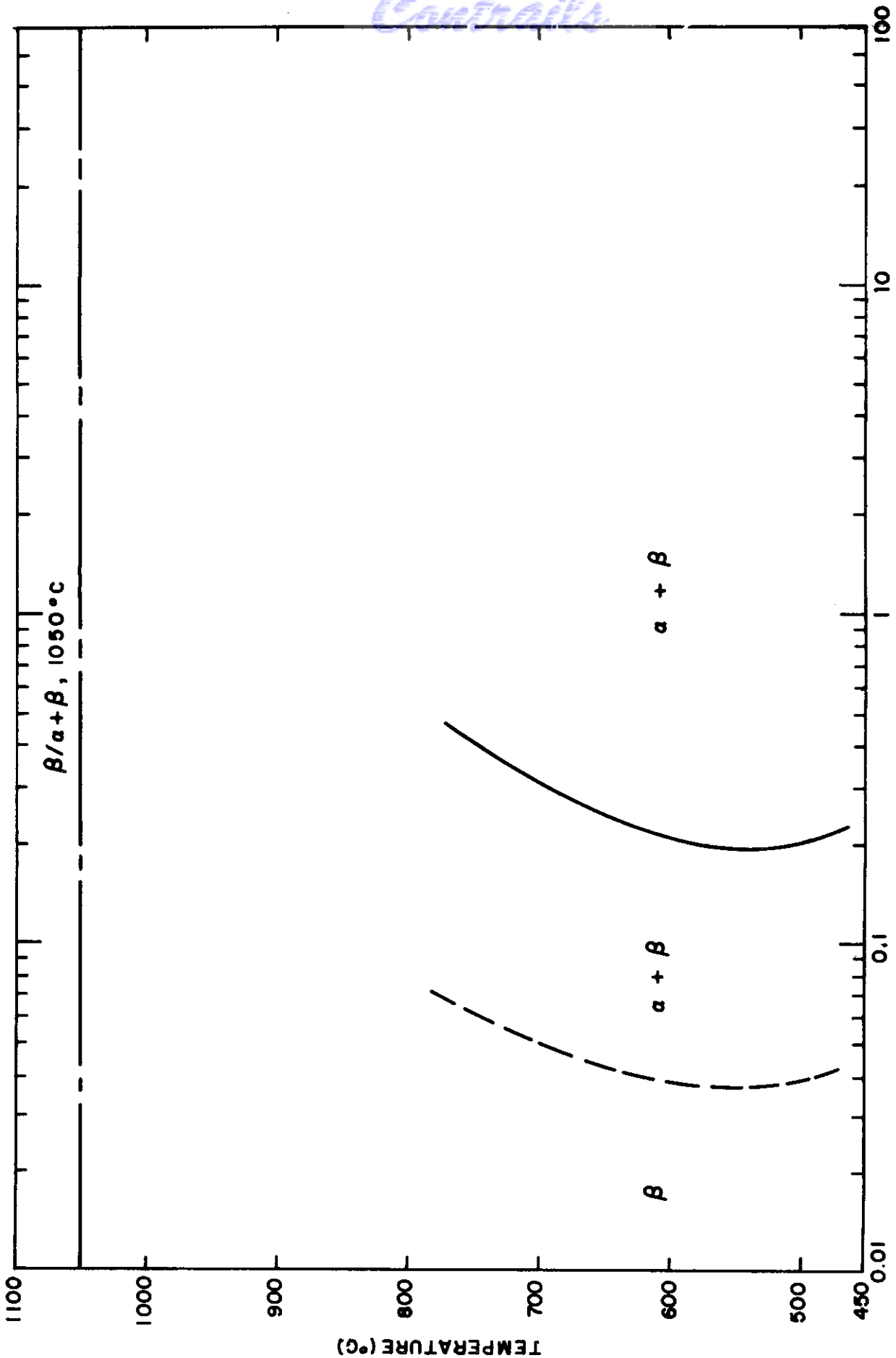

FIG. 6 - TTT CURVES FOR A TITANIUM - 8% ALUMINUM - 4% MOLYBDENUM ALLOY

that there was no apparent tendency for this alloy to transform from the β modification to the equilibrium α + β structure when held at temperatures below the β/α + β boundary for periods of 100 hours and more. Furthermore, investigations of weldability of titanium-base alloys conducted at the Foundation under a separate contract showed the β stable Ti-30% Mo alloy to be weldable (10).

It was hoped that by using two β stabilizers in combination, it would be possible to reduce the total of alloy additions needed to produce a stable β alloy. With respect to titanium there are three β stabilizing non-eutectoid forming elements besides molybdenum. They are vanadium, columbium and tantalum and their densities are 6.0, 8.57 and 16.6 g/cu cm, respectively. Tantalum and columbium are scarce materials, while vanadium is in comparatively plentiful supply. As a consequence of considering the relative densities and availability of the three elements, vanadium was selected to be the ternary addition in this investigation.

B. Procedure

In the titanium-molybdenum binary system, soft β is retained on water quenching alloys containing 11% or more of molybdenum (11); in the titanium-vanadium system, β is retained on ice brine quenching alloys of 15% or more of vanadium (12). Assuming that a straight line in the ternary system joined the retained β boundary points of the binary systems 24 ternary alloys with Mo:V ratios of 1:3, 1:1, and 3:1 were judiciously selected to delineate the compositional region where β transforms and the region where soft β is retained on quenching. The highest compositions were Ti-6% Mo-18% V, Ti-11% Mo-11% V and Ti-15.3% Mo-5.1% V for the three Mo:V ratios 1:3, 1:1 and 3:1, respectively. Several binary alloys were later added to the program to round out the picture. The highest binary compositions were 20% Mo and 30% V alloys. Investigation of the binary alloys was limited to aging studies.

High purity (103 BHN) titanium sponge was used in the preparation of the 50-gram ternary alloy buttons. The selected compositions are plotted diagrammatically in Figure 7. Molybdenum was added as 0.003 in. sheet and vanadium as particles -1/4 in. +20 mesh in size. Three samples were cut from each as-cast alloy button to study the effect of quenching rate on structure. A flat surface was ground and polished on each sample prior to solution heat treating, in order to minimize possible structural changes resulting from the heat developed in the grinding operations preparatory to metallographic examination. Parris et al. (13) have shown that age hardening can occur in some titanium-base alloys at temperatures as low as 100°C. In the Ti-Mo-V alloys, it was possible to age an unstable β structure to hard β' during the polishing operation. (β' is here defined as a structure which metallographically appears as retained β, but is abnormally hard.) The three series of ternary alloy samples were sealed in Vycor bulbs under partial pressures of argon, homogenized for 24 hours at 1100°C and quenched in the appropriate medium.

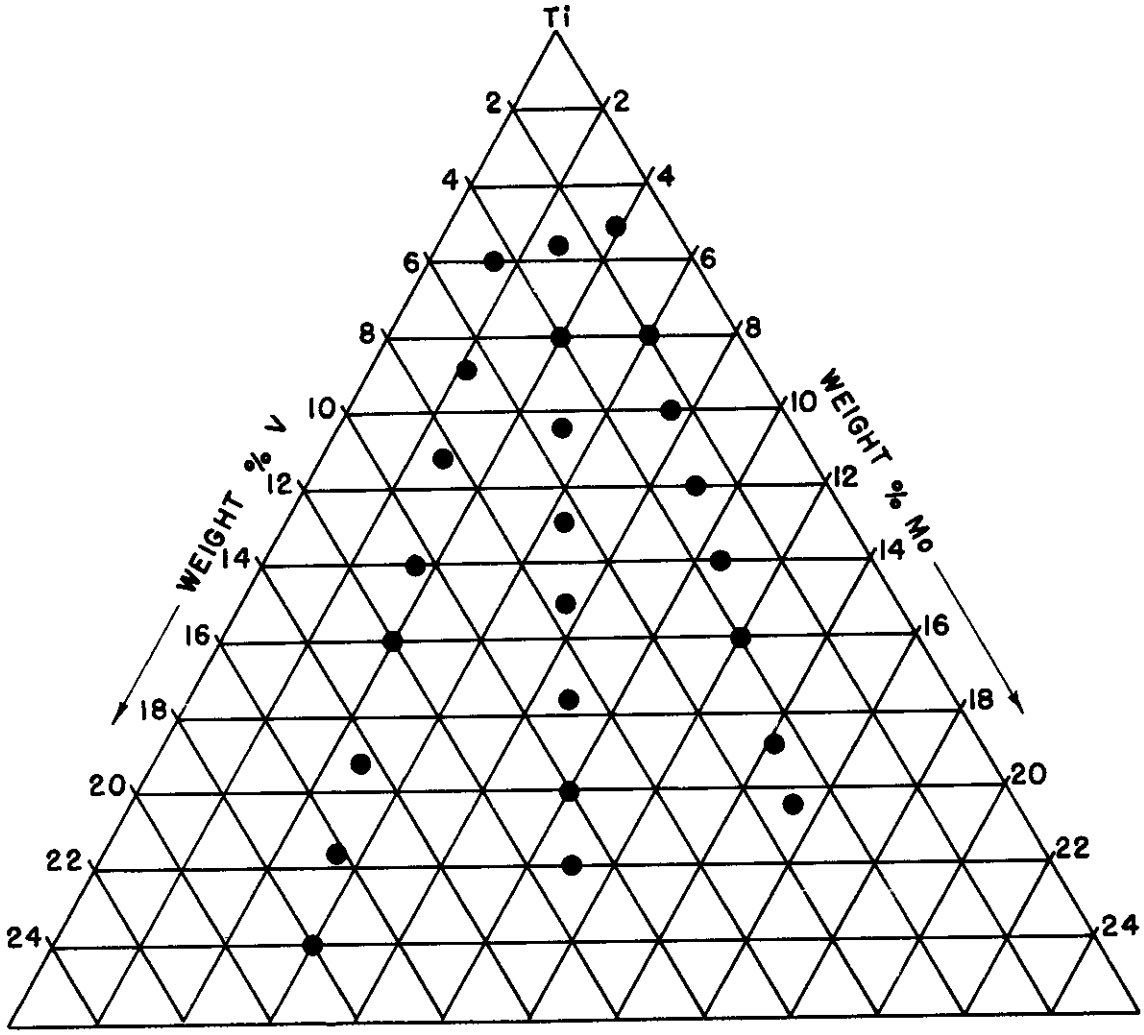

FIG. 7 — COMPOSITION OF Ti-Mo-V INGOTS PREPARED

Since temperatures in excess of 100°C are reached in mounting samples in Bakelite, a plastic which sets at room temperature was used. This was made by mechanically mixing "Epen" resin with triethylene tetramine, using a mixture of 90% by weight of resin to 10% of polymerizer. This mixture hardens in two to three hours at temperatures not exceeding 50°C.

Quenching tints were removed from the previously polished heat treated samples by a light polishing on 4/0 grinding paper to facilitate measurement of hardness indentations. Vickers diamond pyramid hardnesses were taken on all samples using a 10 kilogram load.

Aging was carried out at temperatures of 300°, 425° and 550°C for times of 1, 10, 50, 150 and 350 hours. The low composition (7% or less alloy content) alloys were aged at 300° and 425°C and the high composition (15% or more alloy content) alloys were aged at 425° and 550°C. The compositions selected for aging are shown in Table IV. Aging samples consisted of 1/4 in. thick discs cut from 3/8 in. diameter forged stock. The samples were air cooled after 24 hours at 1100°C in Vycor bulbs preparatory to aging. Air cooling was selected to precede the aging heat treatments as this cooling rate would be expected to give the most severe test of the stability of the β phase.

To conserve time and furnace space, the 120 ternary alloy samples were divided and 60 samples were sealed in each of two Vycor bulbs. These were solution annealed and air cooled in the bulbs. Subsequently, Vickers hardnesses were determined (See Table II) which showed that these samples were harder than the original air cooled samples (used for metallographic examination) by as much as 246 Vickers numbers. This increase was apparently due in part to the larger sample size coupled with the slower cooling rate resulting from having 60 samples in close contact within a sealed container. This slower rate appeared to extend the region of β' formation over the entire field of investigation. This result indicated that there was little hope of obtaining a stable β alloy among the compositions under investigation. However, it was decided to continue with the aging studies.

The ternary alloy samples were re-solution annealed, together with the molybdenum and vanadium binary alloys, to obtain a condition more consistent with the original air cooled samples. This time, only 10 samples were sealed in a Vycor bulb. Hardness values obtained after the solution treatment (presented in Table II) indicated that the ternary alloys more closely approached the hardnesses of the original specimens. The difference in sample size was probably the principal cause for the discrepancies which still remained.

The aging process was followed by hardness measurements and metallographic examination.

TABLE II

HARDNESS OF AIR COOLED Ti-Mo-V SAMPLES*

Alloy		Diamond Pyramid Hardness (10 Kg. Load)		
% Mo	% V	Original Metallographic Samples	60 Samples Per Bulb	10 Samples Per Bulb
5.0				306
15.0				337
17.5				324
20.0				339
	7.0			294
	20.0			351
	25.0			289
	30.0			269
1.5	4.5	286	391	282
4.8	14.5	272	476	319
5.4	16.2	264	427	296
6.0	18.0	236	391	277
2.8	2.8	284	440	320
8.8	8.8	268	473	326
10.0	10.0	273	436	298
11.0	11.0	254	404	282
3.9	1.3	279	457	322
12.0	4.0	300	546	363
14.1	4.7	272	441	319
15.3	5.1	258	443	314

* Solution annealed: 1100°C - 24 hours - air cool.

C. Results and Discussion

Hardness data for the water and oil quenched and air cooled specimens are given in Table III and are plotted in Figures 8 to 10. The hardnesses of the water and oil quenched specimens fell in the range from 218 to 296 DPH whereas a number of the air cooled samples exhibited high hardnesses with major peaks occurring in the plot of hardness versus alloy content between 10 and 13% total alloying addition. The hardness level of each peak was raised and moved to lower total alloy content as the Mo:V ratio increased.

Following the hardness measurements, the samples were examined metallographically to pinpoint the regions where β transforms and where β is retained. Metallographic examination revealed a peculiar microconstituent in the ternary alloys of sufficient alloy content for completely retained β to be expected. The microconstituent is shown in Figure 11. Because no such structures had been reported in the phase diagram work on these systems, it was initially thought that the platelike particles were the result of impurities present in the materials used, perhaps being a hydride phase. Attempts at identification by x-ray methods were unsuccessful, primarily because of the small amounts present. Finally it was concluded that this microconstituent is most probably α for the following reasons:

(1) It was noted that the phase was more abundant in the slower cooled samples, indicating that it did come out on cooling from 1100°C. However, a severe water quench could not suppress its formation completely.

(2) An investigation conducted at the Armour Research Foundation on the structural changes of titanium-base alloys with heat treatment (14) showed very similar microstructures in an 11% Cr alloy quenched isothermally from 1000° to 800°C, held 15 and 30 minutes and water quenched to room temperature (see Figure 12). This specimen showed an α precipitate very similar in appearance to the precipitate present in the Ti-Mo-V alloys. The specimen held for 30 minutes at 800°C showed more of the second phase than the specimen held for 15 minutes indicating that the amount of the second phase increased with time. In this 11% Cr alloy this phase was identified as α.

(3) DeLazaro and Rostoker (15) have shown that oxygen additions to Ti-11% Mo shift the TTT curves for the alloy to shorter times and that at an oxygen content of 0.35%, transformation begins so rapidly that it cannot be suppressed by water quenching. An interesting characteristic of transformation in this alloy is that the initial transformation products delineate grain and subgrain boundaries of the prior β phases and further transformation is comparatively sluggish. However, in an iodide titanium-base Ti-11% Mo containing less than 0.02% oxygen, transformation was readily suppressed by quenching.

TABLE III

AS-QUENCHED HARDNESS OF Ti-Mo-V ALLOYS

Alloy		Diamond Pyramid Hardness (10 Kg. Load)		
% Mo	% V	Water Quench	Oil Quench	Air Cool
1.5	4.5	253	262	286
2.2	6.6	233	227	333
2.8	8.4	225	296	421
3.5	10.5	286	281	425
4.0	12.0	277	254	379
4.8	14.5	223	220	272
5.4	16.2	270	259	264
6.0	18.0	255	235	236
2.8	2.8	250	266	284
4.0	4.0	233	236	321
5.2	5.2	229	274	455
6.5	6.5	261	270	449
7.5	7.5	255	246	360
8.8	8.8	230	232	268
10.0	10.0	257	274	273
11.0	11.0	264	260	254
3.9	1.3	268	252	279
6.0	2.0	227	251	351
7.5	2.5	238	230	561
9.0	3.0	265	260	390
10.5	3.5	247	235	370
12.0	4.0	218	225	300
14.1	4.7	282	280	272
15.3	5.1	268	262	258

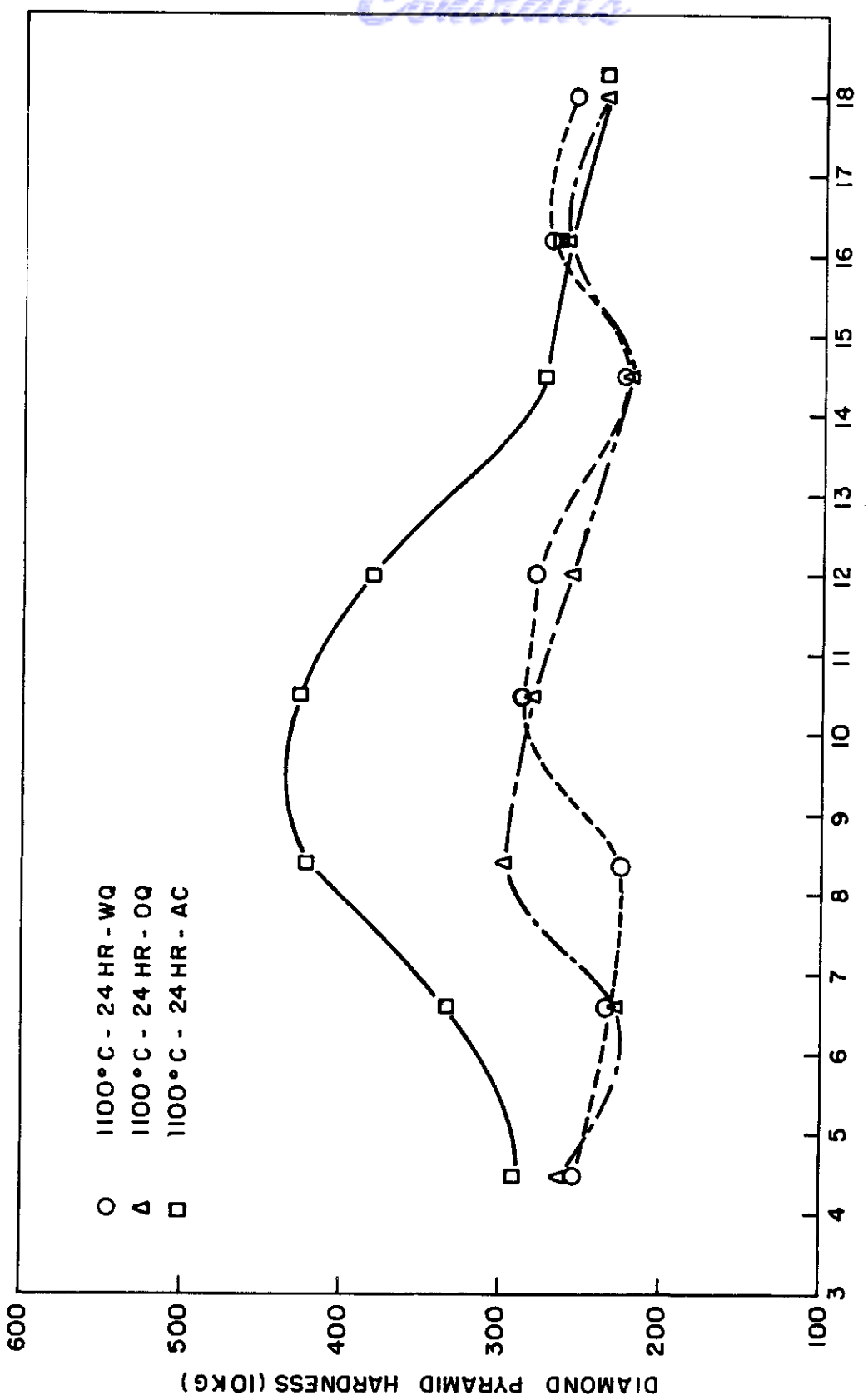

FIG. 8 - AS QUENCHED HARDNESS OF Ti - Mo - V ALLOYS WITH A Mo TO V RATIO OF 1:3

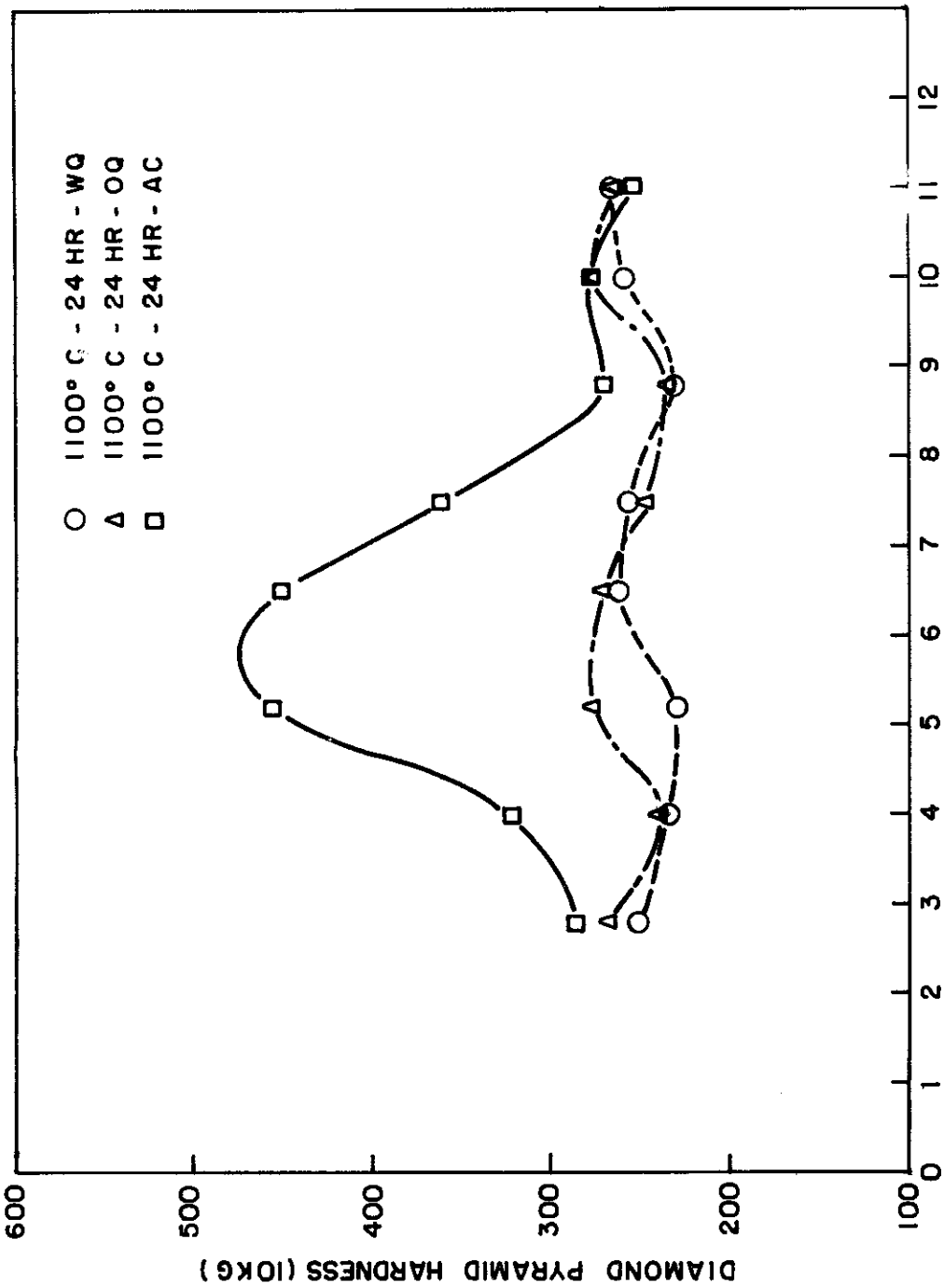

FIG. 9 - AS QUENCHED HARDNESS OF Ti-Mo-V ALLOYS WITH A Mo TO V RATIO OF 1:1

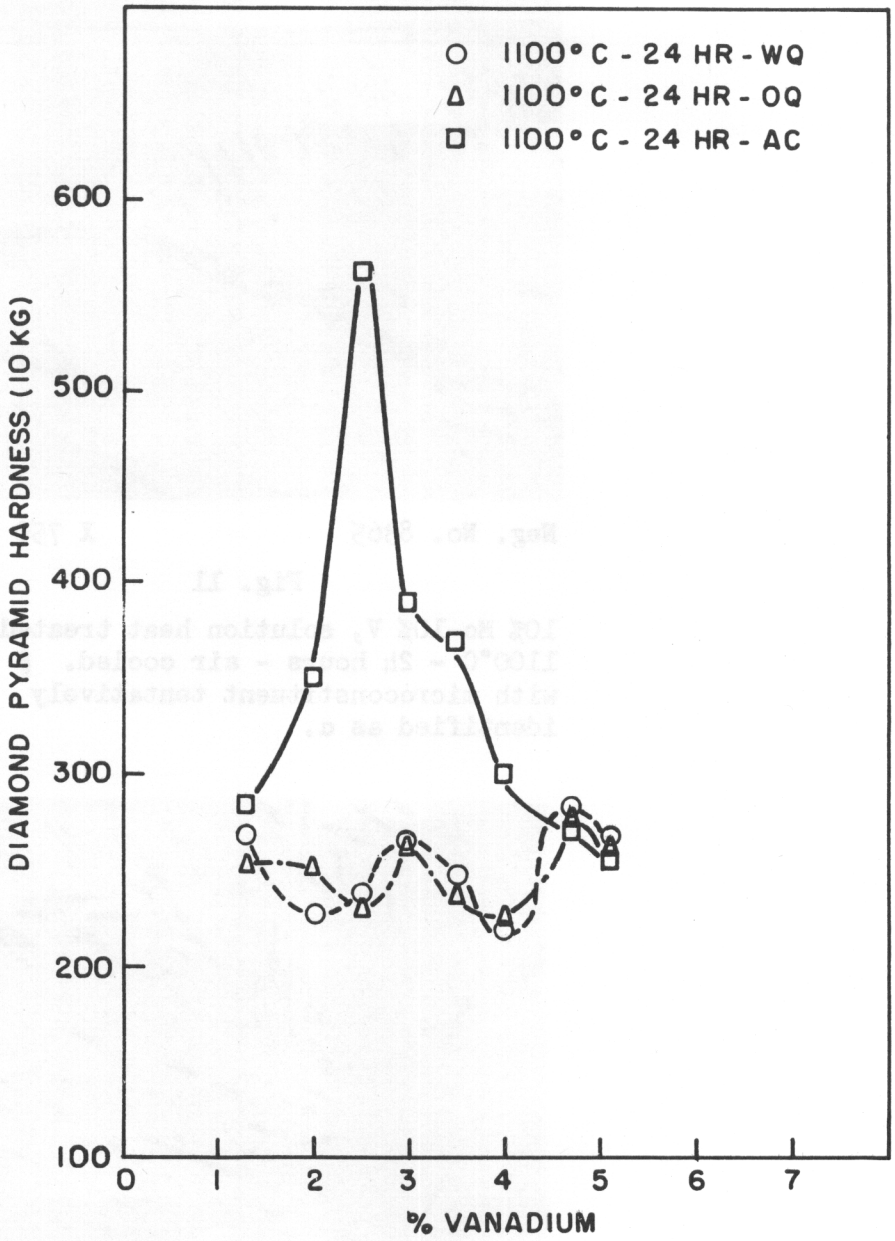

FIG.10 - AS QUENCHED HARDNESS OF Ti - Mo - V ALLOYS WITH A Mo TO V RATIO OF 3:1

Neg. No. 8365 X 750

Fig. 11

10% Mo-10% V, solution heat treated 1100°C - 24 hours - air cooled. β with microconstituent tentatively identified as α.

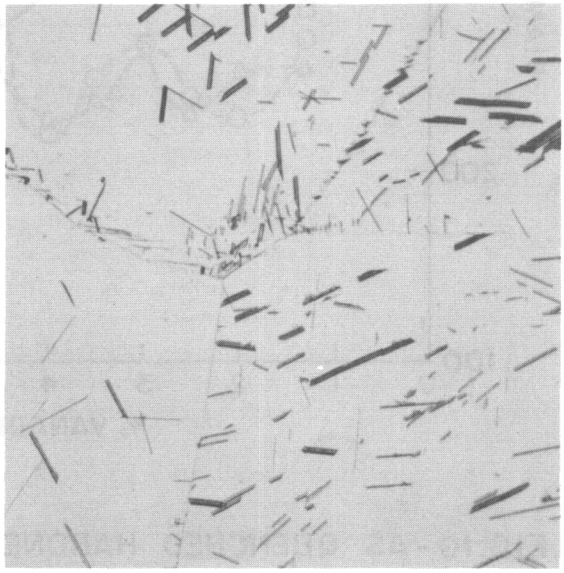

Neg. No. 6914 X 250

Fig. 12

11% Cr, isothermal quench from 1000° to 800°C for 30 minutes - water quenched. β with α precipitate.

Etchant: 60 cc glycerine, 20 cc HNO_3, 20 cc HF.

(4) In the aging work discussed below it was found that the microconstituents under discussion nucleated α and that transformation of β to α occurred last in the regions immediately adjacent to these microconstituents. This is consistent with a hypothesis that this phase which comes out on quenching is α since regions in the immediate vicinity of such α plates would be richer in alloy content than original β matrix and consequently would be more sluggish in transforming.

Although sponge of 103 BHN quality was used in this investigation, it is obviously not as pure as iodide titanium. Apparently, in the high composition sponge base Ti-Mo-V alloys, the presence of oxygen causes α to precipitate on cooling through the high temperature part of the α + β region.

The structures obtained on quenching, together with the hardnesses associated with them, are given in Figures 13 to 15. The structures developed by water quenching are given in Figure 13; the banded zone indicates the transition from transformed β to retained β plus a small amount of α. As anticipated, this band joins the transition points of the binary systems, i.e., approximately 11% molybdenum and 15% vanadium. Although oil quenching represents a slower quenching rate than water quenching, the transition zone is the same for both quenching rates as shown by Figures 13 and 14. However, air cooling from the β field shifts the transition to lower alloy content as shown in Figure 15 so that a straight line in the ternary system now joins the binary points corresponding to approximately 9% molybdenum and 11% vanadium. DeLazaro, et al. (16) found that a 9% Mo alloy, when quenched from 1000° to 700°C and held for two seconds prior to water quenching to room temperature, showed a retained β structure, while water quenching directly from 1000°C to room temperature gave a transformed β structure. In the Ti-Mo-V ternary system a similar stabilization apparently was caused by the relatively show cooling through the high temperature range of the α + β field. Generally one expects, with decreasing cooling rate, to go to higher alloy contents in order to completely retain the β phase.

As shown in the plots of hardness versus total alloy content (Figures 8 to 10) and the ternary plot (Figure 15), a number of air cooled samples immediately beyond the transition zone in the retained β region exhibited abnormally high hardnesses, which presumably identify them as β' structures.

Aging studies were used to check the stability of the promising alloys. The alloys containing the β' structure (see Figure 15) upon air cooling were not included in the aging work because brittleness is associated with this structure. As reported above under "Procedure," air cooling from the β state was selected as the initial condition for the aging experiments since this cooling rate was expected to give the most severe test of the stability of the β phase.

The aging hardness data appear in Table IV together with the observed microstructures. Plots of hardness versus aging time are presented in Figures 16 through 20.

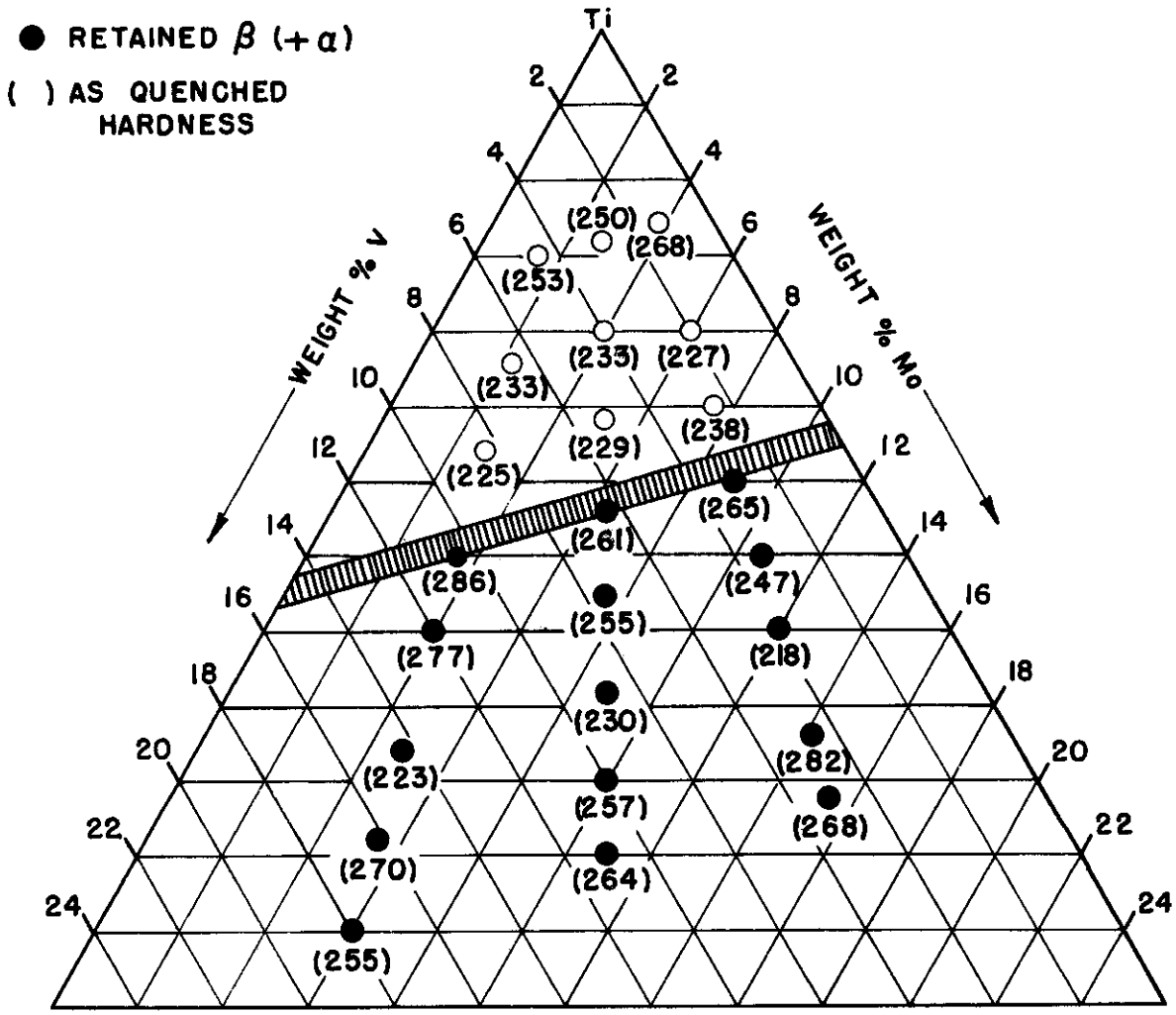

FIG. 13 - STRUCTURES AND CORRESPONDING HARDNESSES OF WATER QUENCHED Ti - Mo - V SAMPLES

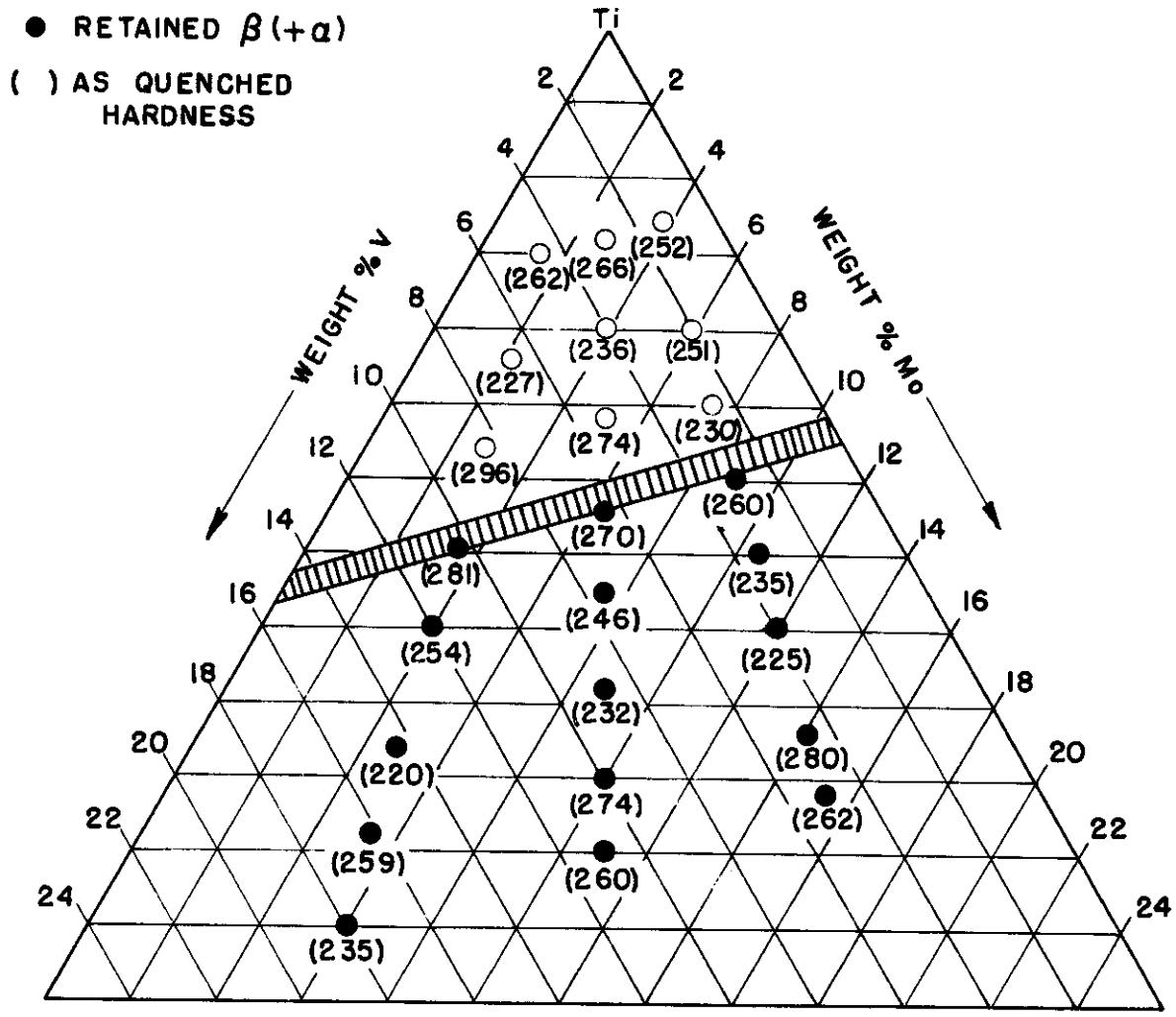

FIG. 14 – STRUCTURES AND CORRESPONDING HARDNESSES OF OIL QUENCHED Ti – Mo – V SAMPLES

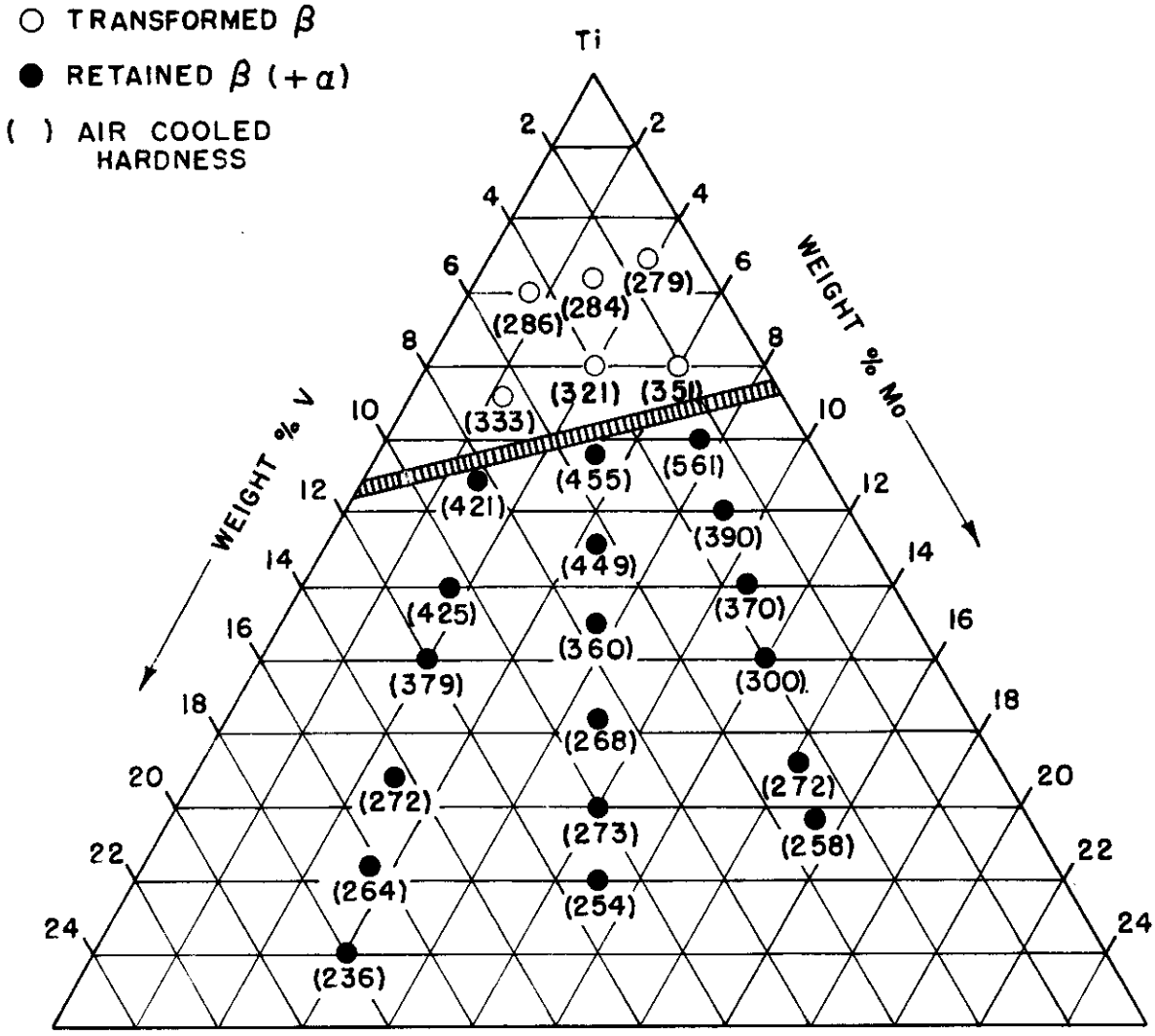

FIG. 15 – STRUCTURES AND CORRESPONDING HARDNESSES OF AIR COOLED Ti–Mo–V SAMPLES

TABLE IV

HARDNESS DATA FROM AGING STUDIES

Alloy		Aging Temp.	VHN (10 Kg. Load) and Related Structures					
% Mo	% V	°C	0 Hr.	1 Hr.	10 Hrs.	50 Hrs.	150 Hrs.	350 Hrs.
5.0		300	306 - (α-β)	314 - (α-β)	296 - (α-β)	311 - (α-β)	306 - (α-β)	351 - (α-β)
		425	306 - (α-β)	304 - (α-β)	306 - (α-β)	320 - (α-β)	288 - (α-β)	285 - (α-β)
15.0		425	337 - (β)	486 - (α-β)	483 - (α-β)	519 - (α-β)	515 - (α-β)	499 - (α-β)
		550	337 - (β)	374 - (α-β)	384 - (α-β)	389 - (α-β)	362 - (α-β)	339 - (α-β)
17.5		425	324 - (β)	400 - (α-β)	443 - (α-β)	433 - (α-β)	510 - (α-β)	508 - (α-β)
		550	324 - (β)	384 - (α-β)	410 - (α-β)	380 - (α-β)	377 - (α-β)	362 - (α-β)
20.0		425	339 - (β)	330 - (α-β)	350 - (α-β)	388 - (α-β)	382 - (α-β)	350 - (α-β)
		550	339 - (β)	366 - (α-β)	394 - (α-β)	373 - (α-β)	373 - (α-β)	361 - (α-β)
	7.0	300	294 - (α-β)	307 - (α-β)	305 - (α-β)	332 - (α-β)	328 - (α-β)	347 - (α-β)
		425	294 - (α-β)	279 - (α-β)	279 - (α-β)	300 - (α-β)	272 - (α-β)	284 - (α-β)
	20.0	425	351 - (β)	457 - (α-β)	452 - (α-β)	399 - (α-β)	431 - (α-β)	412 - (α-β)
		550	351 - (β)	319 - (α-β)	302 - (α-β)	315 - (α-β)	332 - (α-β)	300 - (α-β)
	25.0	425	289 - (β)	464 - (α-β)	335 - (α-β)	385 - (α-β)	400 - (α-β)	395 - (α-β)
		550	289 - (β)	287 - (α-β)	270 - (α-β)	283 - (α-β)	287 - (α-β)	255 - (α-β)
	30.0	425	269 - (β)	276 - (α-β)	256 - (α-β)	296 - (α-β)	322 - (α-β)	357 - (α-β)
		550	269 - (β)	268 - (α-β)	253 - (α-β)	249 - (α-β)	245 - (α-β)	238 - (α-β)
1.5	4.5	300	282 - (α-β)	303 - (α-β)	291 - (α-β)	306 - (α-β)	304 - (α-β)	326 - (α-β)
		425	282 - (α-β)	290 - (α-β)	279 - (α-β)	297 - (α-β)	278 - (α-β)	277 - (α-β)

TABLE IV (Continued)

Alloy		Aging Temp.	VHN (10 Kg. Load) and Related Structures					
% Mo	% V	°C	0 Hr.	1 Hr.	10 Hrs.	50 Hrs.	150 Hrs.	350 Hrs.
4.8	14.5	425	319 - (β)	463 - (α-β)	479 - (α-β)	472 - (α-β)	396 - (α-β)	386 - (α-β)
		550	319 - (β)	307 - (α-β)	275 - (α-β)	288 - (α-β)	287 - (α-β)	271 - (α-β)
5.4	16.2	425	296 - (β)	351 - (α-β)	312 - (α-β)	439 - (α-β)	415 - (α-β)	412 - (α-β)
		550	296 - (β)	295 - (α-β)	299 - (α-β)	295 - (α-β)	295 - (α-β)	278 - (α-β)
6.0	18.0	425	277 - (β)	281 - (α-β)	277 - (α-β)	352 - (α-β)	380 - (α-β)	381 - (α-β)
		550	277 - (β)	273 - (α-β)	258 - (α-β)	280 - (α-β)	279 - (α-β)	279 - (α-β)
2.8	2.8	300	320 - (α-β)	325 - (α-β)	293 - (α-β)	346 - (α-β)	331 - (α-β)	340 - (α-β)
		425	320 - (α-β)	289 - (α-β)	324 - (α-β)	299 - (α-β)	297 - (α-β)	299 - (α-β)
8.8	8.8	425	326 - (β)	486 - (α-β)	491 - (α-β)	499 - (α-β)	481 - (α-β)	432 - (α-β)
		550	326 - (β)	328 - (α-β)	311 - (α-β)	319 - (α-β)	321 - (α-β)	
10.0	10.0	425	298 - (β)	470 - (α-β)	362 - (α-β)	470 - (α-β)	441 - (α-β)	408 - (α-β)
		550	298 - (β)	313 - (α-β)	311 - (α-β)	312 - (α-β)	315 - (α-β)	301 - (α-β)
11.0	11.0	425	282 - (β)	284 - (α-β)	297 - (α-β)	441 - (α-β)	386 - (α-β)	397 - (α-β)
		550	282 - (β)	288 - (α-β)	290 - (α-β)	300 - (α-β)	284 - (α-β)	298 - (α-β)
3.9	1.3	300	322 - (α-β)	317 - (α-β)	305 - (α-β)	342 - (α-β)	328 - (α-β)	392 - (α-β)
		425	322 - (α-β)	314 - (α-β)	326 - (α-β)	333 - (α-β)	310 - (α-β)	316 - (α-β)
12.0	4.0	425	363 - (β)	493 - (α-β)	467 - (α-β)	506 - (α-β)	521 - (α-β)	488 - (α-β)
		550	363 - (β)	356 - (α-β)	358 - (α-β)	364 - (α-β)	343 - (α-β)	342 - (α-β)
14.1	4.7	425	319 - (β)	480 - (α-β)	458 - (α-β)	489 - (α-β)	494 - (α-β)	462 - (α-β)
		550	319 - (β)	330 - (α-β)	370 - (α-β)	351 - (α-β)	356 - (α-β)	328 - (α-β)
15.3	5.1	425	314 - (β)	381 - (α-β)	448 - (α-β)	394 - (α-β)	422 - (α-β)	442 - (α-β)
		550	314 - (β)	321 - (α-β)	316 - (α-β)	355 - (α-β)	326 - (α-β)	354 - (α-β)

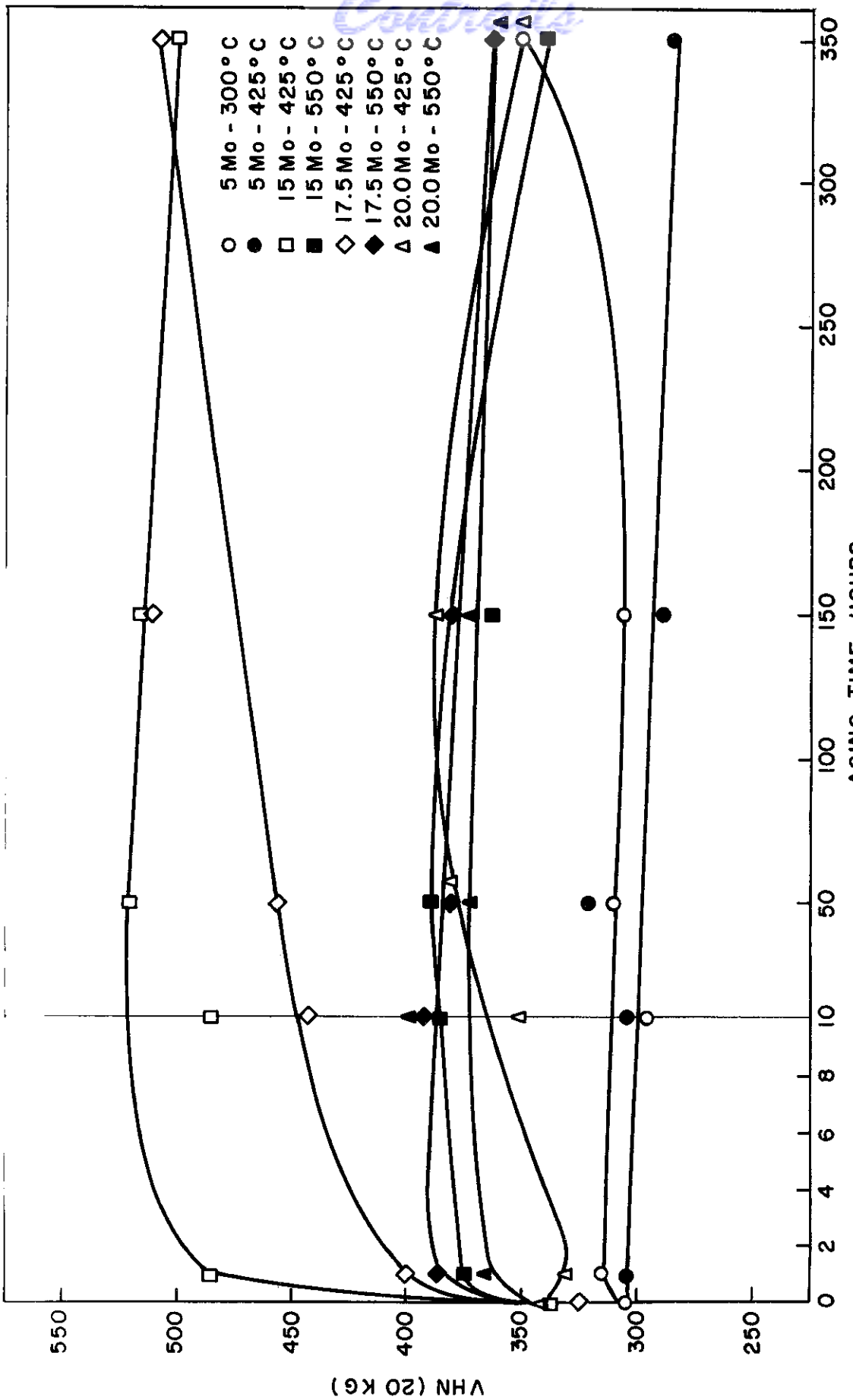

FIG. 16 - HARDNESS VS. AGING TIME AT TEMPERATURES OF 300°, 425°, AND 550°C FOR Ti-Mo BINARY ALLOYS.

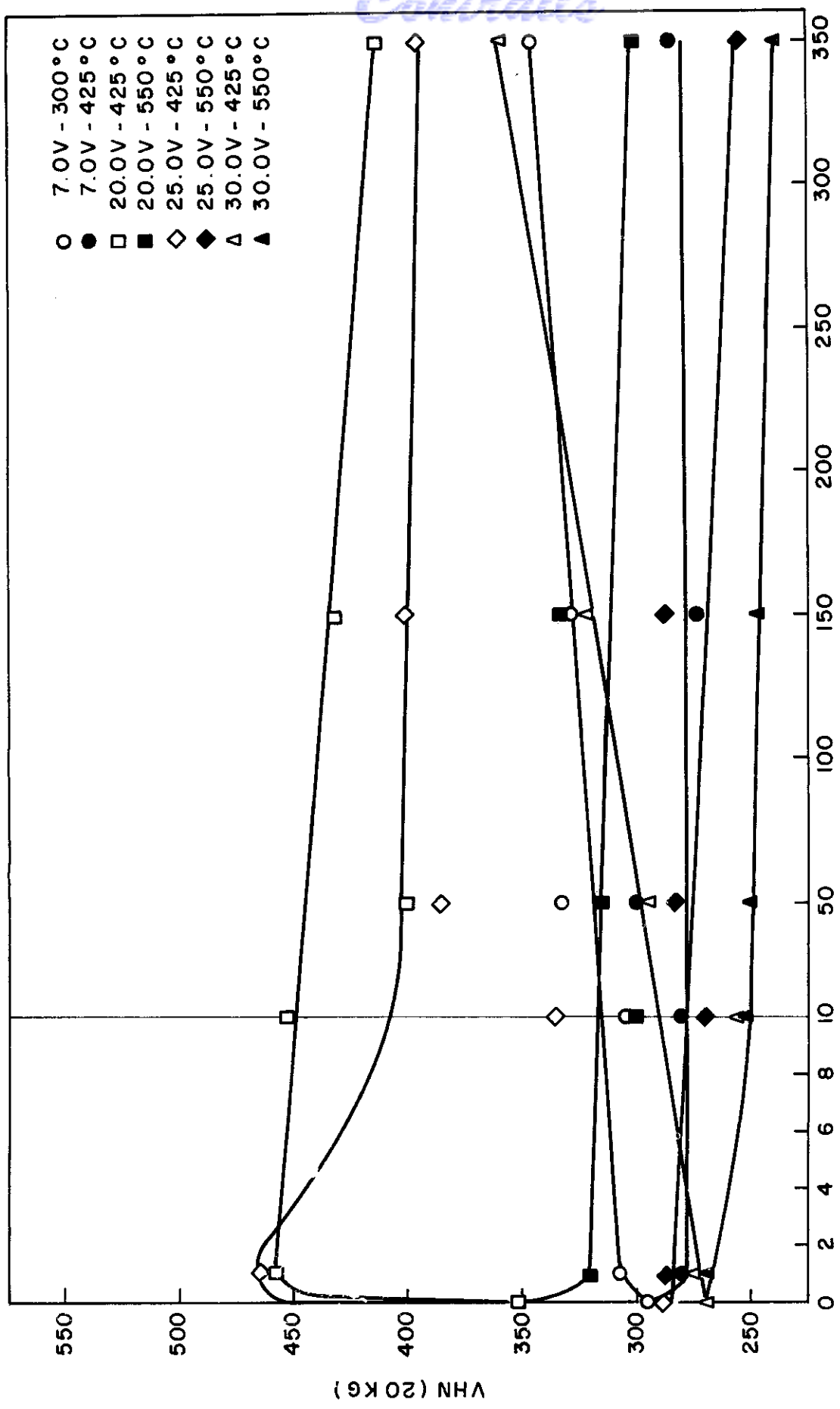

FIG. 17-HARDNESS VS. AGING TIME AT TEMPERATURES OF 300°, 425°, AND 550°C FOR Ti-V BINARY ALLOYS.

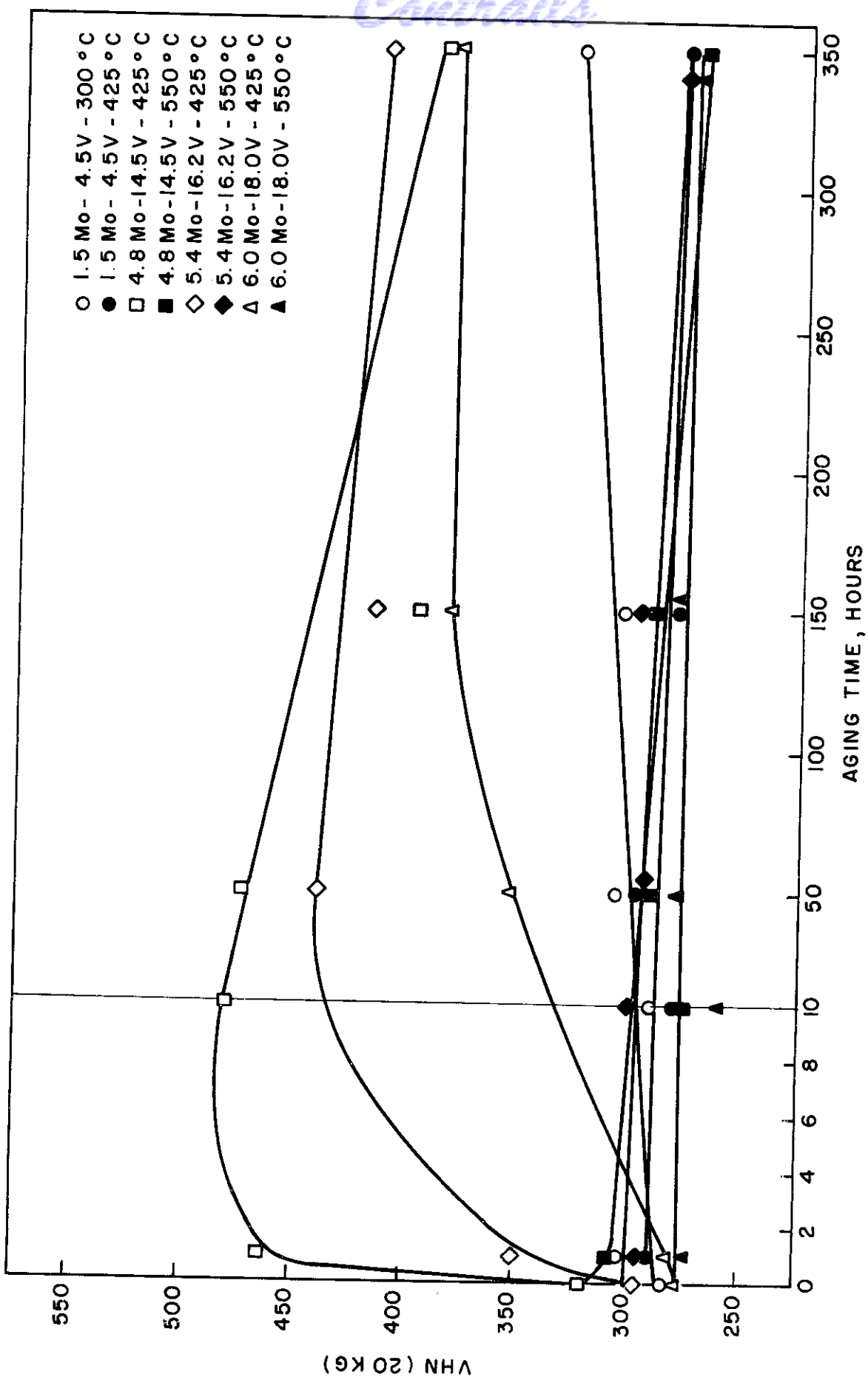

FIG. 18 - HARDNESS VS. AGING TIME AT 300°, 425°, AND 550°C FOR Ti-Mo-V ALLOYS WITH A Mo : V RATIO OF 1 : 3.

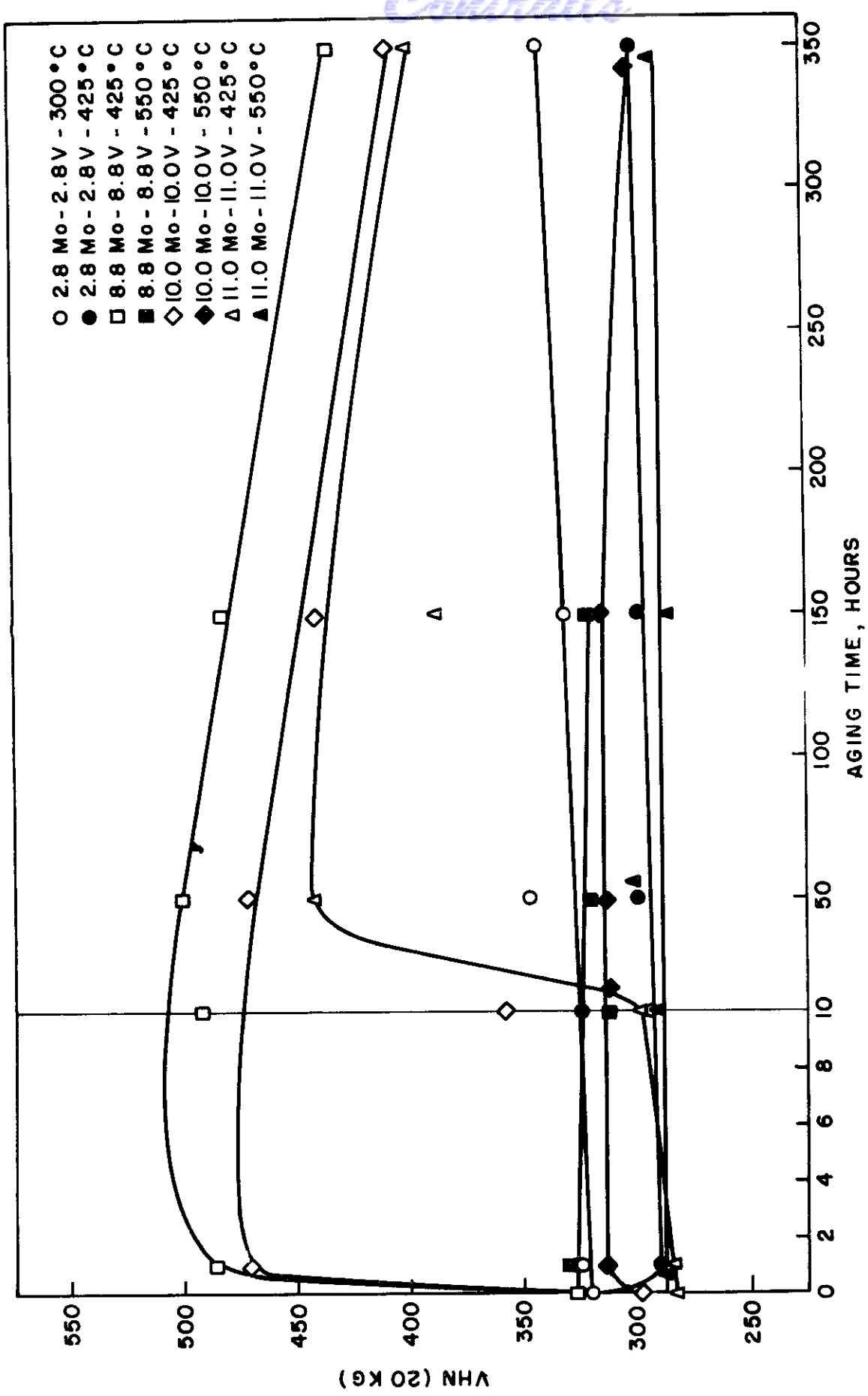

FIG. 19 - HARDNESS VS. AGING TIME AT 300°, 425°, AND 550°C FOR Ti-Mo-V ALLOYS WITH A Mo:V RATIO OF 1:1.

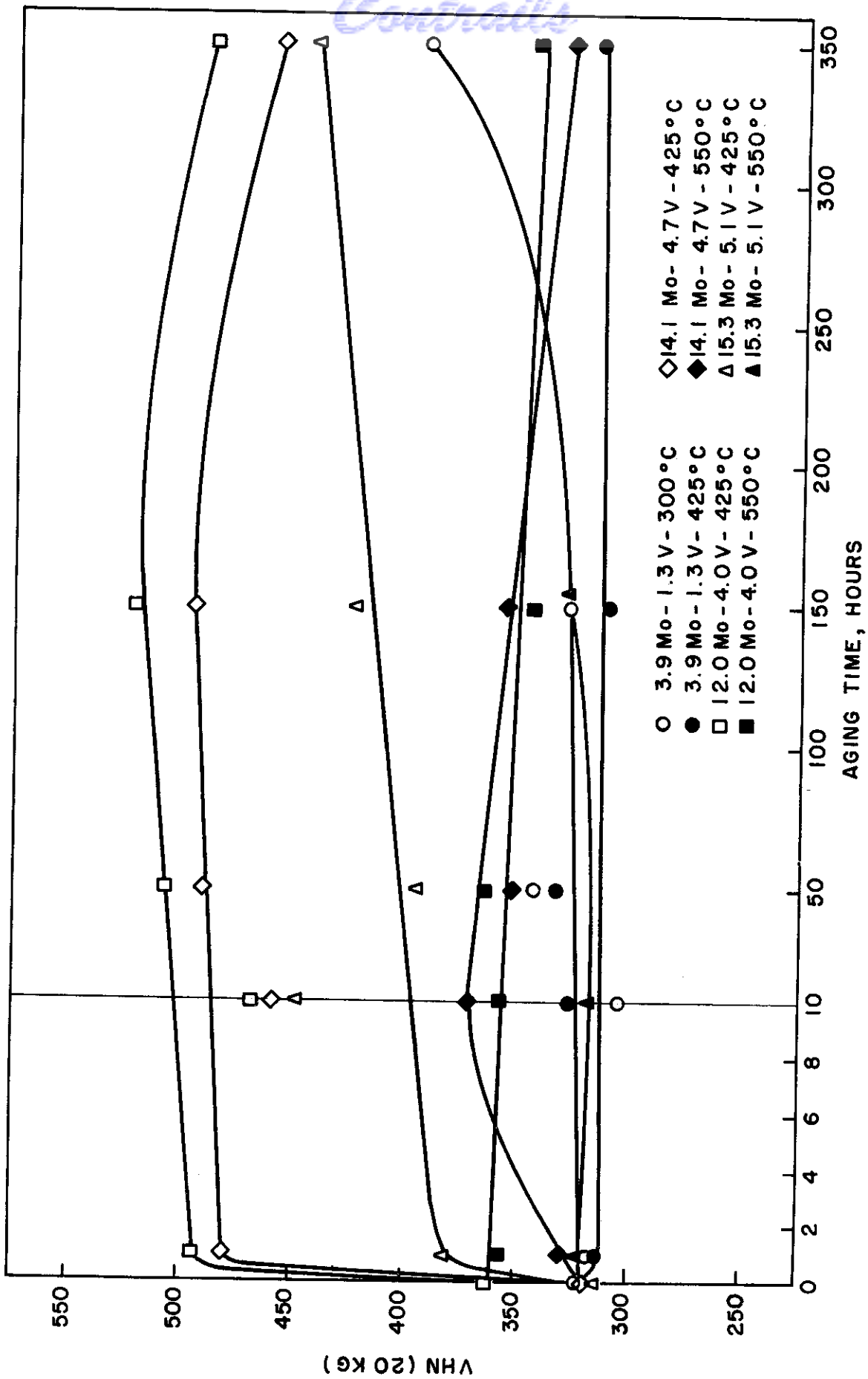

FIG. 20 - HARDNESS VS. AGING TIME AT 300°, 425°, AND 550°C FOR Ti - Mo - V ALLOYS WITH A Mo : V RATIO OF 3:1.

The five alloys with 7.0% or less total alloy content, which were duplex α-β following the solution anneal and air cool, underwent no visible structural change on aging. These alloys had hardnesses in the range 280-325 DPH as air cooled from the β phase field. At 425°C, the hardnesses remained relatively constant with aging time. At 300°C, the hardnesses increased with time but, with a single exception, did not rise above 351 DPH. A specimen of the 3.9% Mo-1.3% V alloy aged at 300°C for 350 hours had a hardness of 392 DPH. There is a reasonable expectancy for titanium-base alloys to be brittle when they are heat treated to a hardness of 400 DPH or more. With the single exception noted, the observed hardness increases in these low composition alloys do not justify any conclusion concerning embrittlement on aging. In order to get a certain answer to the question of embrittlement on aging these alloys at 300°C, it would be necessary to tensile test aged specimens.

Figures 21 to 25 show microstructures which resulted from aging Ti-10% Mo-10% V at 550°C. The structures are typical of those observed for alloys with 15% or more total alloy content aged at 550°C. After only one hour, transformation was well under way. The needle shaped microconstituent present from the air cool from the β field was observed to nucleate α. In the 10% Mo-10% V alloy, transformation at 550°C was completed between 50 and 150 hours. There was coarsening of the structure during aging. After 10 hours at 550°C the structure could be resolved at a magnification of 1160 X only in the vicinity of grain boundaries and the needles, while after 350 hours the entire structure could be resolved. No hardening was observed upon aging the alloys at 550°C. However, hardening may occur for aging times under one hour, the shortest aging time used in these studies.

In general, transformation in the high composition alloys was much less complete after 50 hours at 425°C than for this time at 550°C. Transformation appeared to be complete in all alloys after 350 hours at 550°C. However, transformation did not appear to be complete in Ti-20% Mo and Ti-15.3% Mo-5.1% V after 350 hours at 425°C. The needles were observed to nucleate α at 425°C also. The structures developed at 425°C were very fine and could not be resolved at a magnification of 1160 X after 350 hours of aging. Considerable hardening was associated with the transformation as may be seen from the aging curves. It is quite evident that none of the alloys studied are stable with respect to complete β retention.

D. Conclusions

The results of this study of ternary and binary titanium-base alloys with molybdenum and vanadium show that, for stability of the high temperature β phase with respect to transformation at temperatures below the β transus, the following additions are insufficient:

1. 30% for binary alloys with vanadium.

2. 20% for binary alloys with molybdenum.

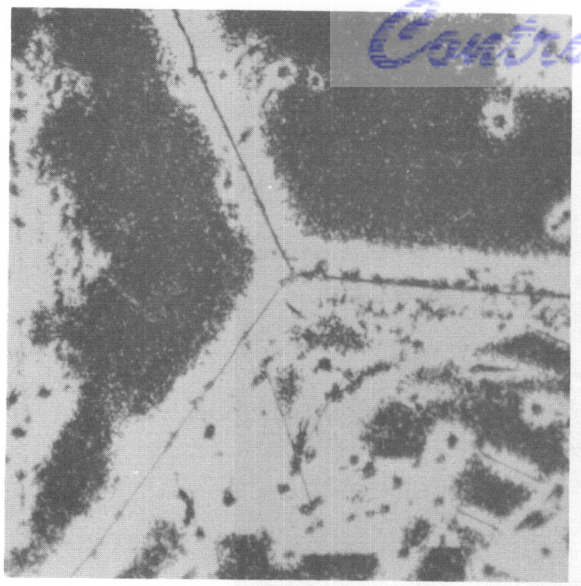

Neg. No. 8363 X 750

Fig. 21

10% Mo-10% V, solution heat treated 1100°C - 24 hours - air cooled, aged at 550°C - 1 Hour - air cooled.

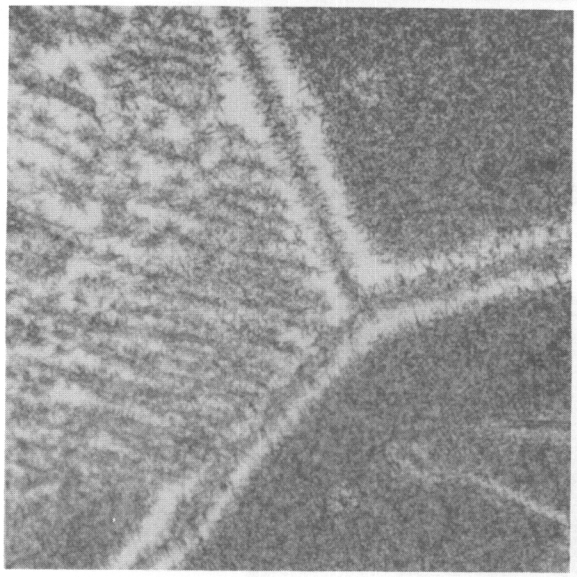

Neg. No. 8364 X 750

Fig. 22

Same as Fig. 21, aged at 550°C - 10 hours - air cooled.

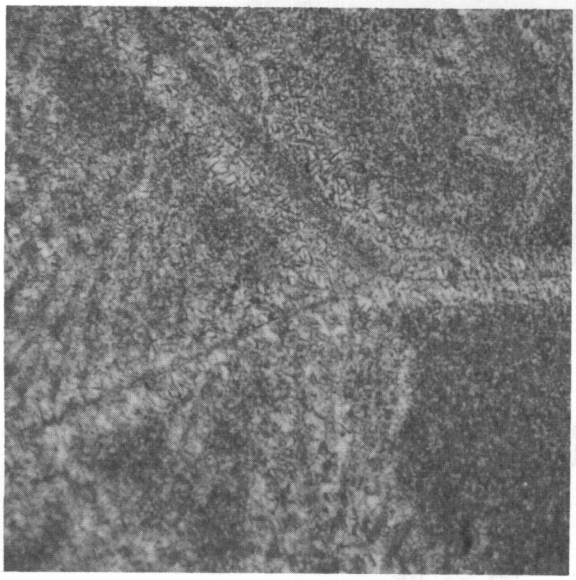

Neg. No. 8361 X 750

Fig. 23

Same as Fig. 21, aged at 550°C - 50 hours - air cooled.

Etchant: 60 cc glycerine, 20 cc HNO_3, 20 cc HF

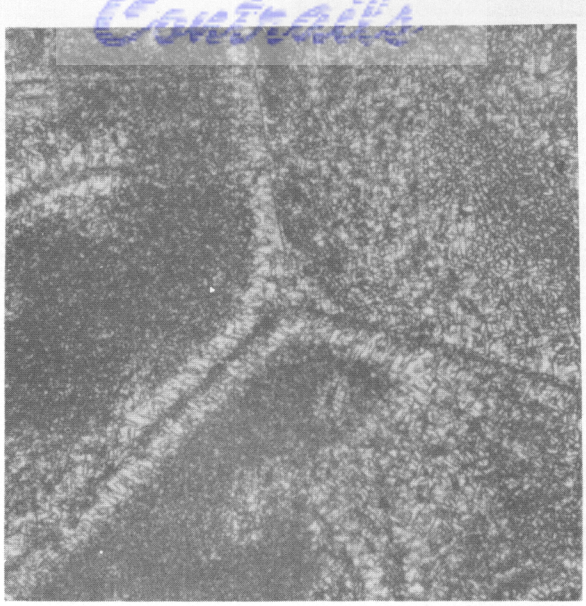

Neg. No. 8362 X 750

Fig. 24

Same as Fig. 21, aged at 550°C - 150 hours - air cooled.

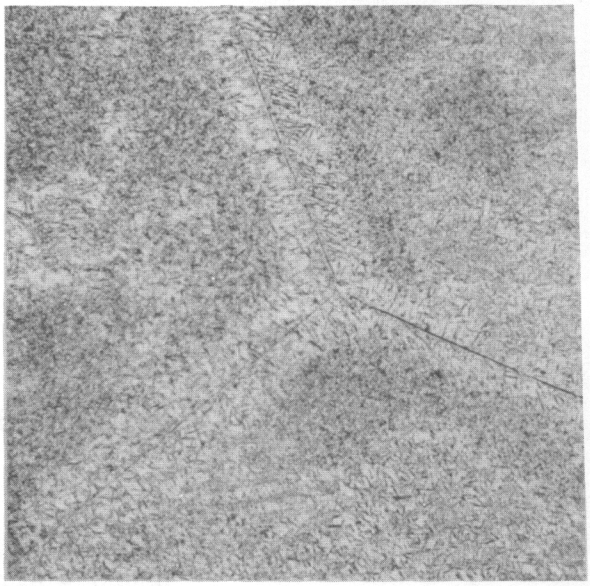

Neg. No. 8360 X 750

Fig. 25

Same as Fig. 21, aged at 550°C - 350 hours - air cooled.

Etchant: 60 cc glycerine, 20 cc HNO_3, 20 cc HF

3. 24% total for ternary alloys with a 1:3 Mo:V ratio.

4. 20% total for ternary alloys with a 1:1 Mo:V ratio.

5. 20.4% total for ternary alloys with a 3:1 Mo:V ratio.

Also, it appears that for stability under stress, more than 30% alloy addition is needed for binary alloys with molybdenum (5,6).

Since, in general, no significantly hard structures, i.e., of 400 DPH or more hardness, developed in the compositions of 7% or less total alloy content upon air cooling from 1100°C and subsequently aging at 300° and 425°C, these alloys may prove useful from the standpoint of retaining ductility under service conditions. A Ti-3% Mo alloy will soon be evaluated under Contract No. AF 33(038)-22806. When the results of this evaluation become available, it will be appropriate to consider whether one of the low composition alloys should be further investigated.

The structures resulting from air cooling the high composition alloys from the β phase region are not necessarily associated with brittleness. However, the fine α precipitates which form upon aging these alloys at temperatures of 425° and 550°C are associated with embrittlement (7,17). It is concluded that ternary Ti-Mo-V alloys in the total alloy content range of 15 to 24% and binary alloys in the range of 15 to 30% offer no promise for a service application at 425° to 550°C where ductility throughout service life is required of members applied in the as-welded state. Further, for compositions in the vicinity of 30% alloy additions, attempts to obtain a stable ductile α + β structure by post-weld heat treatment would very probably prove futile. These alloys have such low β transus temperatures that only fine α + β structures such as are associated with loss of ductility could be produced by heat treatment.

V. THE TITANIUM-RICH CORNER OF THE Ti-Al-V SYSTEM

by J. J. Rausch and F. A. Crossley

A. Introduction

The phase relationships in the titanium-rich corner of the Ti-Al-V system were investigated because of the promise shown by alloys of this system for elevated temperature application. Thirty alloys were prepared in the region from 1 to 22% aluminum and 2 to 17% vanadium. The temperature range studied was from 600° to 1200°C.

B. Procedure

The alloy ingots, weighing 15 grams, were melted in a non-consumable tungsten electrode arc furnace. The alloy charges and resultant ingots were weighed to the nearest one-tenth of a milligram. With the exception of a few alloys high in the vanadium region, negligible weight losses were obtained. Four alloys, 1% Al-11, 14, 17% V and 4% Al-14% V, which had been reported in some of the quarterly reports, have been eliminated from consideration in the final report. These alloys were not used since it was found that there were serious discrepancies between their nominal and actual compositions. Unfortunately, this was discovered too late to make additional alloys and repeat the annealing schedules. However, these four alloys were of such compositions that they were not essential to the successful determination of the part of the ternary system of greatest interest.

Cold deformation was not possible for the majority of the alloys in this investigation prior to annealing. It was felt that the annealing times would be of sufficient duration to allow the alloys to approach equilibrium. The annealing times and temperatures were as follows:

Annealing Temperature	Annealing Time
1200°C	24 hours
1100°C	24 hours
1000°C	48 hours
900°C	72 hours
800°C	1 week
700°C	2 weeks
600°C	1 month

Equilibrating anneals of specimens at temperatures below 1000°C were preceded by a one-hour treatment at this temperature, followed by a furnace cool to the desired equilibrium temperature. This heat treatment was used to eliminate coring in alloys containing more than 7% aluminum and those containing more than 8% vanadium.

C. Results and Discussion

The Ti-Al and Ti-V diagrams as given by Hansen et al. (18) were used to extend the phase boundaries determined by the ternary data to the binary axes of the partial isothermal sections. Although the binary systems were based on investigations in which iodide titanium was used, it was felt that the sponge used in this investigation was of sufficient purity (103 BHN) to justify this extension. However, the results from the determination of phase relationships in the titanium-rich corner of the Ti-Al-Si system (Section VI) indicate that some differences may be expected between alloys made with iodide titanium and with 103 BHN quality sponge.

Seven isothermal sections were made at 100°C intervals from 1200° to 600°C. These are presented in Figures 26 to 32. The isothermal

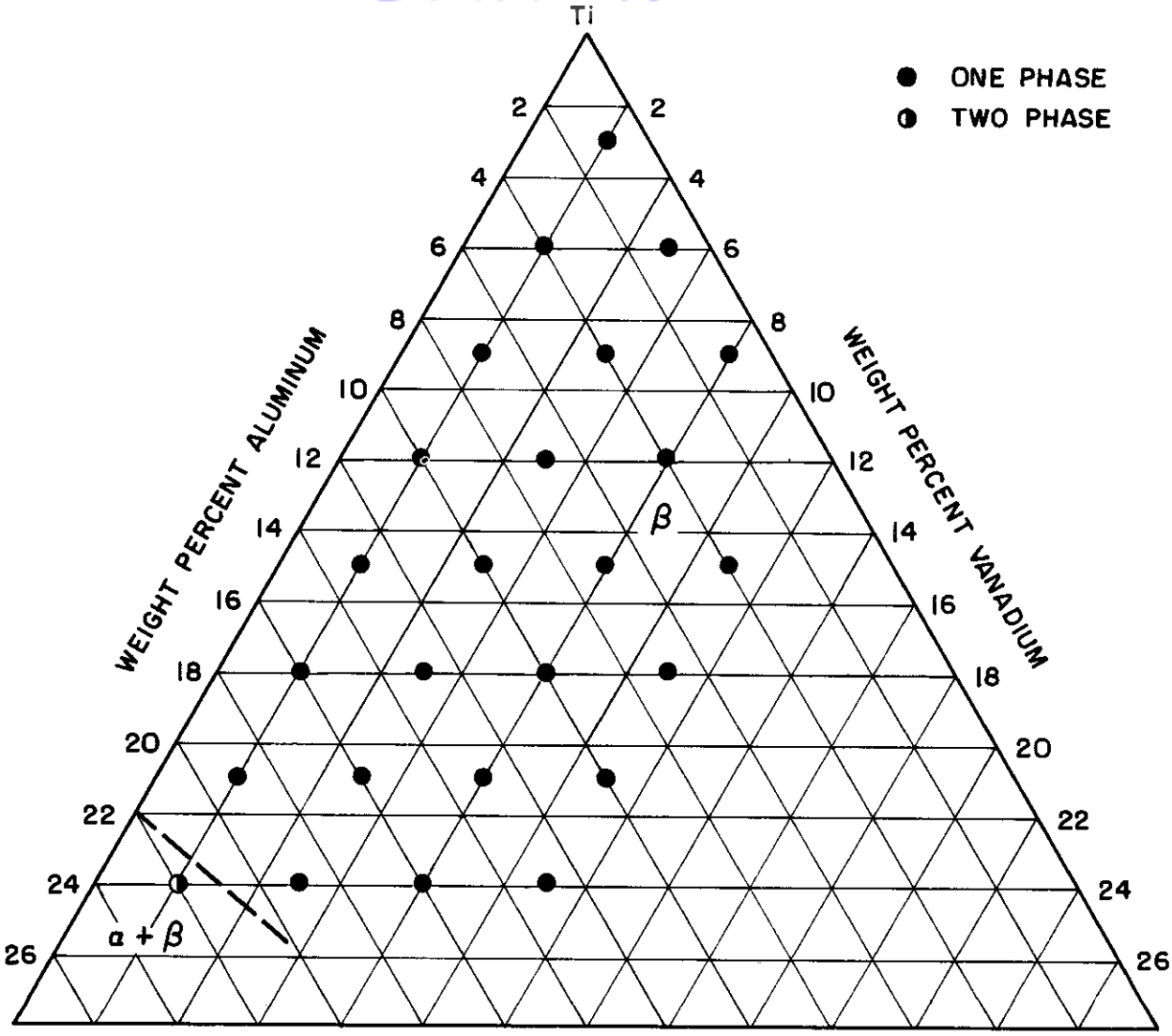

FIG.26 - PARTIAL ISOTHERMAL SECTION OF
Ti - Al - V SYSTEM AT 1200 °C

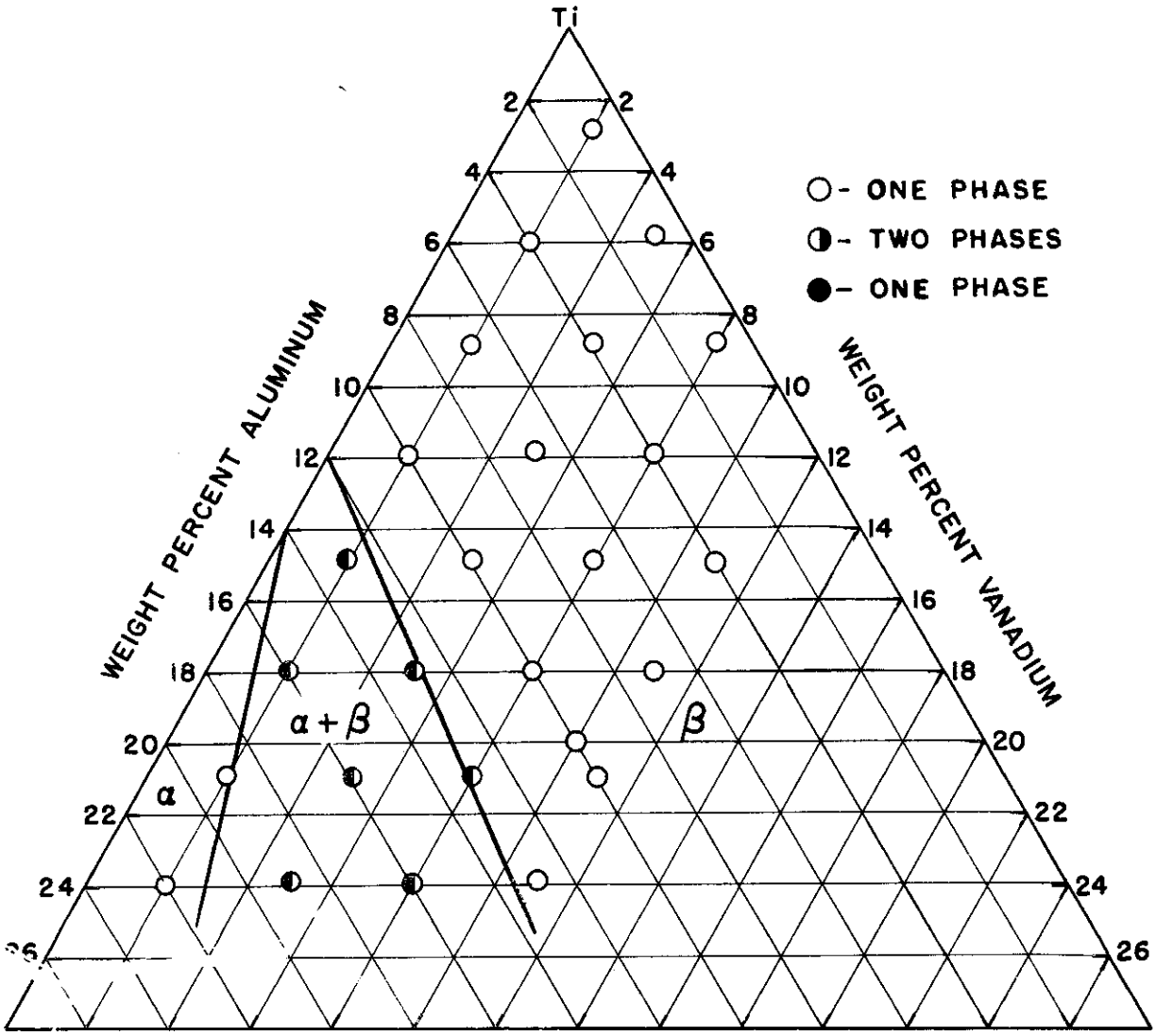

FIG.27-PARTIAL ISOTHERMAL SECTION OF Ti-Al-V SYSTEM AT 1100°C

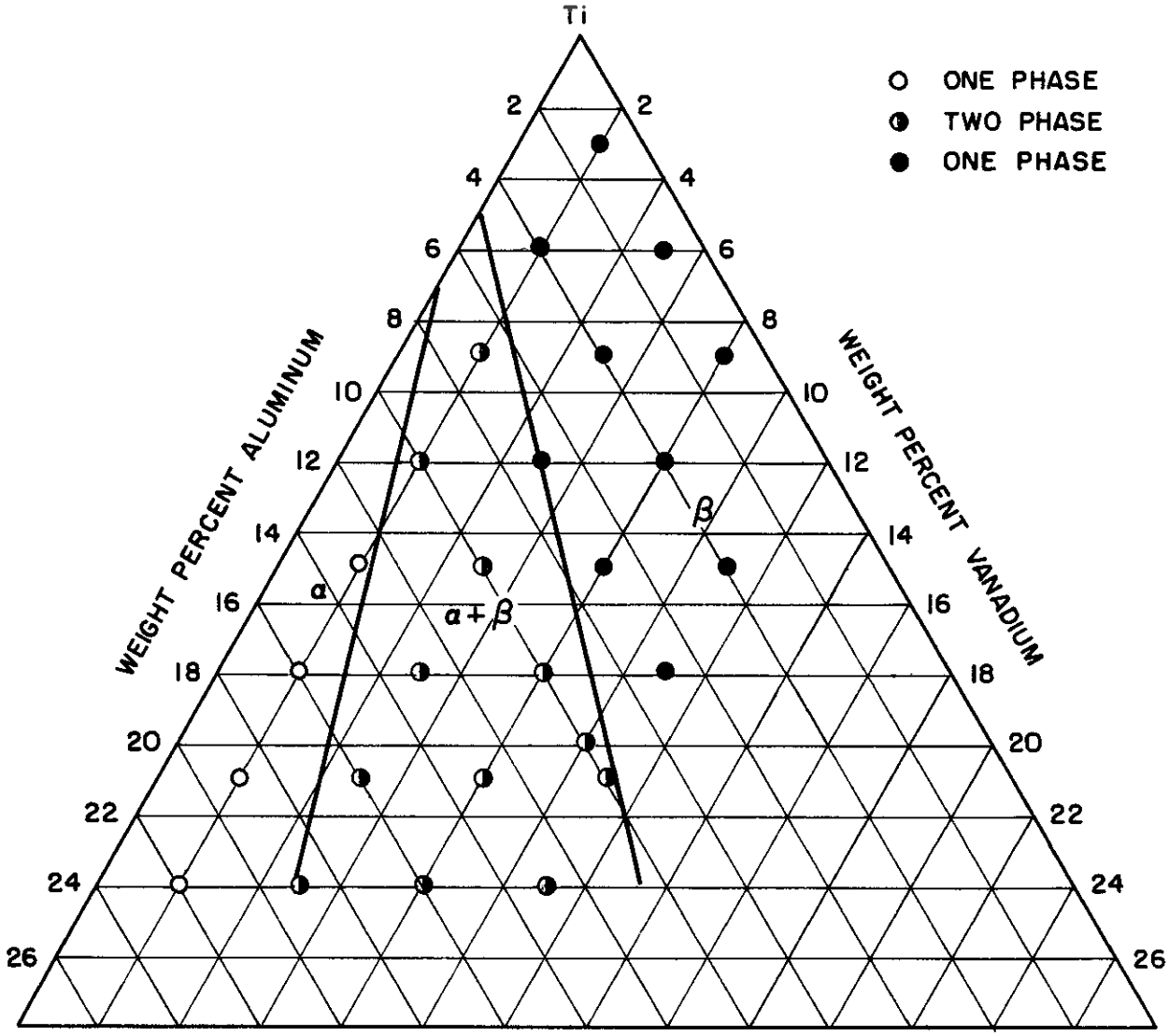

FIG.28 - PARTIAL ISOTHERMAL SECTION OF
Ti - Al - V SYSTEM AT 1000°C

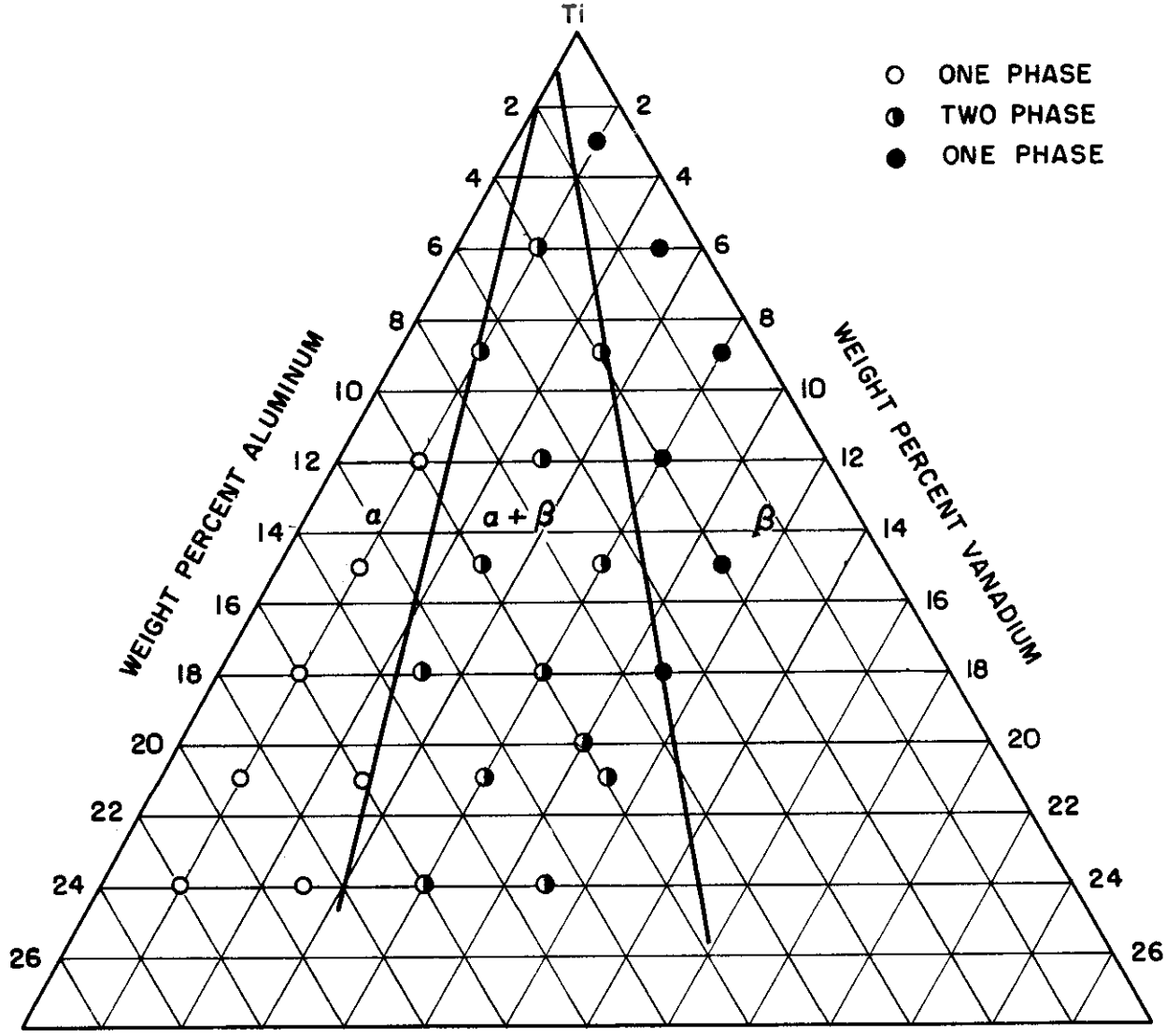

FIG.29 - PARTIAL ISOTHERMAL SECTION OF
Ti - Al - V SYSTEM AT 900 °C

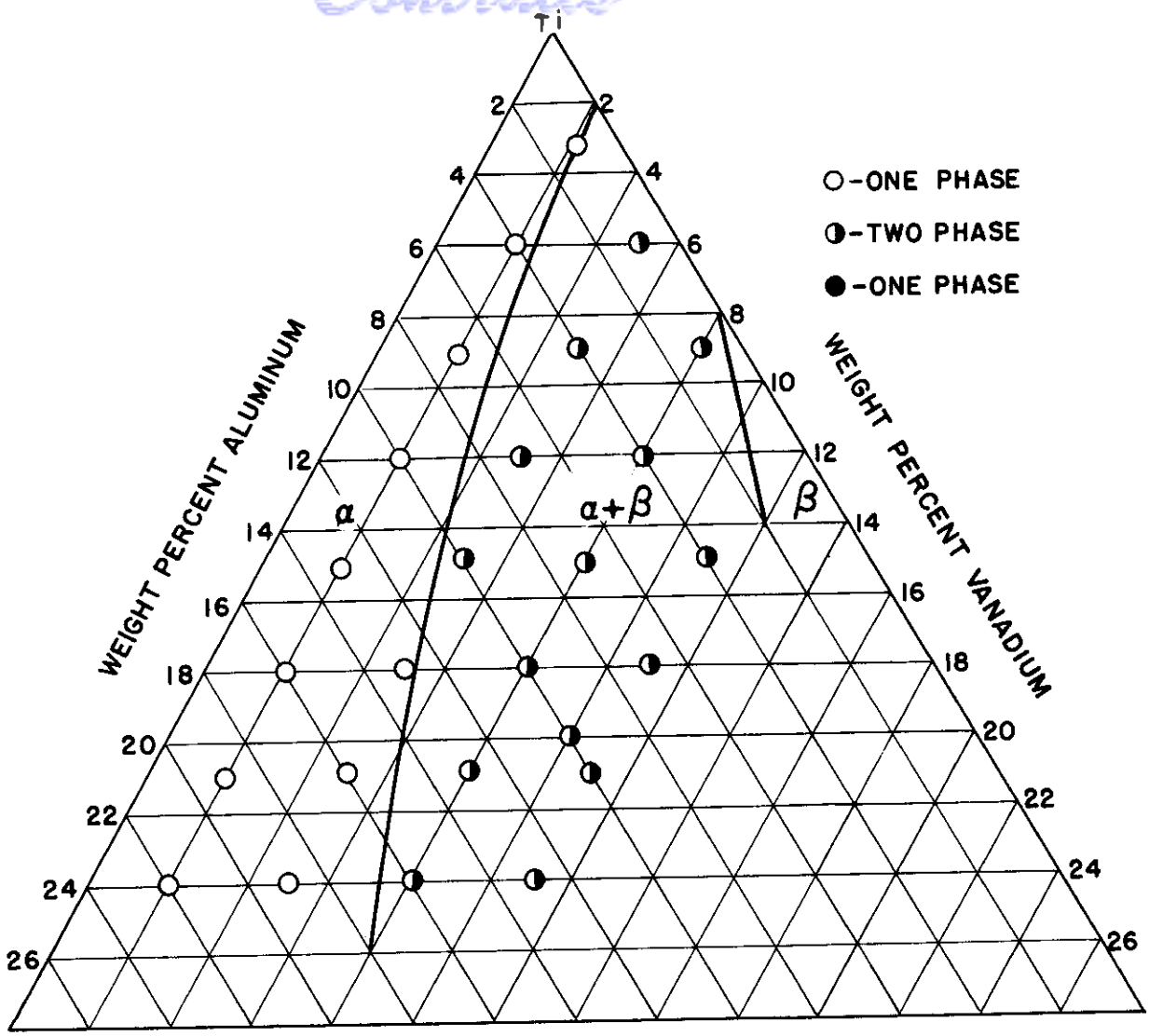

FIG.30-PARTIAL ISOTHERMAL SECTION OF Ti-Al-V SYSTEM AT 800°C

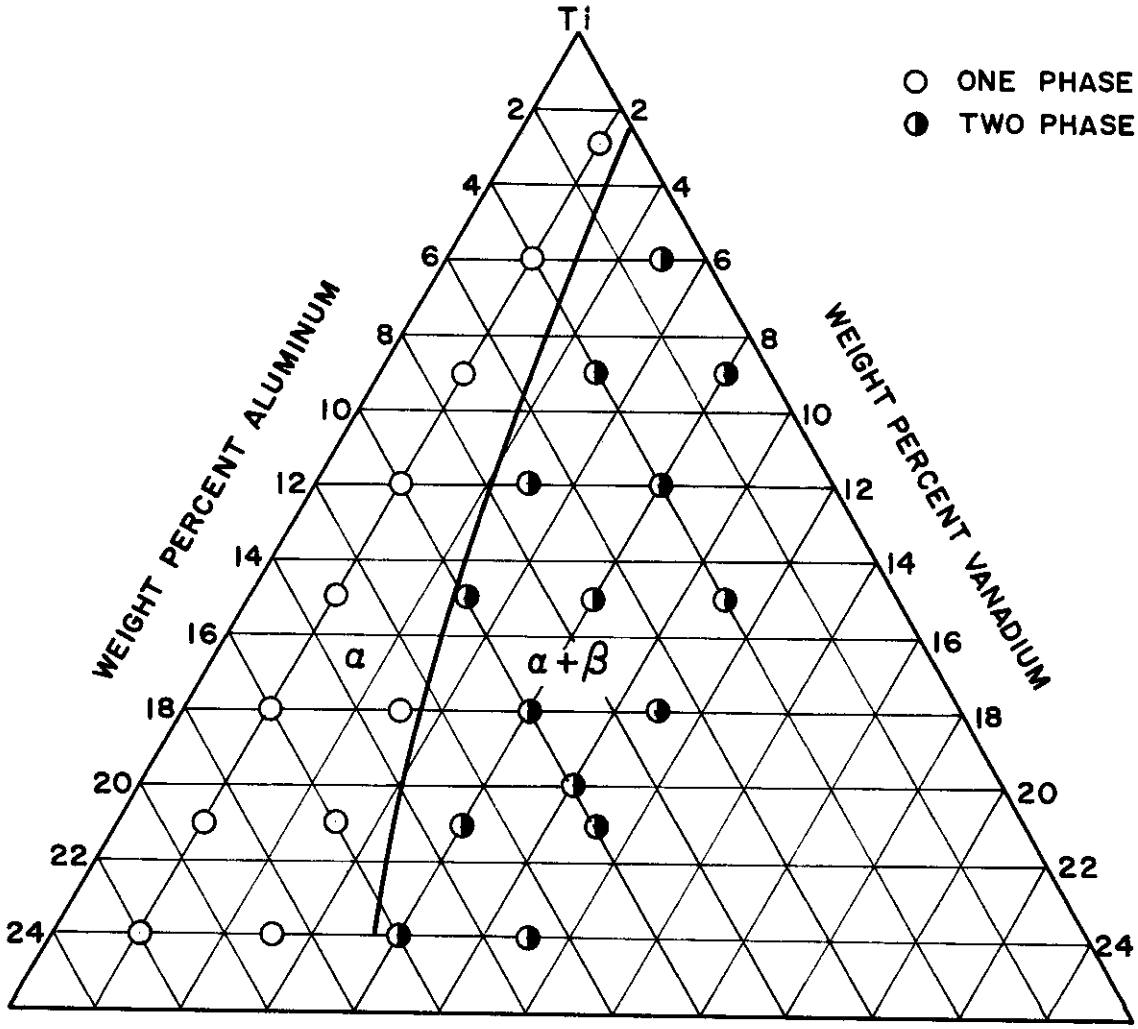

FIG. 31 - PARTIAL ISOTHERMAL SECTION OF Ti-Al-V SYSTEM AT 700°C

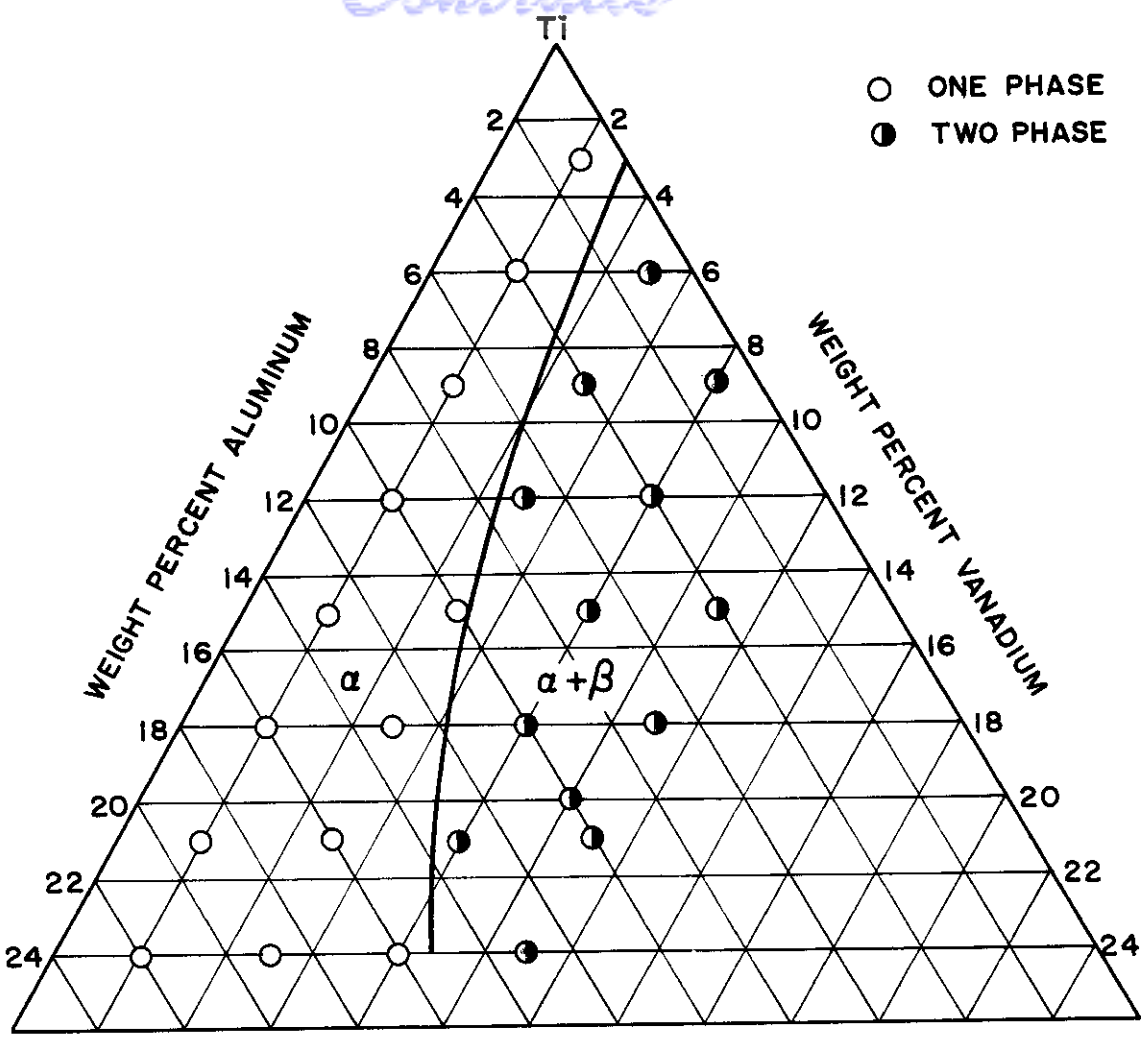

FIG. 32 - PARTIAL ISOTHERMAL SECTION OF Ti-Al-V SYSTEM AT 600°C

sections show that increasing the aluminum content expands the α field at a given temperature.

Vertical sections at both constant aluminum and constant vanadium contents are shown in Figures 33 to 35. Comparison of Figures 33 and 34 show that increasing the aluminum content of Ti-Al-V alloys from 4 to 7% increases the solubility of vanadium in α from approximately 3.5 to 4.5%.

The addition of vanadium to Ti-Al alloys has little effect on the β/α + β boundary as may be seen in Figure 35. Raising the vanadium from 2 to 8% lowers the β/α + β boundary approximately 60°C at the 2% aluminum level and approximately 40°C at the 8% aluminum level.

A few faint unidentified lines were obtained in the Debye powder pattern of a 5% V-19% Al alloy. These lines could be ascribed to neither α nor β. Extra lines were also obtained in the Debye powder patterns of other alloys near the 5% V-19% Al composition. No positive identification of the lines could be made as they were few in number and very faint. Also, no metallographic confirmation of the existence of another phase could be found. Since alloys in this compositional region are not of practical importance, no further effort was made to determine the origin of these lines.

The hardness of alloys water quenched from 1000°C is shown in Table V. These hardness data are plotted versus aluminum content in Figure 36. The curves show that minima occur at about 16% aluminum, independent of the vanadium content. The same phenomenon had also been observed in the Ti-Al-O, N, C systems (19). Although most of the alloys shown in the figure were in the α + β field when quenched, the fact that the most pronounced dip occurred in the curve for 2% vanadium alloys was proof that the minima were due to softening of the α phase. The last four points in the curve for 2% vanadium alloys were entirely in the α field when quenched. These results suggested that Ti-16% Al might be ductile. Therefore, it was decided to investigate the properties of a binary 16% Al alloy.

Three 100-gram buttons of this composition were made using high purity sponge titanium (103 BHN) and aluminum shot. An 800°C anneal, for 92 hours followed by water quenching showed the hardness of this alloy to be 260 DPH. This compared favorably to the hardness of the ternary alloys. The alloy showed no room temperature ductility in this condition. Attempts to cold press and cold roll failed. Hot rolling at temperatures up to 1050°C also resulted in cracking after one or two passes. Since practical ductility does not appear to be a virtue of this alloy no further work was done.

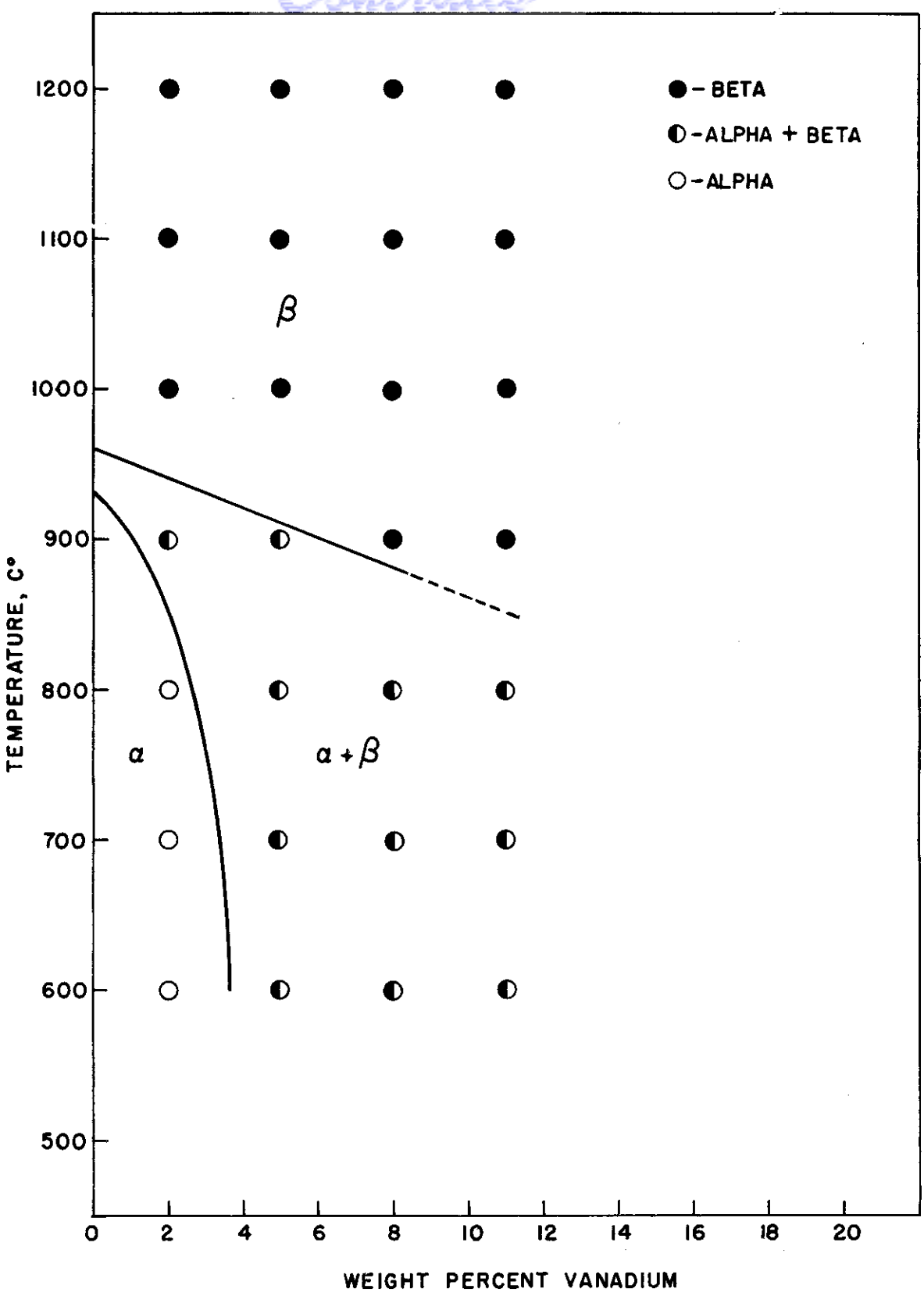

FIG.33- VERTICAL SECTION OF Ti-Al-V SYSTEM AT 4% Al

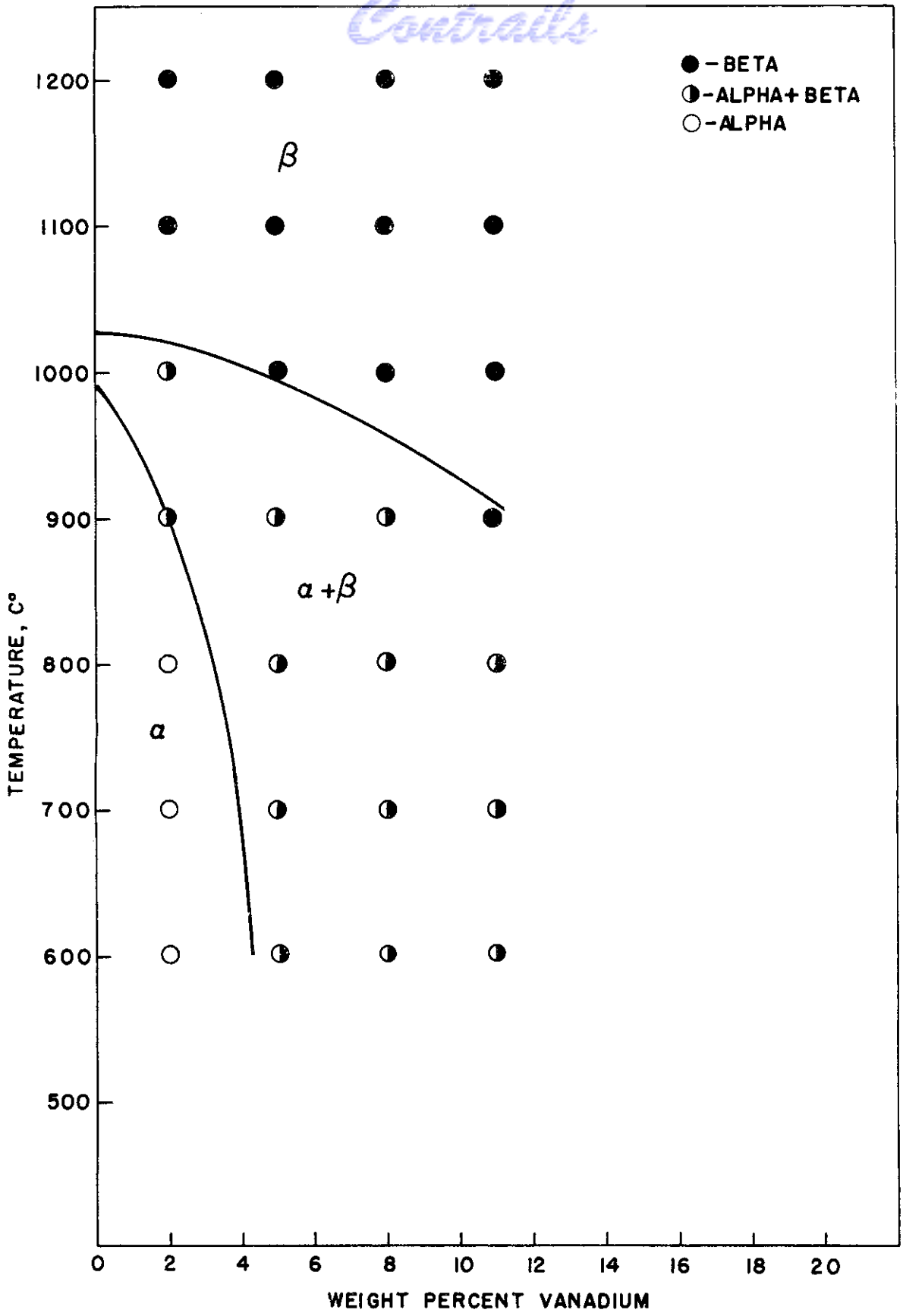

FIG.34 - VERTICAL SECTION OF Ti-Al-V SYSTEM AT 7% Al

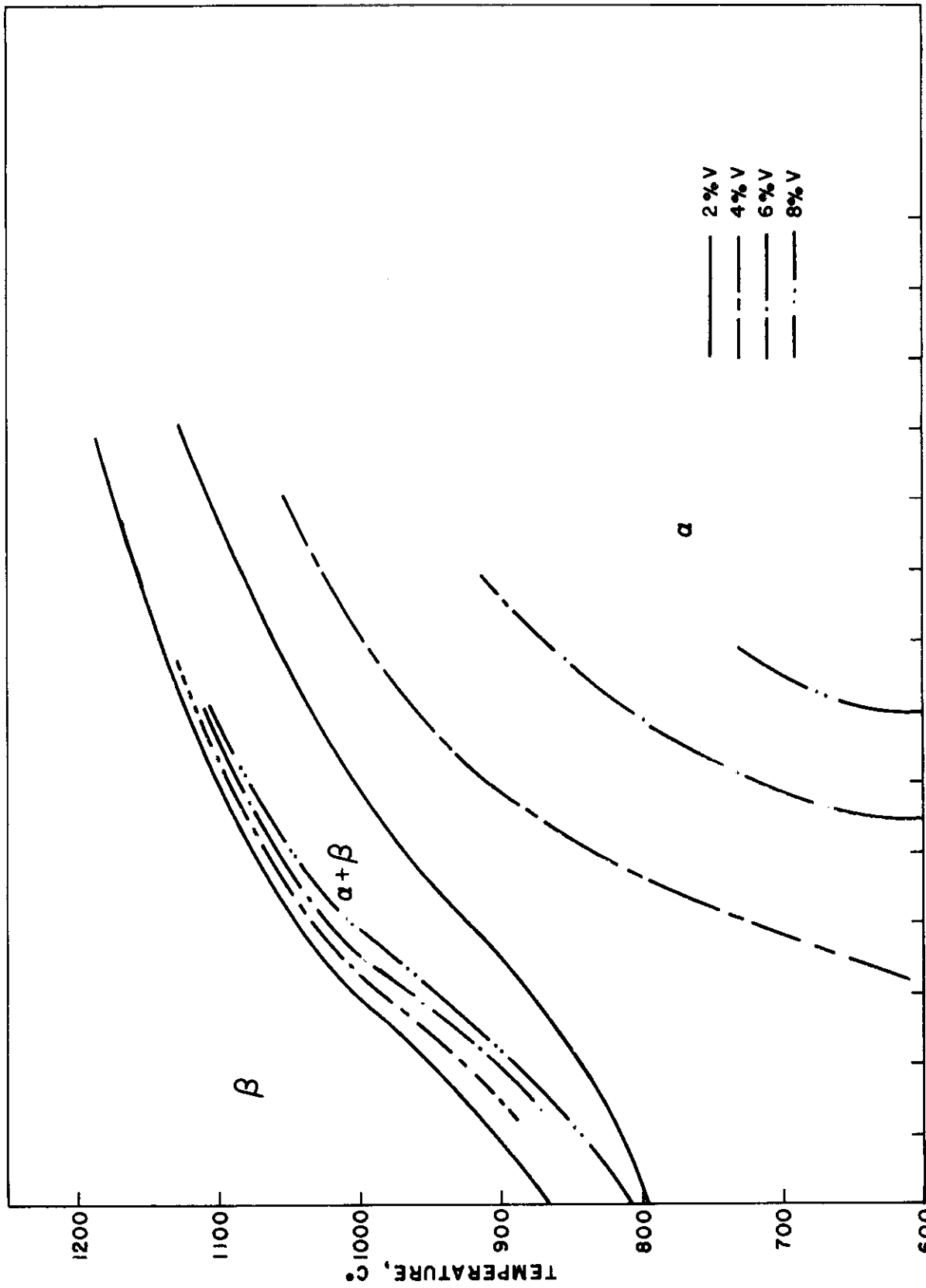

FIG.35-VERTICAL SECTIONS OF Ti-Al-V SYSTEM AT CONSTANT VANADIUM CONTENTS

TABLE V

HARDNESS OF Ti-Al-V ALLOYS WATER QUENCHED FROM 1000°C

2% Vanadium		5% Vanadium		8% Vanadium	
Aluminum Content (Wt. %)	Hardness (DPH)	Aluminum Content (Wt. %)	Hardness (DPH)	Aluminum Content (wt. %)	Hardness (DPH)
1	251	1	257	1	327
4	251	4	316	4	335
7	334	7	360	7	491
10	331	10	353	10	313
13	308	13	279	13	346
16	244	16	278	16	283
19	344	19	303		

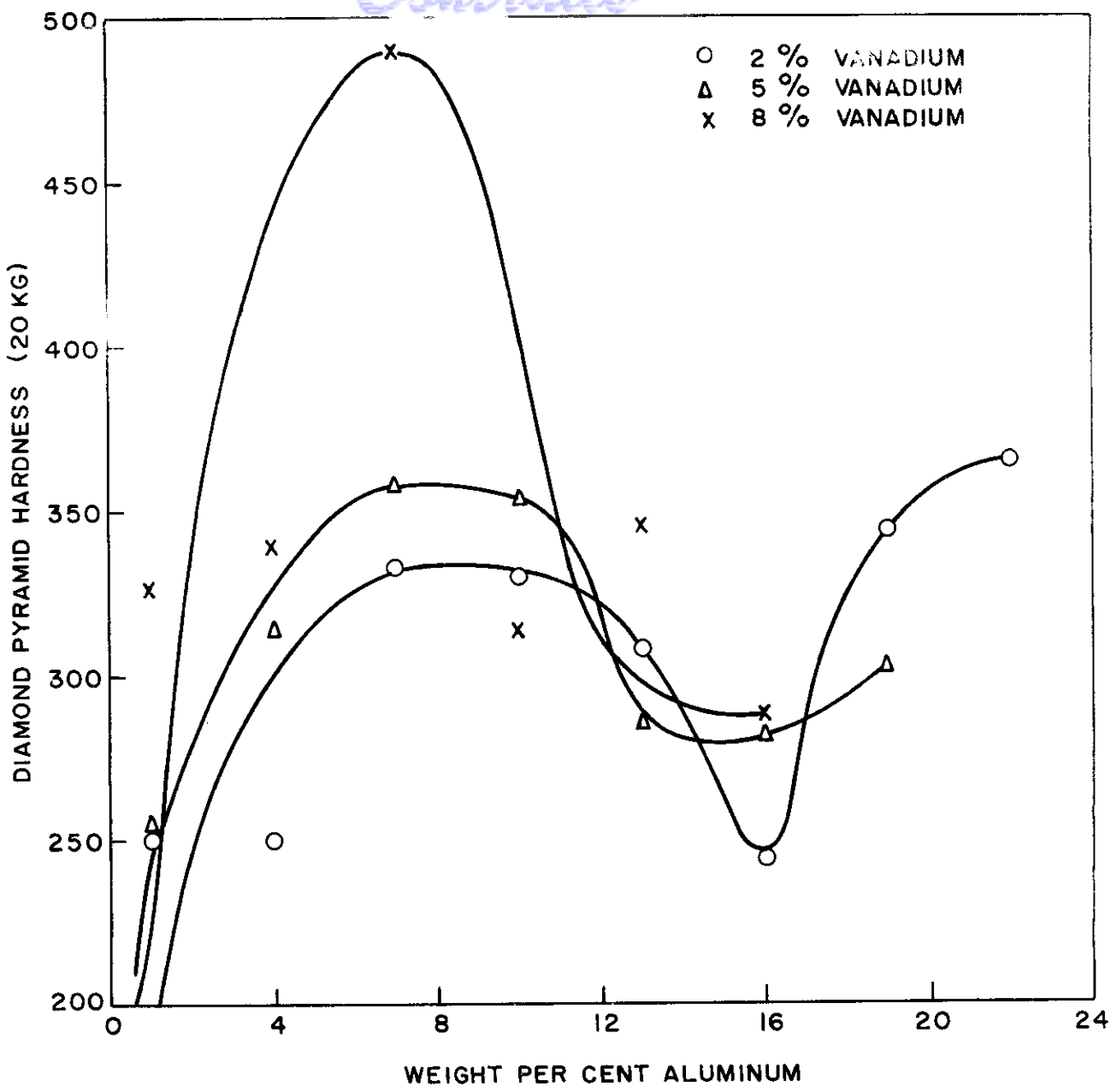

FIG. 36 - HARDNESS OF Ti-Al-V ALLOYS AT CONSTANT VANADIUM CONTENTS, WATER QUENCHED FROM 1000°C.

VI. THE TITANIUM-RICH CORNER OF THE Ti-Al-Si SYSTEM

by D. H. Turner and F. A. Crossley

A. Introduction

An investigation of the titanium-rich corner of the Ti-Al-Si system was initiated to determine the solubility of silicon in the α and β fields so that optimum additions of silicon to the Ti-Al alloys could be determined for the development of promising alloys for elevated temperature application. No information on the titanium-rich corner of this ternary system was available prior to the initiation of this work. This investigation covered the titanium-rich corner up to 8% aluminum and 2% silicon in the temperature range of 600° to 1200°C.

B. Procedure

One-hundred gram arc melted ingots were carefully weighed after melting to detect possible losses. Weight changes were negligible so it was assumed that the actual compositions were very close to the nominal compositions. Alloys were prepared using high purity (103 BHN) sponge. All isothermal anneals below 1000°C were preceded by a solution treatment at 1000°C for one hour and furnace cooled to the annealing temperature. Treatments up to 1000°C were carried out with the specimens sealed in evacuated Vycor bulbs. The higher temperature anneals were done with the specimens sealed in quartz bulbs under a partial pressure of argon. The annealing schedule was as follows:

Temperature, °C	Time, Hours
1200	24
1100	24
1000	48
900	72
800	168
600	720

C. Results and Discussion

Partial isothermal sections at temperatures between 1200° and 600°C are presented in Figures 37 to 42. The binary intercepts used in the diagrams were taken from Hansen, et al (18) in the regions not covered by this investigation. At 1200°C the β field extends over most of the compositional area shown; see Figure 37. The solubility of silicon in β at this temperature appears to be slightly less than 2% and does not seem to be affected by aluminum content in the composition range investigated. Only a small amount of precipitate was observed in the series of alloys containing 2% silicon at 1200°C.

The partial isothermal section at 1100°C is shown in Figure 38. The $\beta/\beta + Ti_5Si_3$ boundary was estimated from the vertical sections.

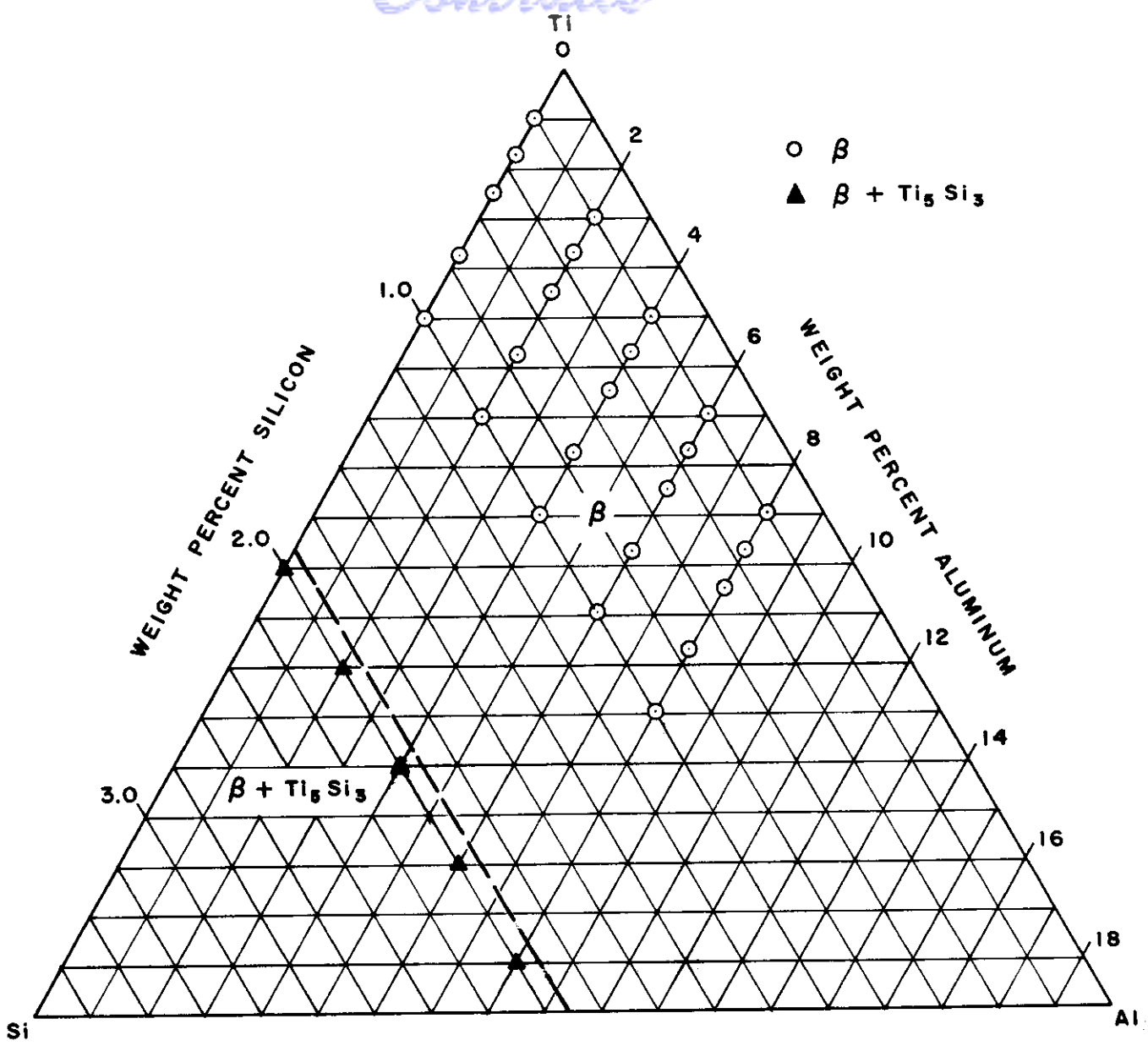

FIG. 37 – PARTIAL ISOTHERMAL SECTION AT 1200° C OF THE Ti-Al-Si SYSTEM.

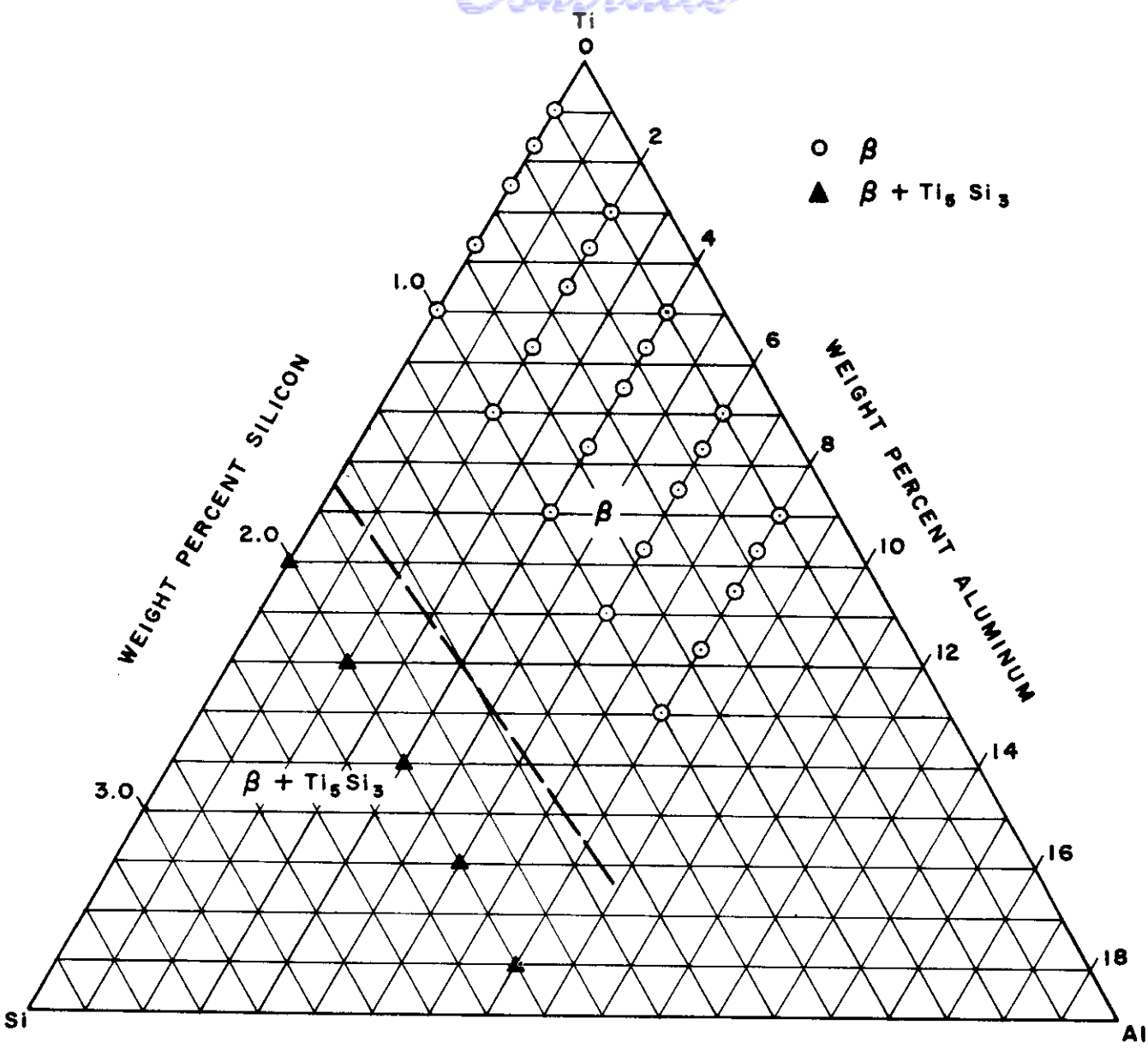

FIG. 38 – PARTIAL ISOTHERMAL SECTION AT 1100° C OF THE Ti-Al-Si SYSTEM.

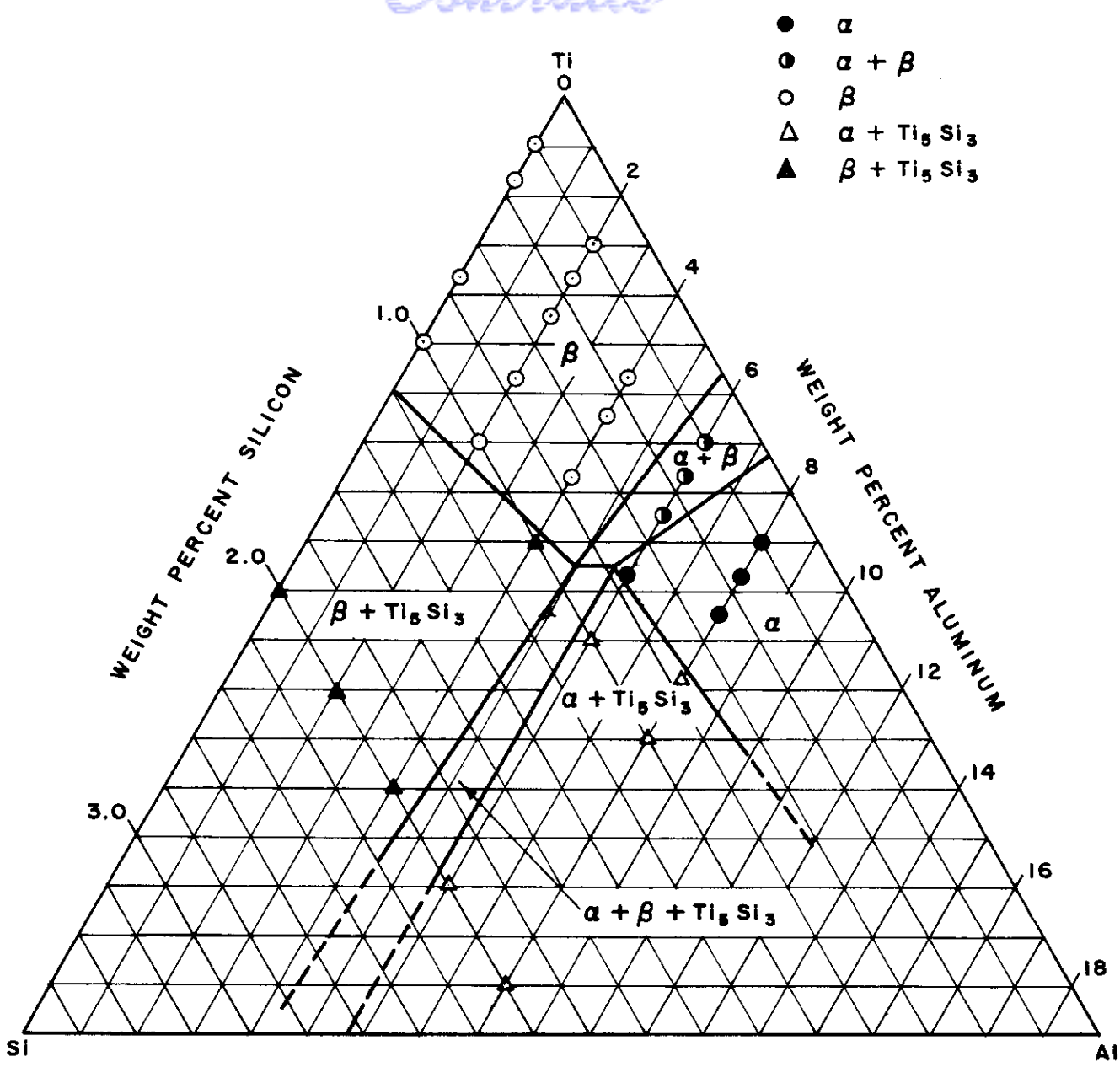

FIG. 39 – PARTIAL ISOTHERMAL SECTION AT 1000° C OF THE Ti-Al-Si SYSTEM

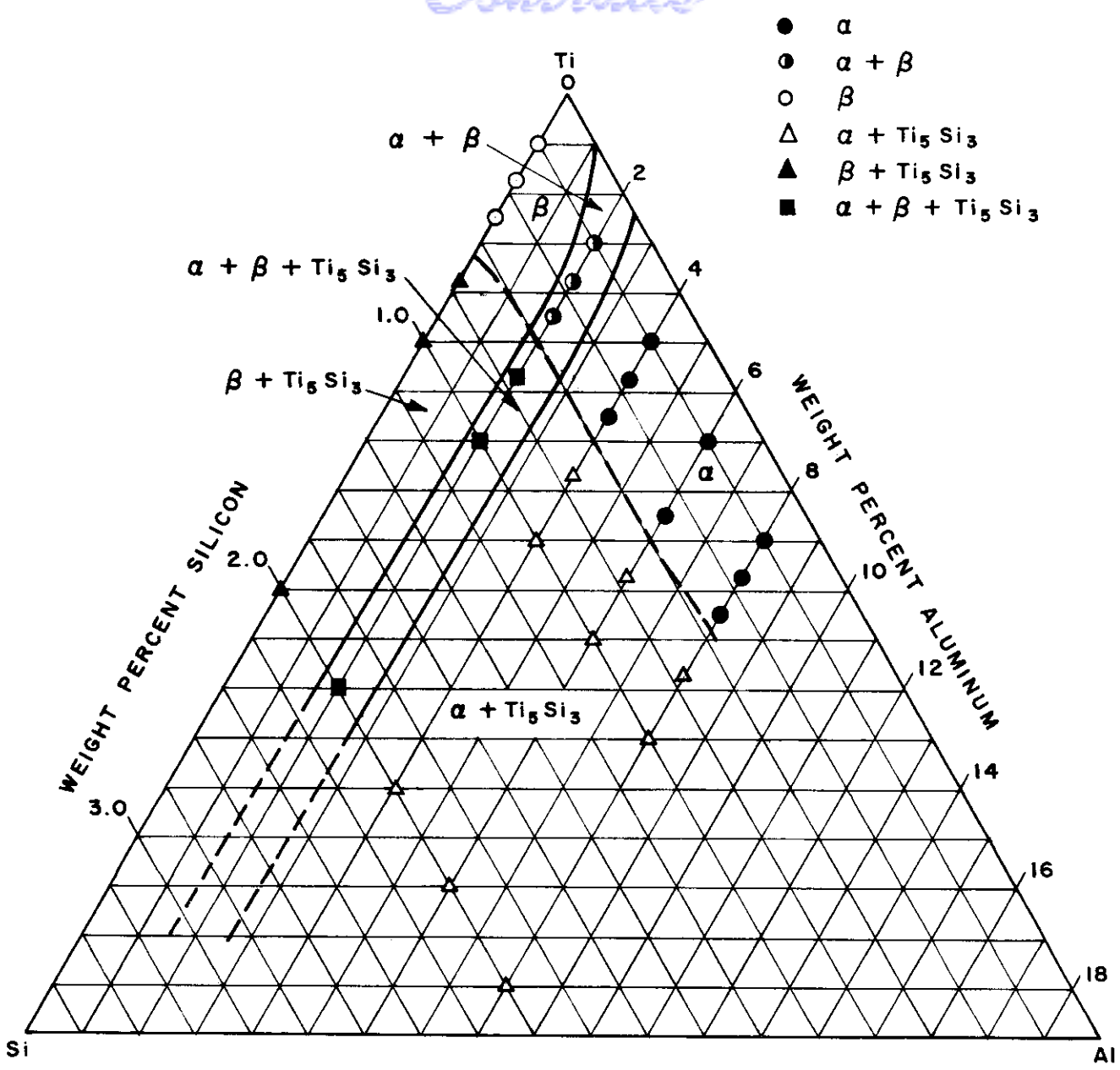

FIG. 40 - PARTIAL ISOTHERMAL SECTION AT 900° C OF THE Ti-Al-Si SYSTEM.

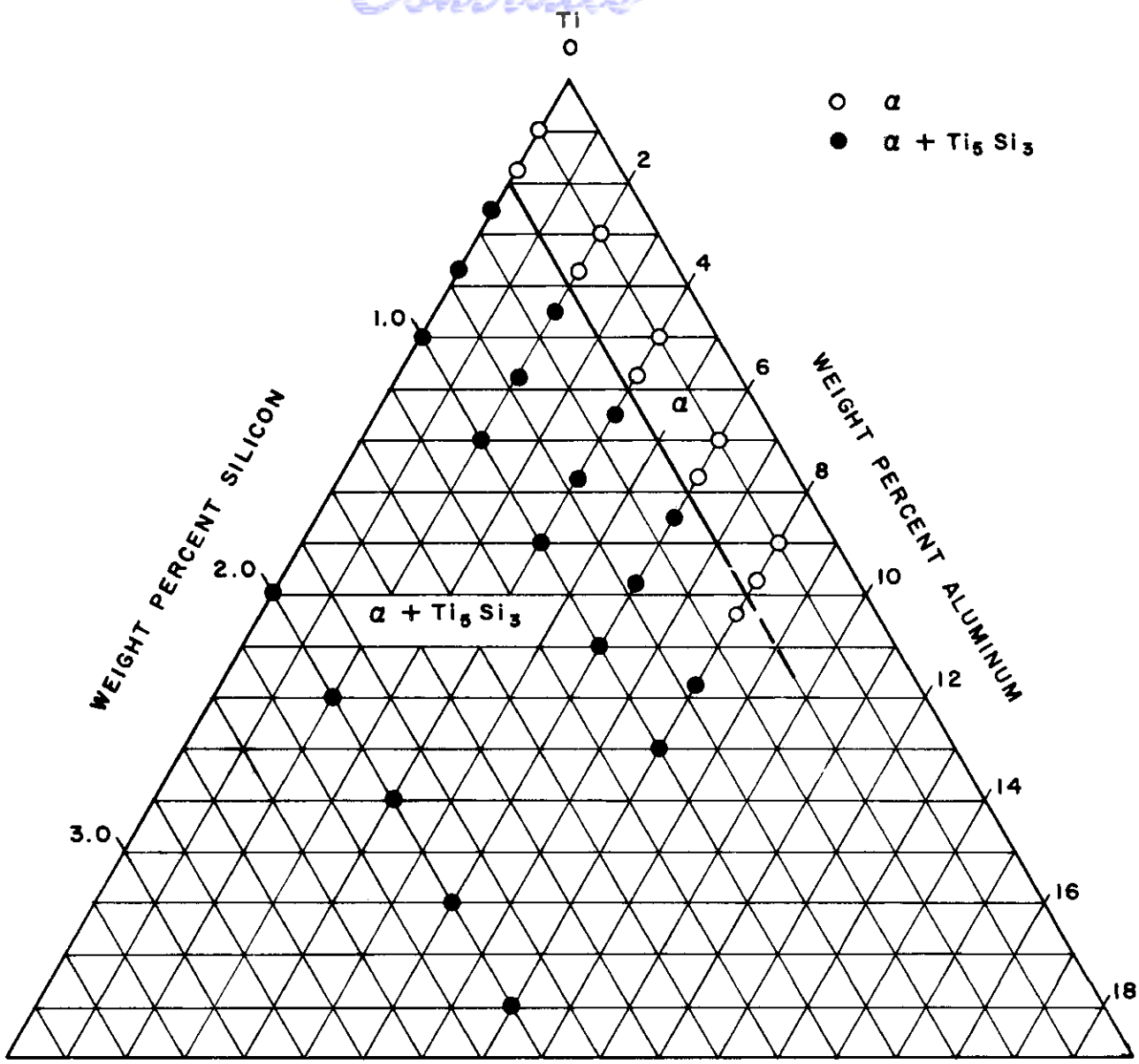

FIG. 41 – PARTIAL ISOTHERMAL SECTION AT 800° C OF THE Ti-Al-Si SYSTEM.

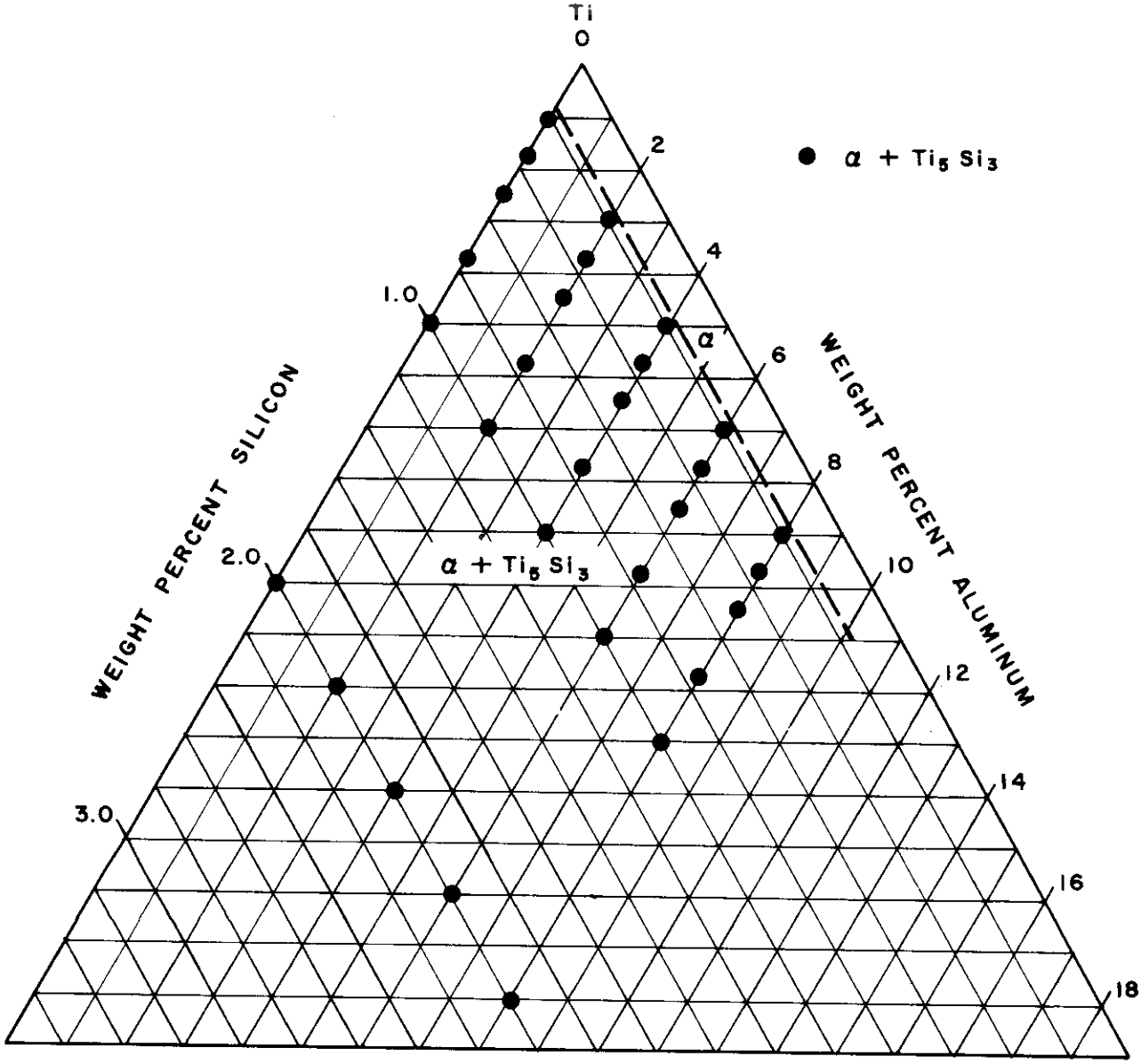

FIG. 42 — PARTIAL ISOTHERMAL SECTION AT 600° C OF THE Ti-Al-Si SYSTEM

In the partial isothermal section for 1000°C, Figure 39, the α field appears. The solubility of silicon in β at 1000°C is reduced to 0.9% at about 5% aluminum from 1.2% in the Ti-Si binary system. Due to the fact that aluminum extends the range of stability of α to higher temperatures it is possible to get more silicon into solution in the α phase of the ternary system than in the α of the binary system. For example, at 1000°C the maximum solubility of silicon in the α of the ternary system is about 0.75%. The maximum solubility of silicon in the α of the binary system occurs at the eutectoid temperature, 860°C, and is about 0.5% (18).

The partial isothermal section at 900°C, Figure 40, shows expansion of the α and α + Ti_5Si_3 phase fields at the expense of the β and β + Ti_5Si_3 fields when compared to the 1000°C isothermal section. The solubility of silicon in α and in β is between 0.5 and 0.75% over the range of aluminum contents studied. Hansen et al. give the solubility of silicon in titanium at this temperature as about 0.9% (18). The difference between these two values can probably be attributed to the fact that sponge titanium was used in the preparation of these alloys whereas iodide titanium was the basis of the work reported by Hansen.

In the partial isothermal sections at 800° and 600°C, Figures 41 and 42, only the α and α + Ti_5Si_3 fields remain. The solubilities of silicon in α at 800° and 600°C are slightly less than 0.5 and 0.2%, respectively.

Aluminum appears to have little, if any, effect upon the solubility of silicon in titanium.

Vertical sections at constant aluminum contents are presented in Figures 43 to 46.

Microstructures representative of those encountered in this investigation are shown in Figures 47 to 52. Figure 47 shows the large grained equiaxed α structure obtained in the 6% Al-0.75% Si alloy water quenched from 1000°C.

The α + Ti_5Si_3 structure shown in Figure 48 is for 8% Al-1.0% Si alloy water quenched from 900°C. The Ti_5Si_3 precipitate is concentrated at the grain boundaries.

Figure 49 shows the transformed β structure of the 6% Al-0.5% Si alloy water quenched from 1200°C.

An α + transformed β structure is presented in Figure 50. The 6% Al-0.5% Si alloy annealed at 1000°C shows transformed β at the grain boundaries of the large equiaxed α grains.

Figure 51, an example of an α + transformed β + Ti_5Si_3 structure, represents a 2% Al-0.75% Si specimen water quenched from 900°C. The fine precipitate at the α grain boundaries is Ti_5Si_3. Transformed β appears as platelets in the α grains and as globules at the grain corners.

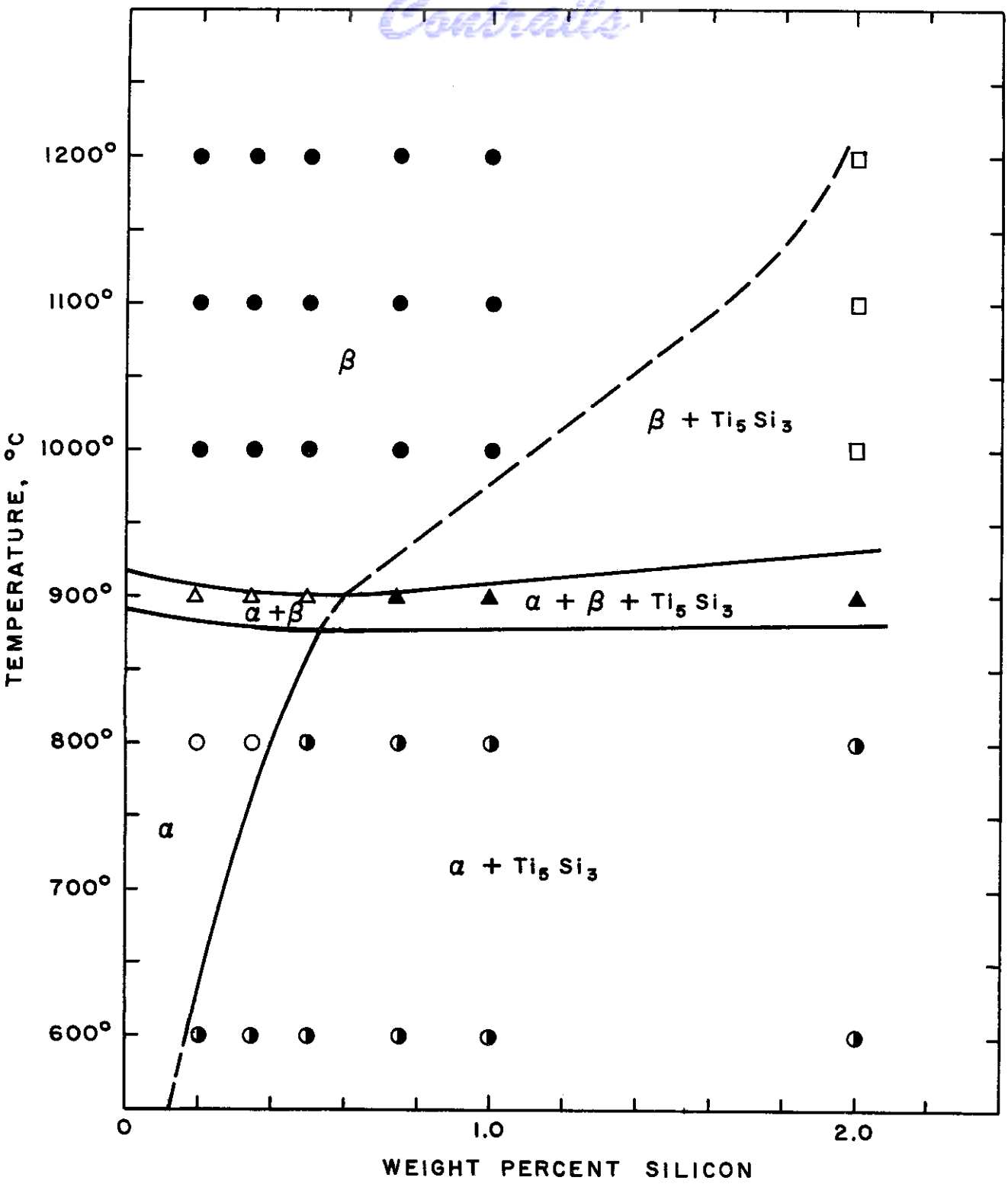

FIG.43 – PARTIAL VERTICAL SECTION AT 2 PERCENT ALUMINUM OF THE SYSTEM Ti-Al-Si.

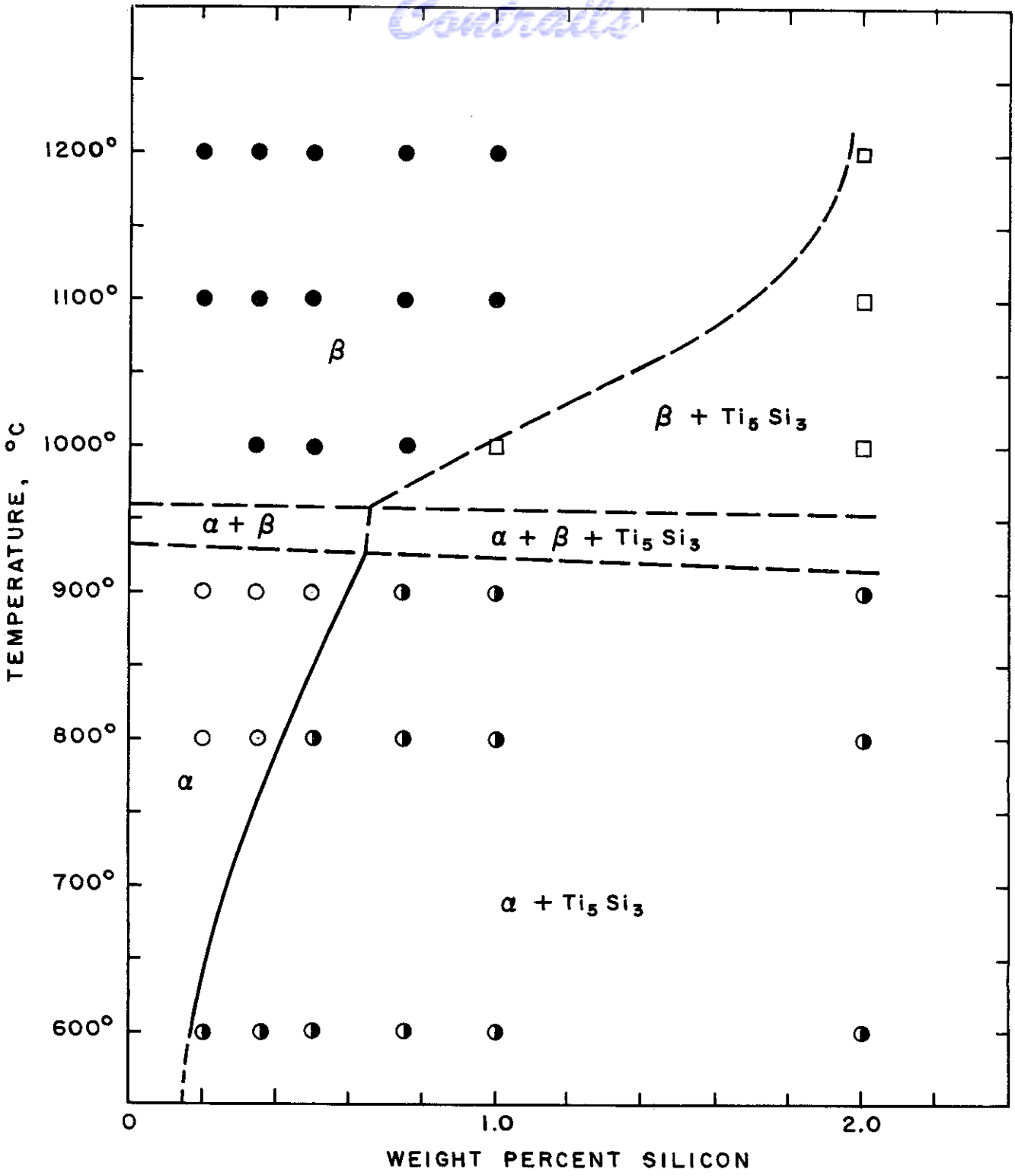

FIG.44-PARTIAL VERTICAL SECTION AT 4 PERCENT ALUMINUM OF THE SYSTEM Ti-Al-Si.

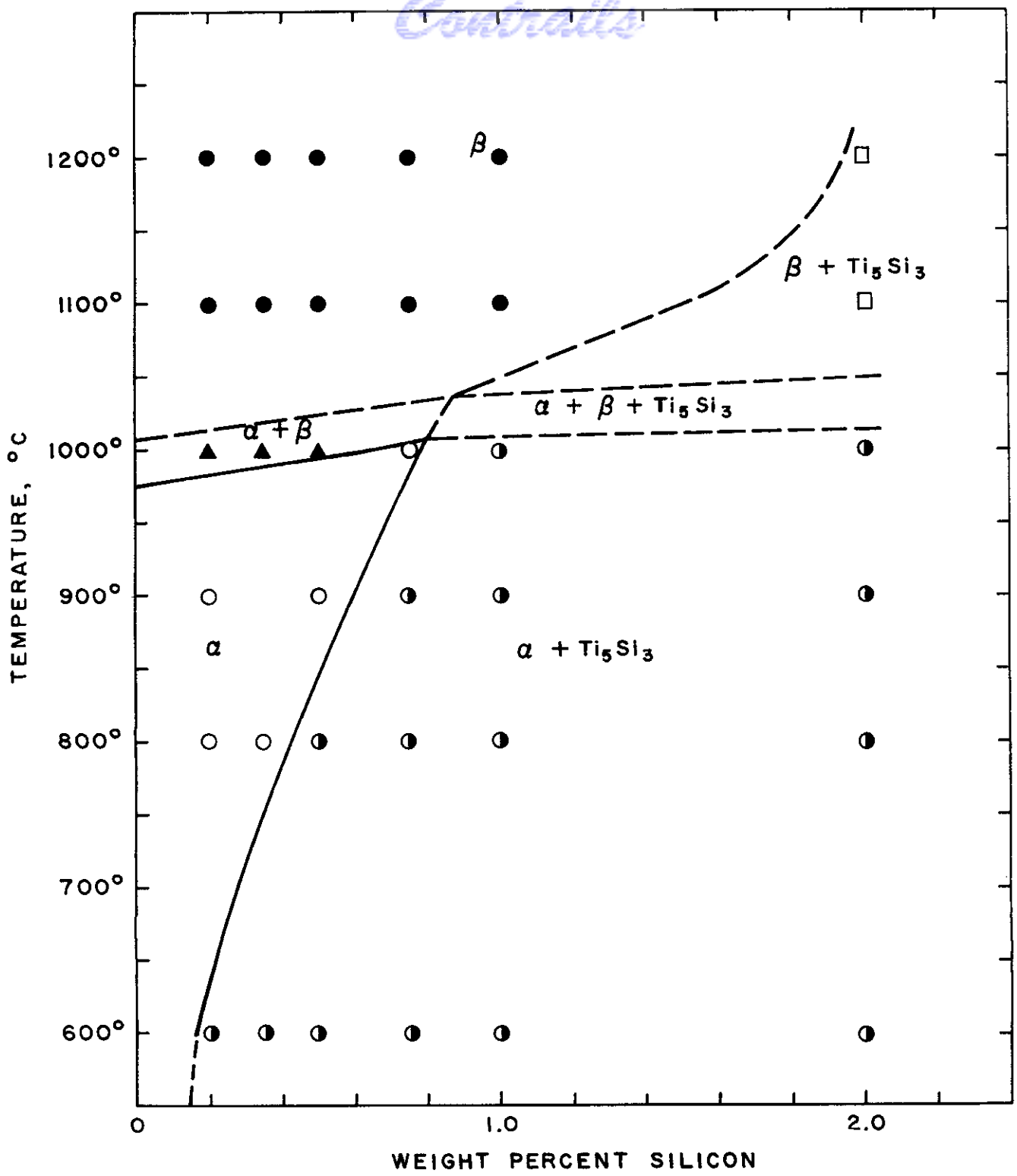

FIG.45 – PARTIAL VERTICAL SECTION AT 6 PERCENT ALUMINUM OF THE Ti-Al-Si SYSTEM.

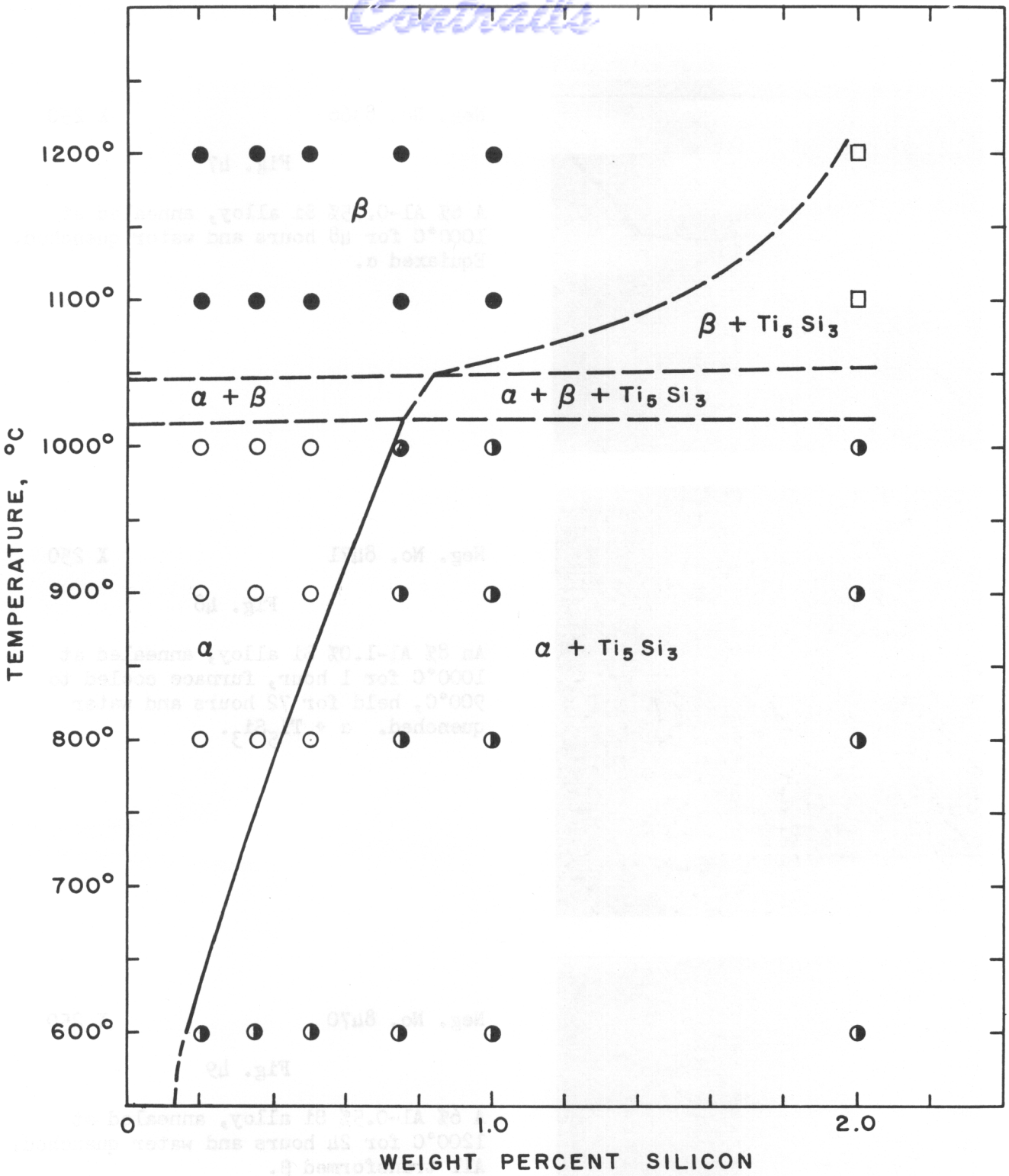

FIG.46 – PARTIAL VERTICAL SECTION AT 8 PERCENT ALUMINUM OF THE SYSTEM Ti-Al-Si.

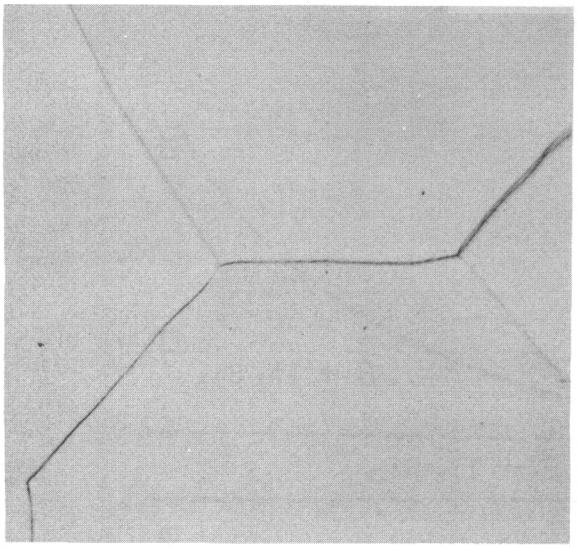

Neg. No. 8366 X 250

Fig. 47

A 6% Al-0.75% Si alloy, annealed at 1000°C for 48 hours and water quenched. Equiaxed α.

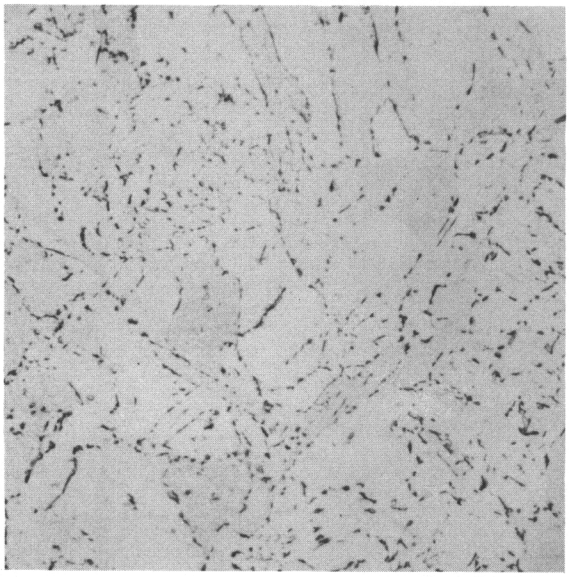

Neg. No. 8471 X 250

Fig. 48

An 8% Al-1.0% Si alloy, annealed at 1000°C for 1 hour, furnace cooled to 900°C, held for 72 hours and water quenched. $\alpha + Ti_5Si_3$.

Neg. No. 8470 X 250

Fig. 49

A 6% Al-0.5% Si alloy, annealed at 1200°C for 24 hours and water quenched. All transformed β.

Etchant: 60 cc glycerine, 20 cc HNO_3, 20 cc HF

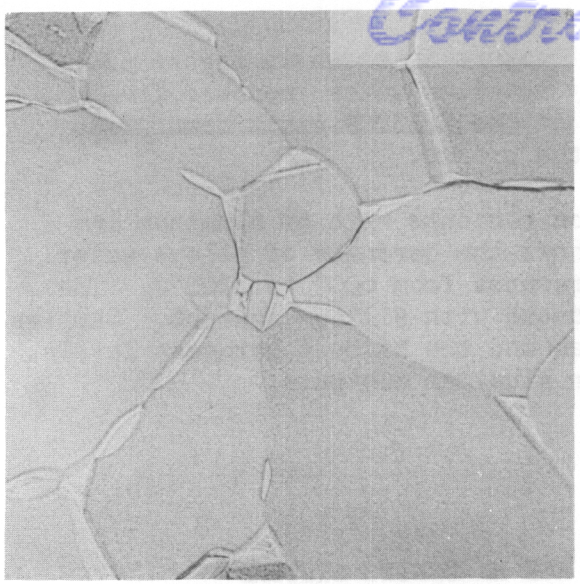

Neg. No. 8233 X 250

Fig. 50

A 6% Al-0.5% Si alloy, annealed at 1000°C for 48 hours and water quenched. $\alpha + \beta$. β at grain boundaries.

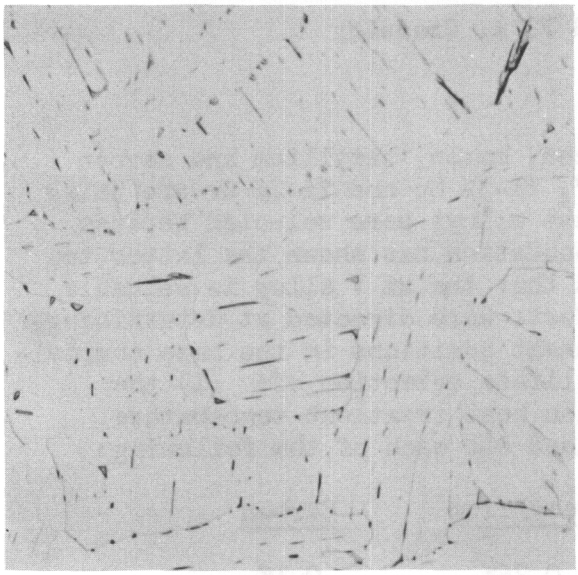

Neg. No. 8230 X 250

Fig. 51

A 2% Al-0.75% Si alloy, annealed at 1000°C for 1 hour, furnace cooled to 900°C, held for 72 hours and water quenched. $\alpha + \beta + Ti_5Si_3$.

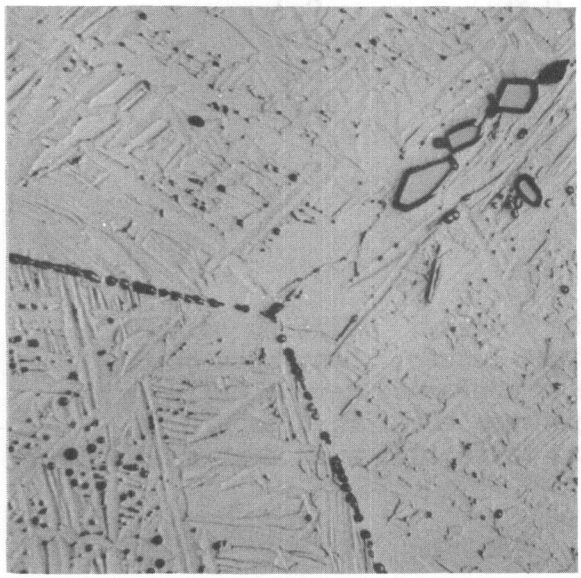

Neg. No. 8607 X 250

Fig. 52

A 2% Al-2% Si alloy, annealed at 1200°C for 24 hours and water quenched. Transformed $\beta + Ti_5Si_3$.

Etchant: 60 cc glycerine, 20 cc HNO_3, 20 cc HF

A transformed β + Ti_5Si_3 microstructure is shown in Figure 52 which represents a 2% Al-2.0% Si alloy specimen water quenched from 1200°C. The Ti_5Si_3 appears primarily at the prior β grain boundaries along with some precipitation within the grains.

Hardness data for varying silicon contents with 6% aluminum are presented in Figure 53. The figure shows the hardness of alloys water quenched from various annealing temperatures from 600° to 1200°C. The curves show a gradual increase in hardness with silicon content. Samples water quenched from 1100° and 1200°C showed the highest hardness levels. Similar results were obtained at other aluminum contents.

VII. STUDY OF POSSIBLE AGE HARDENING SYSTEMS

by J. J. Rausch and F. A. Crossley

A. Introduction

Age hardening systems with silicon, boron, beryllium and carbon added to the base compositions Ti-4% V, Ti-3% Mo and Ti-2% Cr are being studied. The 4% V, 3% Mo and 2% Cr base alloys were selected because current research at Armour Research Foundation has shown the latter two to be weldable (10) and it was assumed that the 4% V alloy is weldable by analogy. During the past year, efforts were directed at determining the solubility limits of the third element additions in the base compositions. This was done in order to facilitate selection of: (1) the amount of addition, and (2) the solution heat treatment temperature. The third element additions have included one each of the following:

Silicon	Boron	Beryllium	Carbon
0.10%	0.020%	0.25%	0.1%
0.20	0.035	0.50	0.2
0.30	0.050	0.75	0.3
0.40	0.100	1.00	0.4
0.50		1.50	0.5
0.75		2.00	0.75
1.00			
1.50			
2.00			

B. Experimental Procedure

The alloys were melted as 100-gram charges. Weighing before and after melting showed no appreciable weight losses. Many spot checks were made by wet chemical analysis; these conformed very closely to the nominal compositions. All of the alloys were hot forged to 3/8 in. diameter rods. Specimens sectioned from these rods were sealed in Vycor

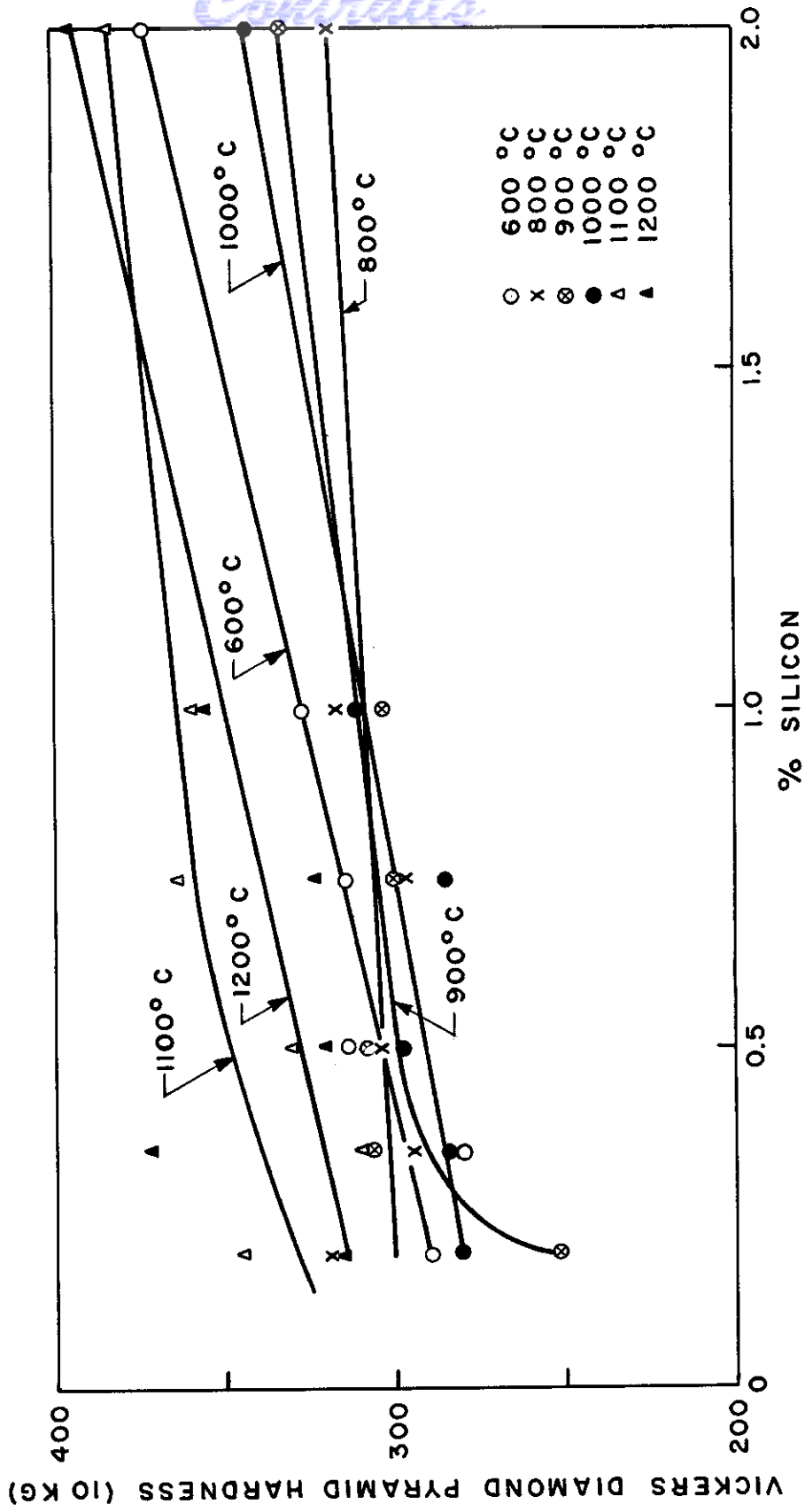

FIG. 53 – WATER QUENCHED HARDNESS OF Ti-Al-Si ALLOYS WITH 6% ALUMINUM

bulbs for heat treatment with the exception of those annealed at 1200°C, which were sealed in quartz bulbs. Annealing times and temperatures were as follows:

Annealing Temperature, °C	Annealing Time
1200	24 hours
1050	48 hours
1000	48 hours
950	72 hours
900	96 hours
850	120 hours
800	168 hours
700	288 hours
600	507 hours

C. Results and Discussion

The systems containing carbon were not completed and will be reported later. Nine partial vertical sections were made, corresponding to the other three compound-forming alloy additions to each of the three base compositions. These are shown in Figures 54-56, 58-60, 64 and 68-69. Metallographic examination was used exclusively in determining these phase boundaries. In all of the systems there is some question concerning the microstructures at 600°C. The annealing time at this temperature might not have been of sufficient duration for equilibration. The phase relationships reported are correct on the basis of microscopic evidence but are subject to this condition. In the alloys in which a eutectoid decomposition occurs between 600° and 700°C, an arbitrary temperature of 650°C was selected to separate the phase fields. In some cases the temperature at which the $\alpha/\alpha + \beta$ (or α + compound/$\alpha + \beta$ + compound) transformation occurred was placed arbitrarily at the transformation temperature of the binary alloy systems. This was done in the systems containing boron and silicon. No attempt was made to determine the phase boundaries more precisely, since such precision was unnecessary to our limited objectives.

The three systems Ti-2% Cr-B, Ti-3% Mo-B and Ti-4% V-B, in the region from 0.02 to 0.1% B and from 600° to 1200°C, are shown in Figures 54 to 56. The partial diagrams are very similar. At all temperatures between 600° and 1200°C the boron solubility appears to be less than 0.02%. Solubility limits are not indicated for it was felt that the data obtained is not sufficient to warrant this. The microstructures of the alloys containing 0.02% boron did not indicate that these alloys were close to the solubility limits. A photomicrograph showing evidence of TiB in the Ti-2% Cr-0.02% B alloy at 600°C is shown in Figure 57.

Figures 58 to 60 show partial vertical sections of the systems Ti-2% Cr-Be, Ti-3% Mo-Be and Ti-4% V-Be in the region from 0.25 to 2% beryllium and from 600° to 1200°C. At temperatures of 700°C and above the solubility of beryllium in all of the alloys was greater than 2%, the limit of the composition range studied. In all of the systems

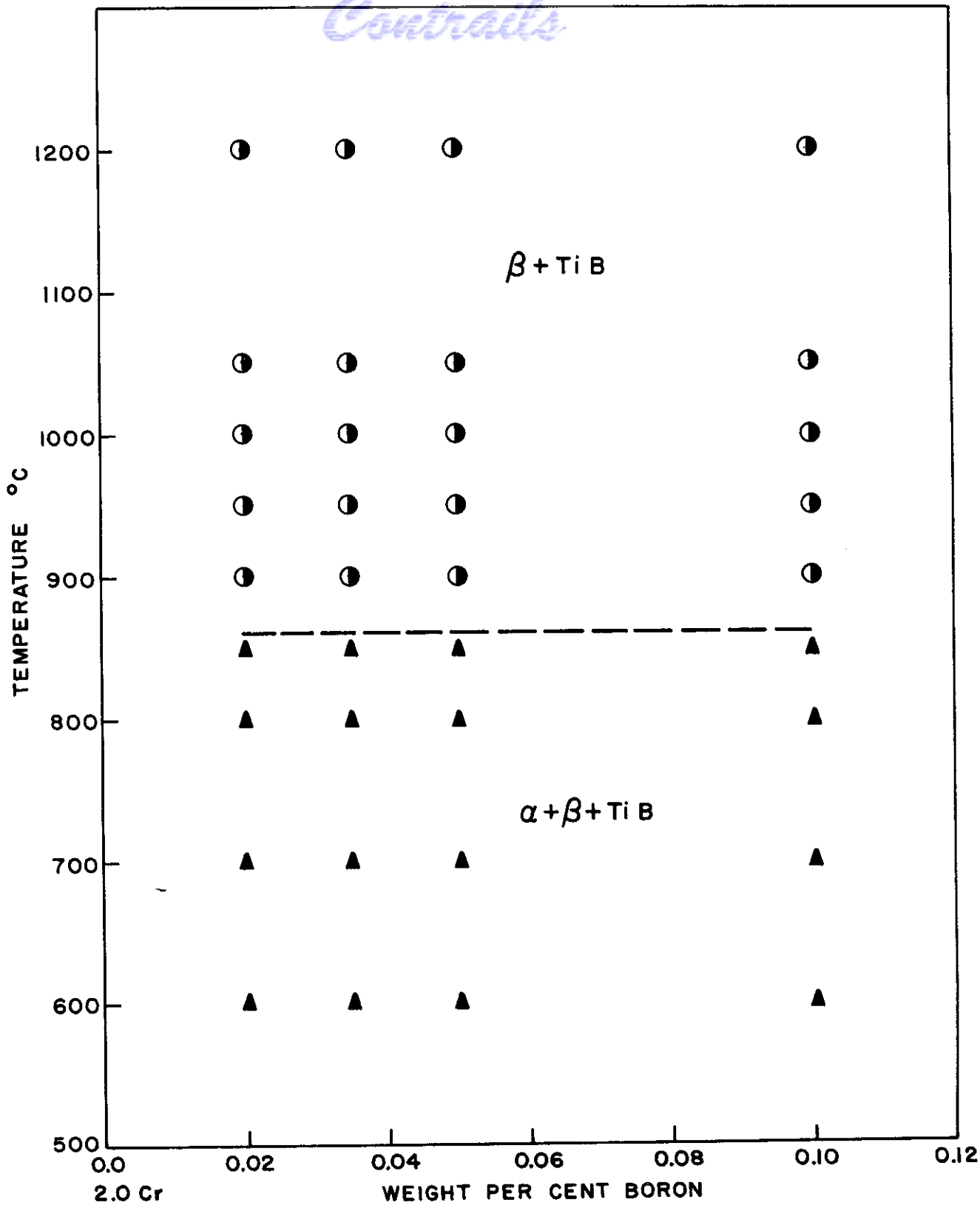

FIG. 54 - PARTIAL VERTICAL SECTION AT 2 PER CENT CHROMIUM OF THE SYSTEM Ti - Cr - B

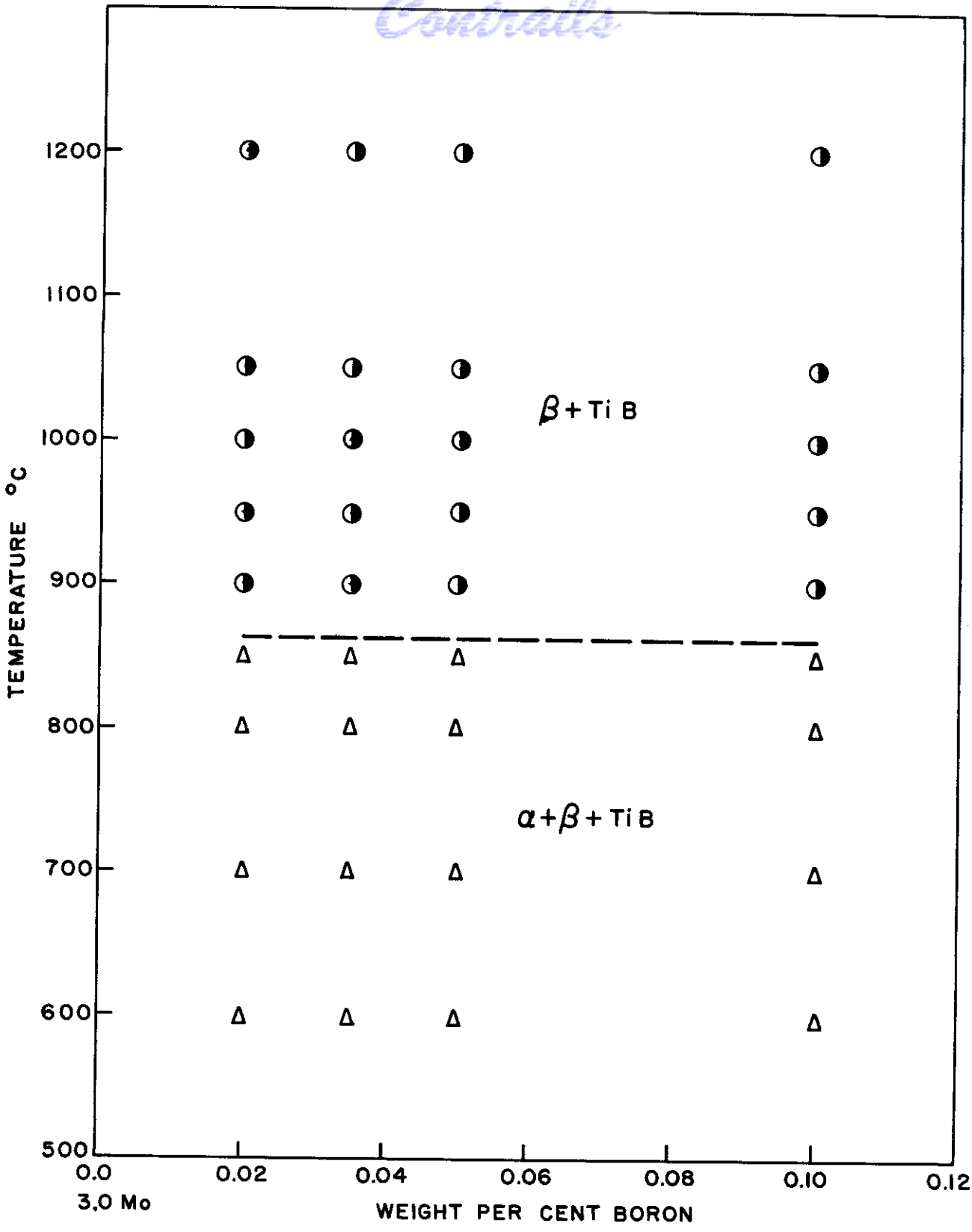

FIG. 55 - PARTIAL VERTICAL SECTION AT 3 PER CENT MOLYBDENUM OF THE SYSTEM Ti - Mo - B

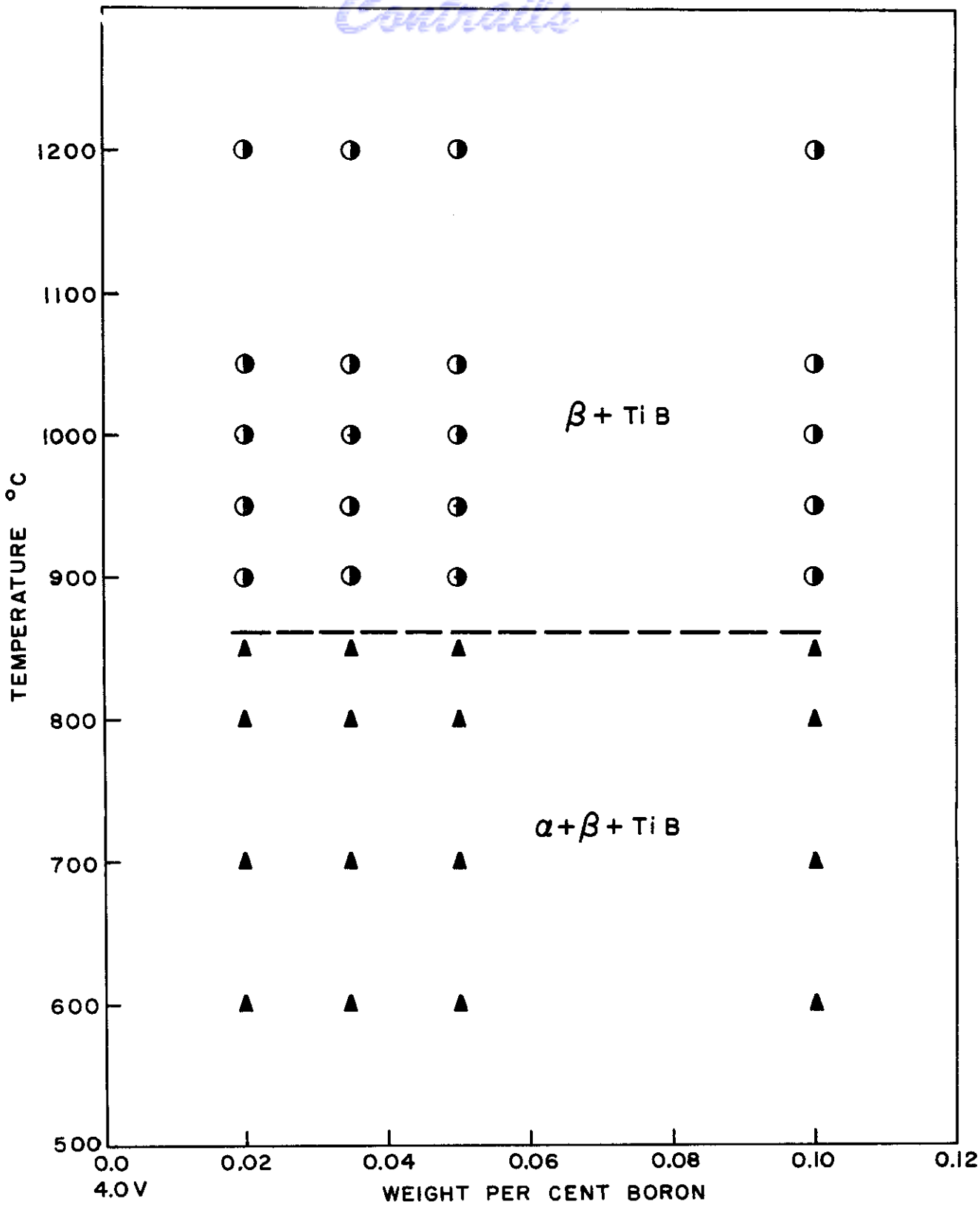

FIG. 56 - PARTIAL VERTICAL SECTION AT 4 PER CENT VANADIUM OF THE SYSTEM Ti - V - B

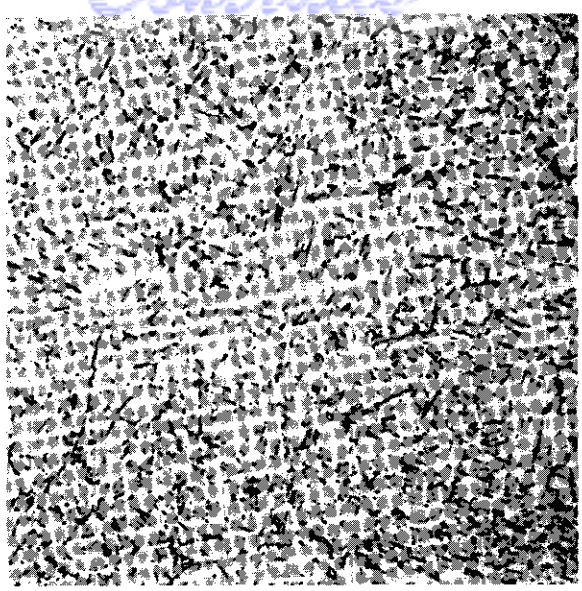

Neg. No. 8582 X 750

Fig. 57

A 2% Cr-0.02% B alloy, annealed at 600°C for 507 hours and water quenched. $\alpha + \beta + TiB$.

Etchant: 60 cc glycerine, 20 cc HNO_3, 20 cc HF

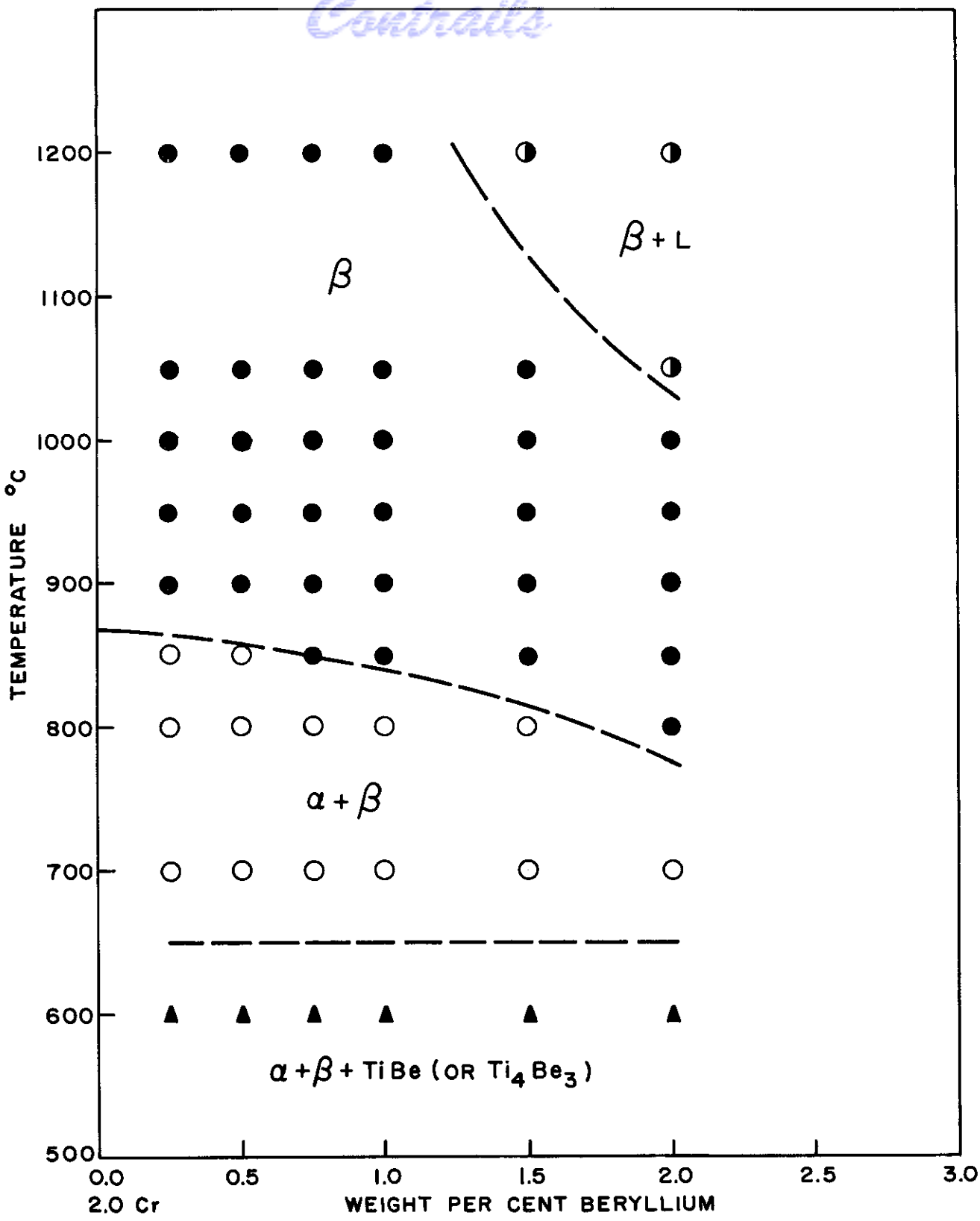

FIG. 58- PARTIAL VERTICAL SECTION AT 2 PER CENT CHROMIUM OF THE SYSTEM Ti-Cr-Be

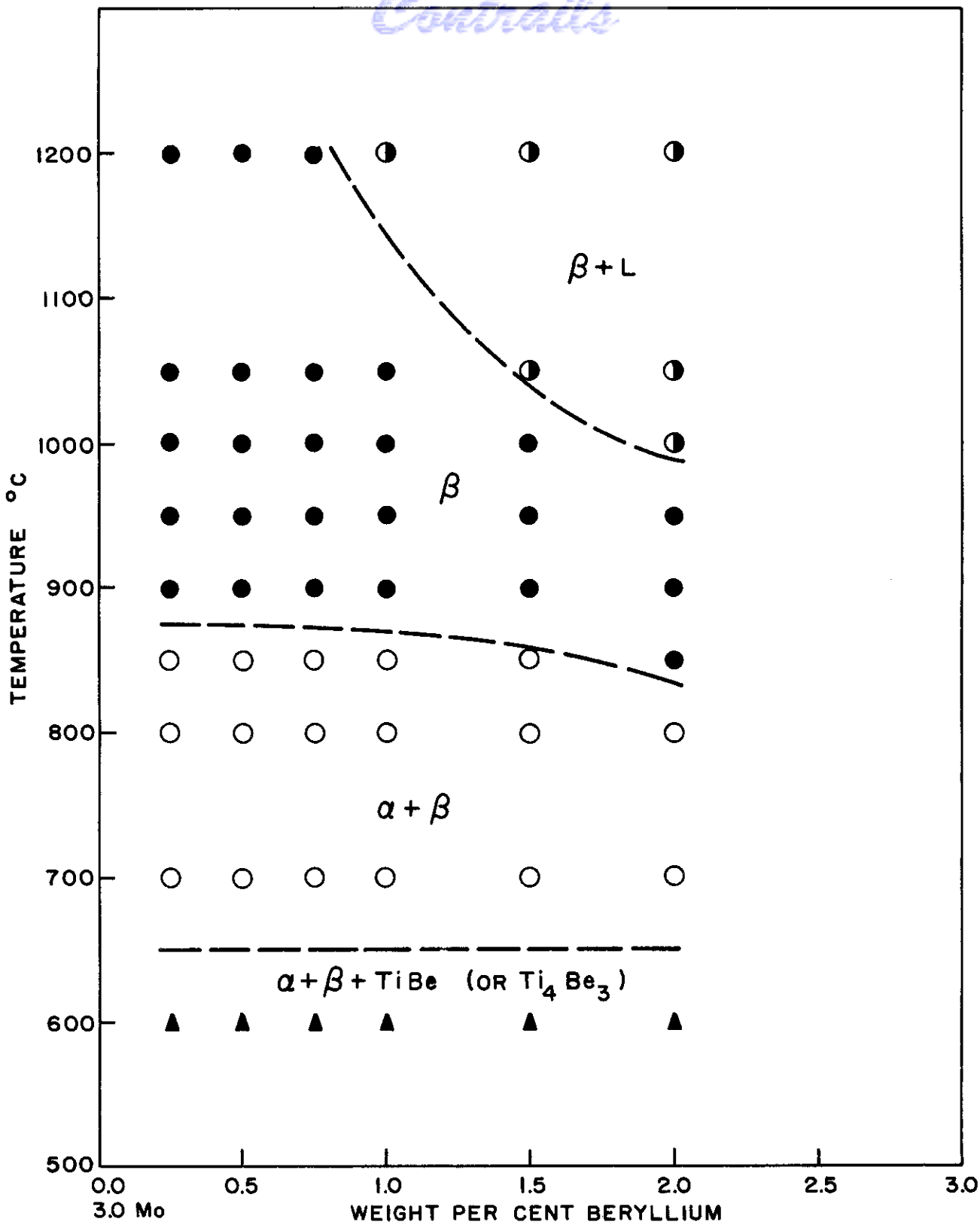

FIG. 59 - PARTIAL VERTICAL SECTION AT 3 PER CENT MOLYBDENUM OF THE SYSTEM Ti - Mo - Be

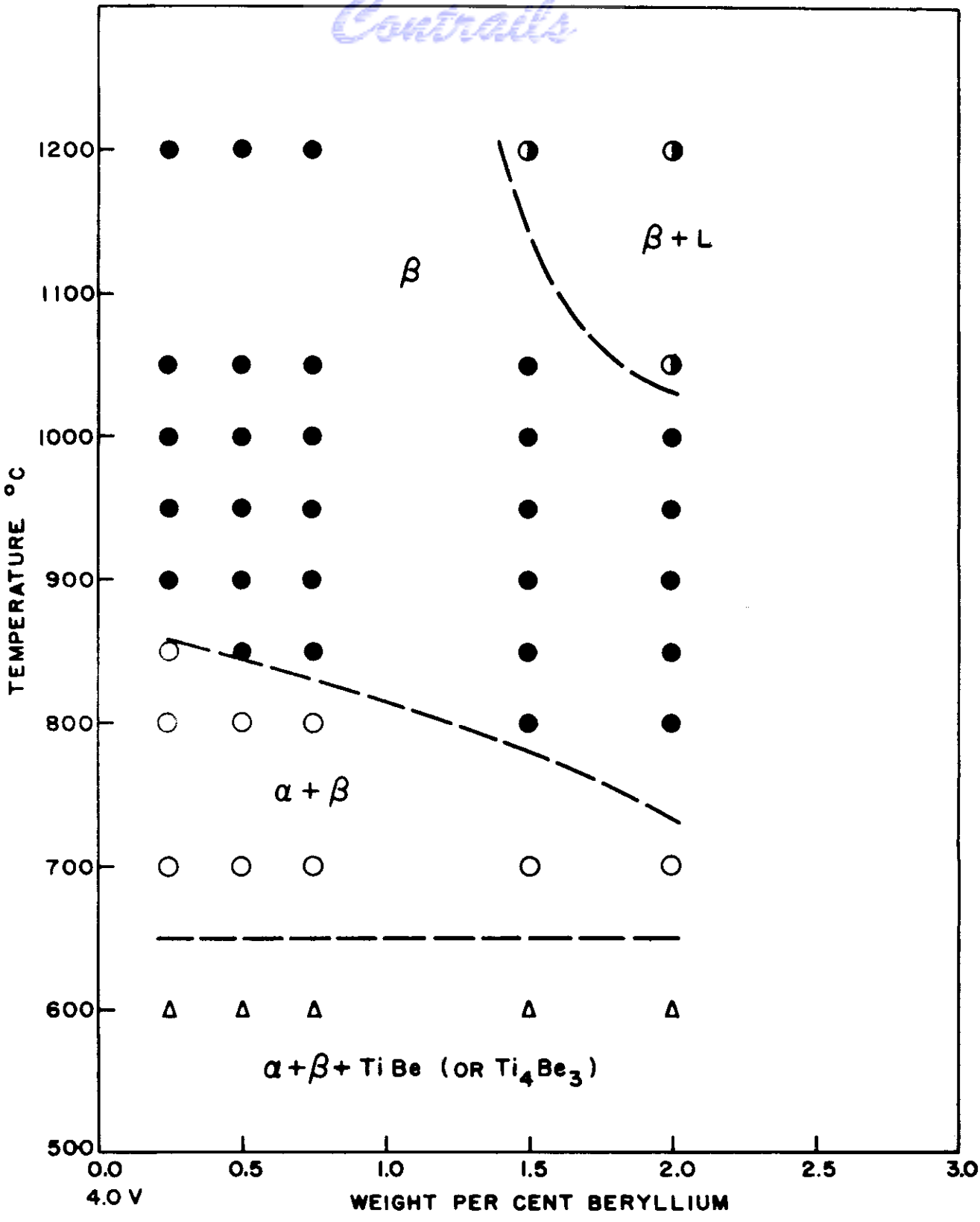

FIG. 60 - PARTIAL VERTICAL SECTION AT 4 PER CENT VANADIUM OF THE SYSTEM Ti - V - Be

containing beryllium there was evidence of a eutectoid decomposition of the β phase to α + TiBe (or Ti_4Be_3) occurring somewhere between 600° and 700°C. At 600°C the solubility of beryllium appeared to be less than 0.25%. Beryllium has a pronounced effect of lowering the solidus of the systems studied as can be seen from the vertical sections. The most severe depression of melting temperature was observed in a sample of Ti-3% Mo-2% Be. This sample showed evidence of melting at 1000°C. These results show that forging temperatures should be selected with great care for alloys containing beryllium in the vicinity of 1-2%. In this work, initial attempts to forge alloys containing 0.75 and 1% beryllium at 950°C resulted in break-up of the ingots. However, these alloys, and alloys containing 2% beryllium, were successfully forged at 870°C. Photomicrographs showing the extensive solubility of beryllium at temperatures of 700°C and above, the eutectoid decomposition product, and the effect of beryllium on the solidus are shown in Figures 61, 62 and 63, respectively.

In the Ti-2% Cr-Be and Ti-2% Cr-B systems no microscopic evidence of $TiCr_2$ could be found. The phase formed in the eutectoid reaction occurring in the Ti-Cr-Be alloys studied is believed not to be $TiCr_2$ since the same phase was found in the microstructures of the alloys containing molybdenum and vanadium.

The systems Ti-2% Cr-Si, Ti-3% Mo-Si and Ti-4% V-Si in the region from 0.1 to 1.5% silicon for the Ti-2% Cr-Si system and from 0.1 to 2% silicon for the other two and from 600° to 1200°C are shown in Figures 64, 68 and 69. In the Ti-2% Cr-Si system, the solubility of silicon in β increases sharply with increasing temperature. However, this system shows the least solubility of silicon at temperatures below 900°C. At 1050°C silicon dissolves in β to the extent of approximately 1.1%. The solubility decreases to a value between 0.1 and 0.2% at 900°C and below. Eutectoid decomposition of β to α + $TiCr_2$ + Ti_5Si_3 occurs between 700° and 600°C. Photomicrographs showing the extensive solubility of silicon in β at 1050°C, evidence of the slight solubility at 850°C, and the eutectoid decomposition product found at 600°C in the Ti-2% Cr-Si system are shown in Figures 65, 66 and 67, respectively.

In the Ti-3% Mo-Si system little change in silicon solubility with temperature was found. The solubility limit of silicon in the alloy is between 0.2 and 0.3% at all temperatures between 600° and 1050°C.

The lowest solubility of silicon in the Ti-4% V base composition is shown at approximately 825°C. The solubility increases with both increasing and decreasing temperature. The α + β/α + β + Ti_5Si_3 boundary changes from approximately 0.3% silicon at 840°C to about 0.45% silicon at 600°C.

During the next research year, the aging characteristics of the systems Ti-4% V-B, Ti-4% V-Be, Ti-4% V-C and Ti-4% V-Si will be studied. If these systems show promise and if the Ti-2% Cr and Ti-3% Mo are shown to be stable with respect to retention of room temperature ductility

Neg. No. 8584 X 750

Fig. 61

A 3% Mo-2% Be alloy, annealed at 700°C for 288 hours and water quenched. $\alpha + \beta$, beryllium in solution.

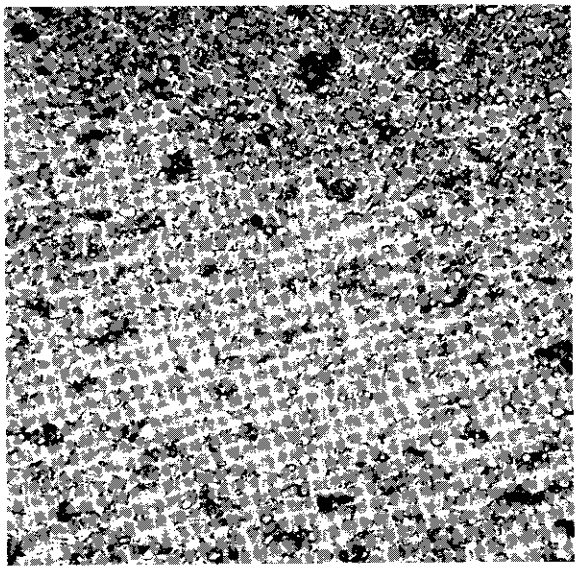

Neg. No. 8606 X 750

Fig. 62

A 3% Mo-1.5% Be alloy, annealed at 600°C for 507 hours and water quenched. $\alpha + \beta$ + TiBe (or Ti_3Be_4).

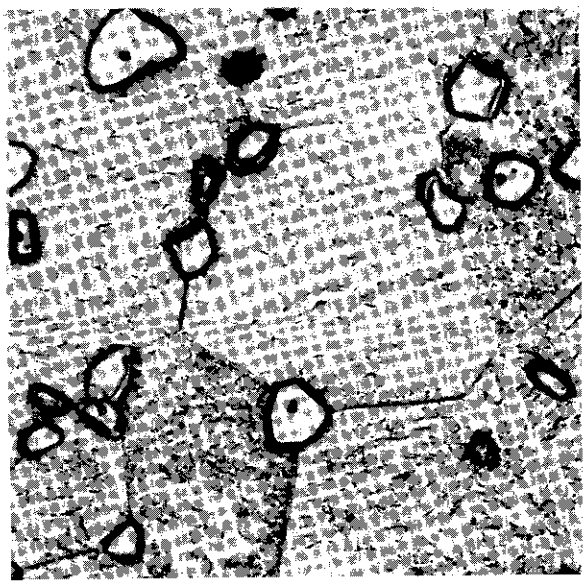

Neg. No. 8583 X 750

Fig. 63

A 3% Mo-2% Be alloy, annealed at 1000°C for 48 hours and water quenched. Light etching areas show melting. Transformed β matrix.

Etchant: 60 cc glycerine, 20 cc HNO_3, 20 cc HF

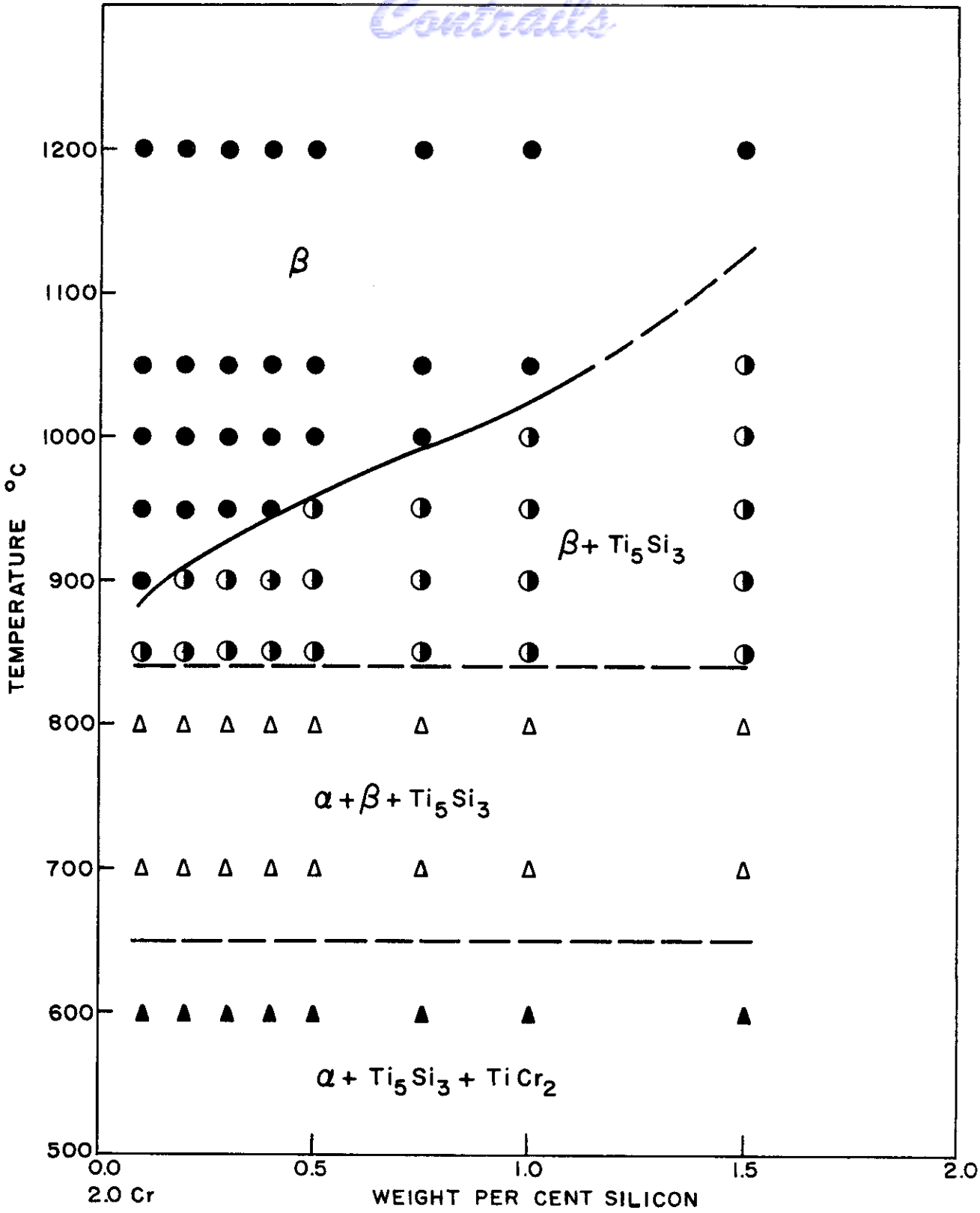

FIG. 64 - PARTIAL VERTICAL SECTION AT 2 PER CENT CHROMIUM OF THE SYSTEM Ti - Cr - Si

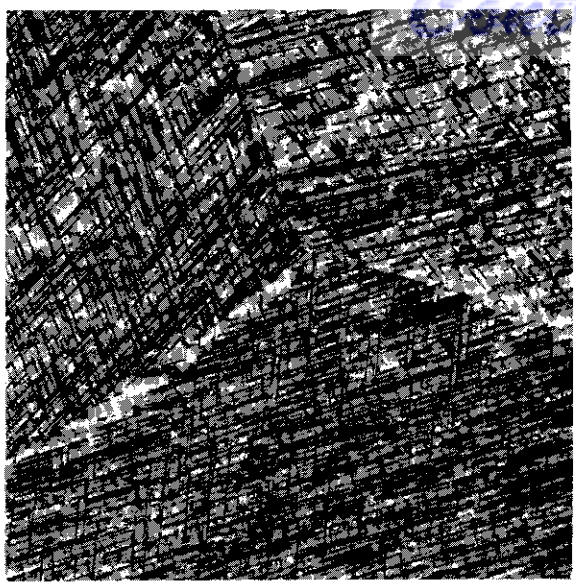

Neg. No. 8586 X 750

Fig. 65

A 2% Cr-1% Si alloy, annealed at 1050°C for 48 hours and water quenched. Transformed β, silicon in solution.

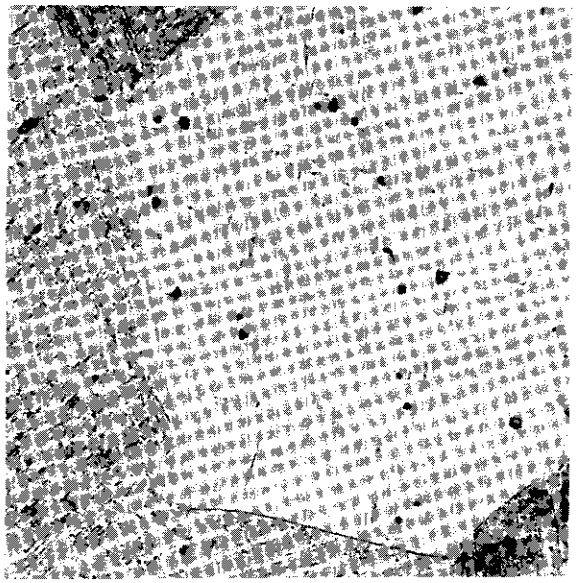

Neg. No. 8598 X 750

Fig. 66

A 2% Cr-0.1% Si alloy, annealed at 850°C for 120 hours and water quenched. Transformed β + Ti_5Si_3.

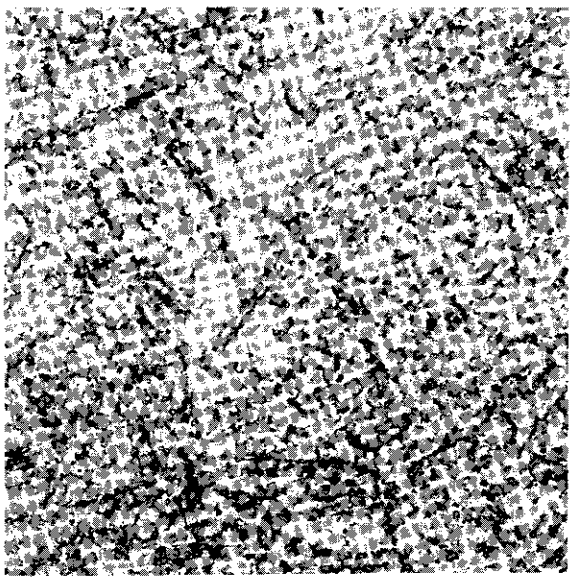

Neg. No. 8588 X 750

Fig. 67

A 2% Cr-0.5% Si alloy, annealed at 600°C for 507 hours and water quenched. α + Ti_5Si_3 + $TiCr_2$.

Etchant: 60 cc glycerine, 20 cc HNO_3, 20 cc HF

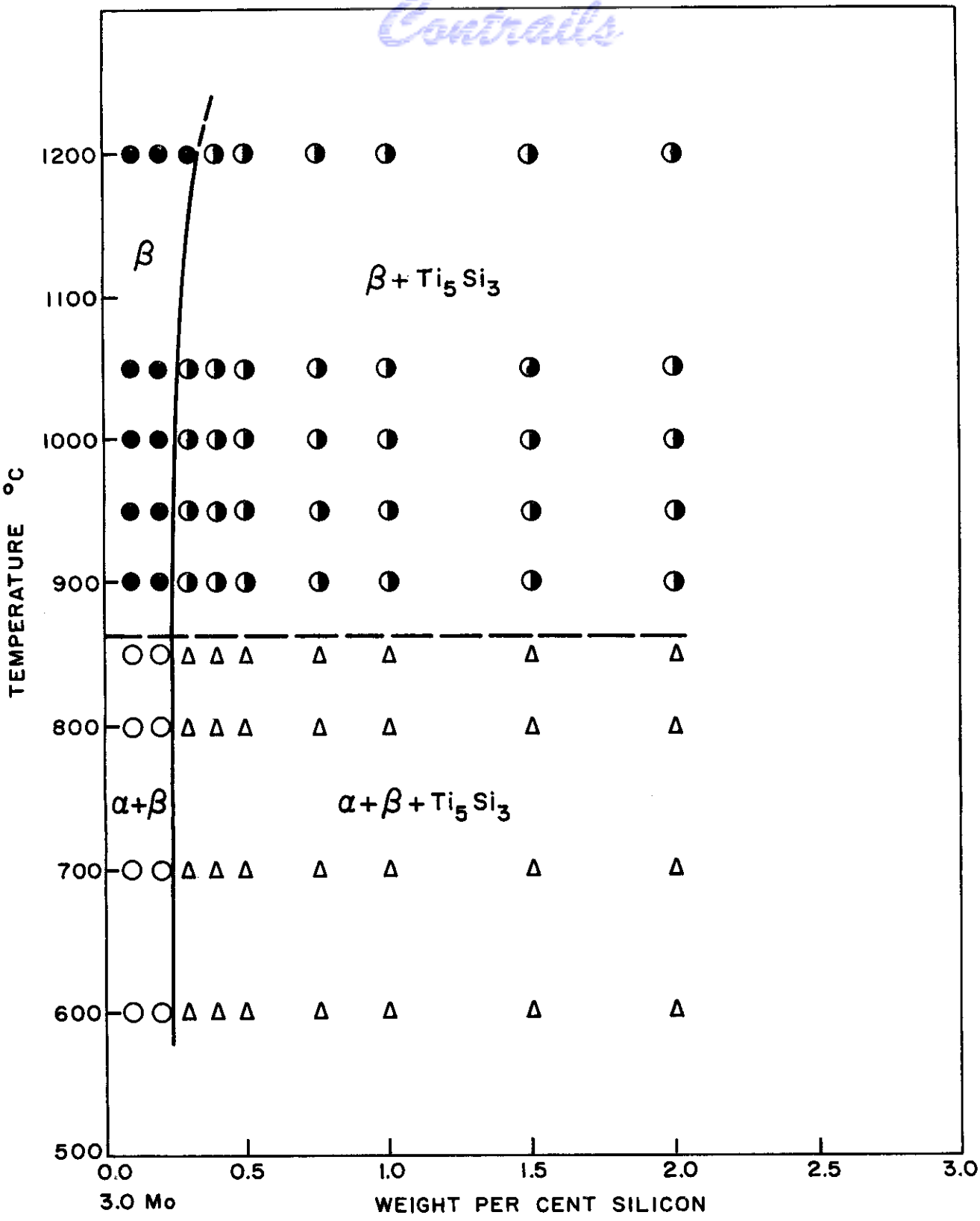

FIG. 68 - PARTIAL VERTICAL SECTION AT 3 PER CENT MOLYBDENUM OF THE SYSTEM Ti - Mo - Si

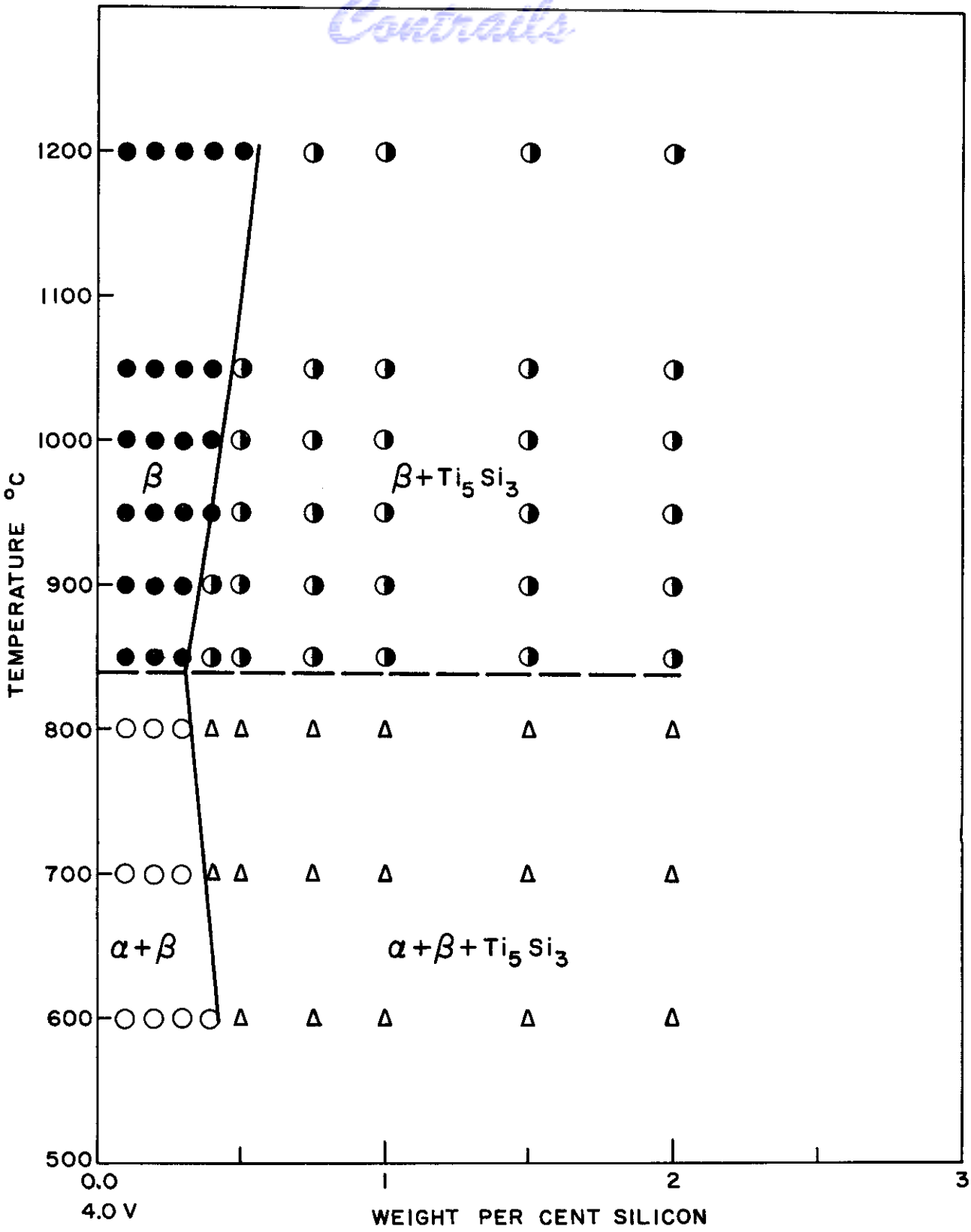

FIG. 69 – PARTIAL VERTICAL SECTION AT 4 PER CENT VANADIUM OF THE SYSTEM Ti – V – Si

upon exposure to creep test conditions, the work will be extended to Ti-2% Cr-B, Be, C, Si and Ti-3% Mo-B, Be, C, Si.

Phase diagram studies of the Ti-Ag system have shown the solubility of silver in α to decrease from about 9% at 850°C to 5% at lower temperatures (20). In the interest of developing age hardening alloys, it was considered worthwhile to investigate an alloy with silver plus aluminum additions. The alloy Ti-5% Al-5% Ag was selected. Work was carried out to determine the proper solution treatment temperature. However, when results of chemical analyses on the alloy became available, it was discovered that the ingot was off composition.

Two additional 100-gram ingots were made which analyzed as follows: (1) 5.5% Al, 2.1% Ag and (2) 4.7% Al, 7.1% Ag. The amount of silver lost due to volatilization is indicated from the nominal compositions of these alloys which were (1) 5% Al-5% Ag and (2) 5% Al-10% Ag, respectively. The ingots were forged to 3/8 in. diameter and were cut into 1/4 in. specimens. One sample of each alloy was annealed at 850°C for 24 hours and water quenched. Both alloys were completely in the α field. Aging studies of the alloys will be made during the next contract period.

VIII. THE FORMATION OF THE α' PHASE

by R. P. Elliott and W. Rostoker

A. Introduction

In severe quenching from elevated temperatures, it is known that β transforms to an acicular product called α'. X-ray diffraction studies have shown this phase to be structurally the same as the α modification of titanium, i.e., hexagonal close packed. The breadth of diffraction lines encountered indicate either a severe stress gradient in the individual particles of the phase, or a very small plate thickness causing the well-known "particle broadening" effect. The fact that the α' formation cannot be suppressed, and the characteristic metallographic appearance of the phase have led to a general assumption that a martensitic type of transformation is responsible.

The α' phase is encountered very frequently in the heat treated structures of lower alloy content. Actually, most of the present commercial alloys show α' as a quench product. There has been no general appreciation of the specific contribution of the phase to mechanical properties. Furthermore, since no method has been developed for estimating the relative proportions of α' and β, it has not been possible to know in what manner the relative proportions of α' and β can be varied in controlled fashion.

The initial objective of this phase of the work was to study the variables by which the formation of α' could be promoted or inhibited. A necessary prerequisite to these objectives was the development of a means of estimating the relative proportions of α' and β. Similar problems of estimating relative proportions of austenite and martensite in ferrous alloys had been handled by at least three techniques:

a. Lineal analysis of microstructures.

b. Measurement of ferromagnetic saturation flux density.

c. Evaluation of comparative intensities of x-ray diffraction lines.

Since titanium alloys are not ferromagnetic in either allotropic modification and since it is not possible to differentiate metallographically between the phases when they are present in appreciable quantities, methods (a) and (b) are not practical. Of several possible methods (21,22) of using x-ray diffraction techniques to determine proportions of phase mixtures, the integrated intensity method as outlined by Averbach and Cohen (23) seemed the most practical.

Previous work on the crystallographic studies of the α' phase in titanium alloys have been made using powder diffraction techniques. Although such patterns are usually easy to interpret, the most that can be said for such a pattern is that it is representative of a powder that has had the prescribed heat treatment. The question always remains whether the transformation characteristics of powder are identical with the bulk solid and whether the quench effectiveness was comparable to that obtained in a bulk solid. To avoid such uncertainties it was decided that all diffraction work would be done on solid specimens. Thus, the observed data is characteristic of large pieces of material. Such an analysis can be done with a focussing camera or a Geiger counter spectrometer. In both cases there is trouble with the usual coarse grain size of the sample producing spotty or discontinuous Debye rings.

B. Experimental Procedure

Initial work was carried out on titanium alloys containing additions of molybdenum and chromium. These alloys were solution treated and quenched in cold water. Geiger counter spectrometer patterns showed in no case a mixture of the retained body centered cubic β phase with the hexagonal close packed α' phase. Filings heat treated similarly in Vycor tubes showed that only a very slight amount of β was retained.

In the α' pattern, the most predominant lines were 10.1, 00.2, and 10.1. In the β pattern the most predominant line was 110. The other lines in both diffraction patterns were very broad and often not possible to be distinguished from the background. In the transformation from the β to α or α' structure the 110 plane of β is almost equivalent to the 00.2 of α. As a consequence, spectrometer patterns of a mixture of β and α' have their intense lines at the same range of Bragg angles.

It is therefore impossible to evaluate the relative intensity of a mixture of α and β. Had it been possible to develop structures of β and α', it would not have been possible to determine the relative volumes of the phases by the integrated intensity method because the only strong lines of these phases occur at the same Bragg angle.

During the preliminary investigation of the titanium-molybdenum alloys, it was found that certain compositions of the titanium-molybdenum alloys exhibited extra diffraction lines. These lines could not be indexed as β. It was found that these extra lines could be indexed as a second hexagonal close packed structure. The scope of the investigation thus was changed from a study of the integrated intensity method to a study of the quench products of binary titanium alloys. Such a discovery can be correlated with previous knowledge. Work at New York University (24) has shown that in titanium-molybdenum alloys there exist two martensite habit planes, $\{334\}_\beta$ and $\{344\}_\beta$. Martensite formed by deformation was shown to have the habit plane $\{344\}_\beta$. It is entirely plausible that instead of two habit planes, as New York University hypothesizes, that there are two martensites with different habit planes.

Because solid metal specimens are usually coarse grained, diffraction patterns from such specimens are inherently spotty. Thus, spectrometer patterns of such a specimen can give faulty readings. To remedy this situation as much as possible, a spectrometer specimen spinner was purchased as an attachment for the spectrometer. This device served a two-fold purpose. First, it rotated the specimen in the plane of incident x-radiation and thus assisted appreciably in getting quantitative readings of intensities. Second, by the design of this attachment it was possible to place the specimen in the spinner in a reproducible manner. This afforded a better degree of certainty in the calculation of lattice parameters and axial ratios. This matter will be further discussed in a subsequent section. The specimen for this spinner is 1 in. in diameter and 1/8 in. thick.

C. The Quench Products of Ti-Mo, Ti-Cr and Ti-Mn

In view of the discovery of dual martensites in certain of the Ti-Mo alloys, a program was laid out for the investigation of this phenomena in the binary systems Ti-Cr, Ti-Mn and Ti-Mo. Alloys were prepared from commercial sponge titanium and master alloys of the alloy additions. The ingot weight was 150 grams. Alloys were melted in a non-consumable electrode, arc furnace with a water cooled copper crucible. After melting, the ingots were hot forged at temperatures between 1800° and 2000°F into rods 1-1/8 in. in diameter. These rods were then machined into the specimen discs for the spectrometer specimen spinner. Pieces of the machined ingots were then chemically analyzed. Nominal and analyzed compositions of the alloys are shown in Table VI.

TABLE VI

ANALYSIS OF ALLOYS MELTED

Alloy	Analysis	Alloy	Analysis	Alloy	Analysis
3% Mo	3.20	3% Cr	2.93	3% Mn	2.98 to 3.29
5% Mo	5.28	5% Cr	4.94	5% Mn	5.33 to 5.47
7% Mo	7.21	7% Cr	7.06	7% Mn	7.58 to 8.04
9% Mo	9.52	9% Cr	9.02	9% Mn	9.9 to 10.3
11% Mo	11.32	11% Cr	11.0	11% Mn	11.89 to 12.09
13% Mo	12.68	13% Cr	12.9	13% Mn	13.0 to 13.20

Specimens were sealed in evacuated Vycor bulbs and given a solution treatment of 1/2 hour at 1000°C. One sample of each composition was quenched to cold water. At the instant of quenching, the Vycor bulb was broken. An additional sample of each composition was quenched to cold water and then transferred immediately to liquid nitrogen. Such a step quenching has been found to give a more rapid quench than quenching directly to liquid nitrogen. The samples were then ready for the spectrographic examination.

Spectrometer patterns were made on a Norelco Geiger counter spectrometer using the spectrometer specimen spinner previously described. Nickel-filtered copper radiation was used throughout, with a chart speed of 1/2 degree of 2 θ per minute and divergence slits of 1 degree. Various settings of the recording conditions were used to get the most desirable deflection on the chart. The pattern in all cases was scanned from 30 degrees to 75 degrees of 2 θ (15 degrees to 37.5 degrees θ).

Following the reasoning of New York University, attempts were made to develop the martensite structure by cold work. To do this, it was decided to quench spinner samples into cold water and then to cold work the specimens by sand blasting. In this way the specimen is not distorted and may be used directly in the spectrometer.

D. Experimental Data

1. Titanium-Molybdenum Alloys

Titanium-molybdenum alloys containing 3 and 5% molybdenum showed by x-ray to be single-phase structurally composed of a hexagonal close packed structure of α'. The 7 and 9% molybdenum alloys showed a duplex structure consisting of two hexagonal close packed structures. The 9% molybdenum alloy showed trace amounts of retained β. Alloys containing 11 and 13% molybdenum were completely retained β, body-centered cubic. The liquid nitrogen-quenched specimens showed the same phases

as did the water quenched specimens. The relative amounts of the two hexagonal phases in the 7 and 9% molybdenum alloys were independent of the severity of the quench as judged by the relative intensity of the patterns.

The diffraction line widths of the 3% molybdenum alloy were sharper than the 5% alloy. From this, it might be inferred that there is a duplex hexagonal structure in 5% molybdenum alloys also but that the lattice parameters are so nearly identical that they cannot be distinguished. In such case, it would be advantageous to look for resolution in the back reflection lines, but it was found that the α' lines broadened so much at large θ values that accurate measurements could not be made.

The metallographic structures are shown in Figures 70 through 81. A conclusion that may be drawn from this work is that there is a very steep drop of the Ms temperature in the composition range between 9 and 11% molybdenum. The 9% molybdenum alloy shows large quantities of martensitic needles for both the water and liquid nitrogen quenches while the 11% molybdenum alloy is all retained β for both quenches. The β lines are very sharp. The observed and calculated diffraction data for the Ti-Mo alloys is shown in Tables VII and VIII.

2. Titanium-Chromium Alloys

Titanium-chromium alloys containing 3% chromium were completely α' for both the water quenched and liquid nitrogen quenched treatments. The nitrogen quenched 5% chromium alloy was completely α', but the water quenched specimen showed the presence of retained β. The alloys containing 7, 8, 11 and 13% chromium were completely retained β for both quenching treatments. In no case was there evidence to indicate the existence of duplex martensites. Nearly all of the chromium alloys showed a marked subgrain boundary which has been attributed to oxygen contamination. Typical microstructures of the Ti-Cr alloys are shown in Figures 82 and 83.

An attempt was made to determine whether or not the abnormally hard constituent in 5 and 7% chromium (commonly called β') could be associated with diffraction effects. Since nothing was noticeable in the regular alloys, the hardness of the alloys were checked. It was found that these specimens had not developed this material β', i.e., they were not abnormally hard. Accordingly, as had been suggested by Parris, Hirsch and Frost (13), these samples were heat treated for one hour periods at slightly elevated temperatures. The hardness increased as is shown in Table IX.

Neg. No. 7611 X 250

Fig. 70

Ti-3% Mo, solution treated 1/2 hour - 1000°C, water quenched. α' structure.

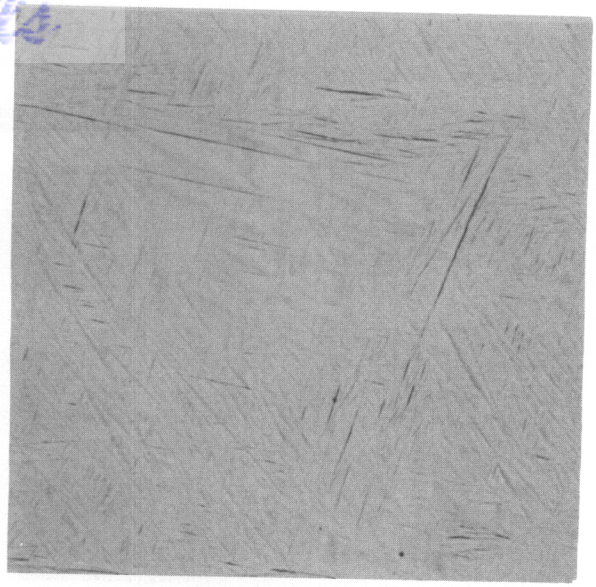

Neg. No. 7612 X 250

Fig. 71

Ti-5% Mo, solution treated 1/2 hour - 1000°C, water quenched. α' structure.

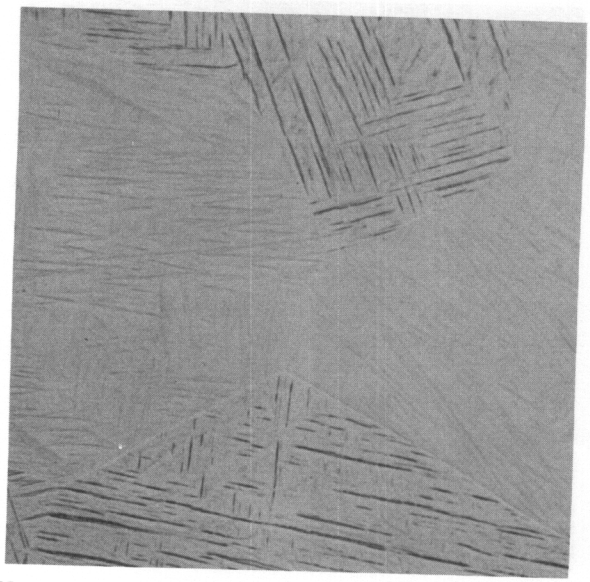

Neg. No. 7613 X 250

Fig. 72

Ti-7% Mo, solution treated 1/2 hour - 1000°C, water quenched. α' structure (x-ray diffractions show two separate α' structures).

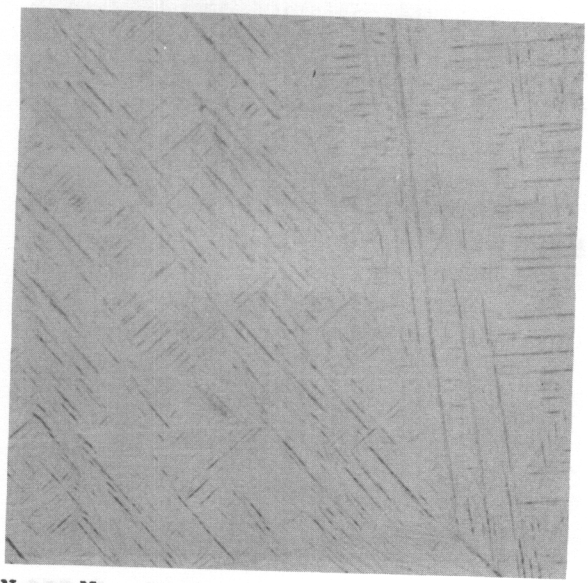

Neg. No. 7733 X 250

Fig. 73

Ti-9% Mo, solution treated 1/2 hour - 1000°C, water quenched. α' structure (x-ray diffraction shows two separate structures with a trace of retained β).

Etchant: 60 cc glycerine, 20 cc HNO_3, 20 cc HF

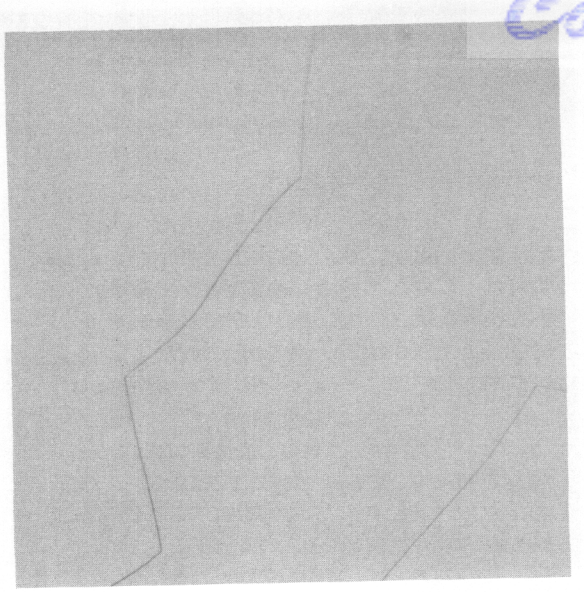

Neg. No. 7734 X 250

Fig. 74

Ti-11% Mo, solution treated 1/2 hour - 1000°C, water quenched. Completely retained β.

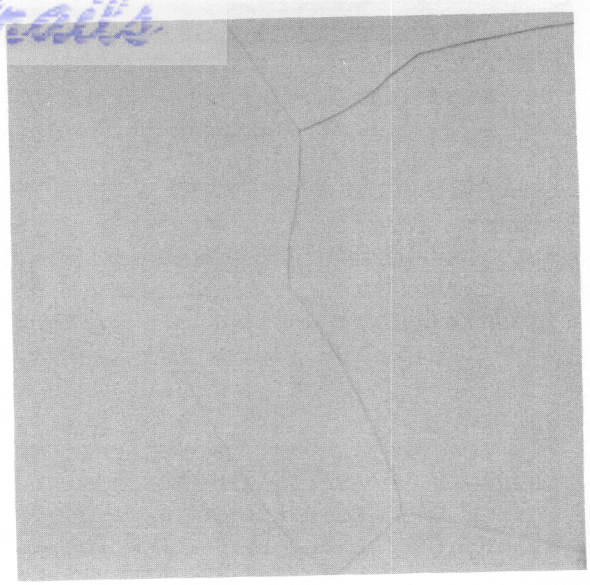

Neg. No. 7735 X 250

Fig. 75

Ti-13% Mo, solution treated 1/2 hour - 1000°C, water quenched. Completely retained β.

Neg. No. 7719 X 250

Fig. 76

Ti-3% Mo, solution treated 1/2 hour - 1000°C, liquid nitrogen quenched. α' structure.

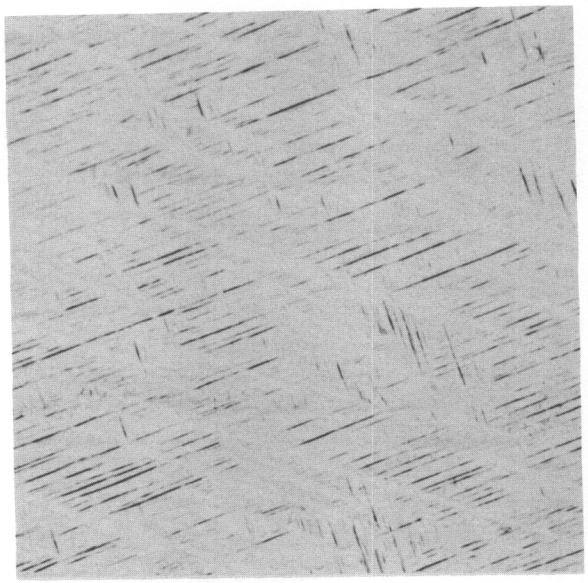

Neg. No. 7720 X 250

Fig. 77

Ti-5% Mo, solution treated 1/2 hour - 1000°C, liquid nitrogen quenched. α' structure.

Etchant: 60 cc glycerine, 20 cc HNO_3, 20 cc HF

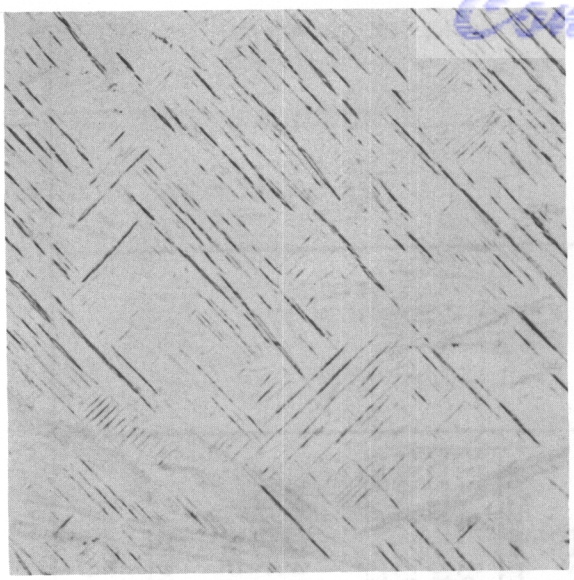

Neg. No. 7721 X 250

Fig. 78

Ti-7% Mo, solution treated 1/2 hour - 1000°C, liquid nitrogen quenched. α' structure (x-ray diffraction shows this to be two α' structures).

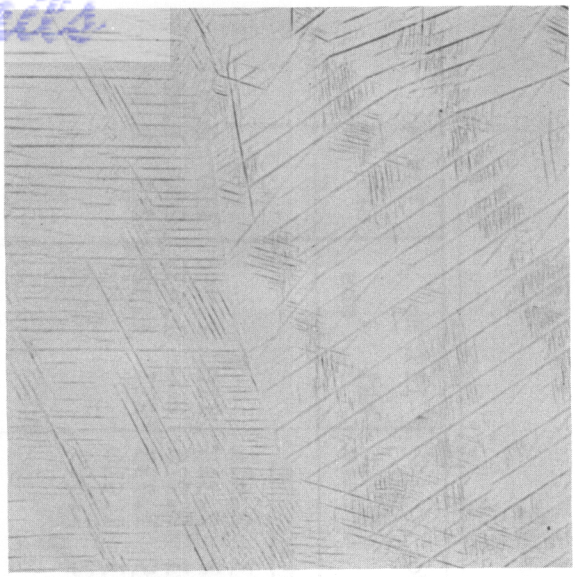

Neg. No. 7722 X 250

Fig. 79

Ti-9% Mo, solution treated 1/2 hour - 1000°C, liquid nitrogen quenched. α' structure (x-ray diffraction shows this to be two α' structures with a trace of retained β).

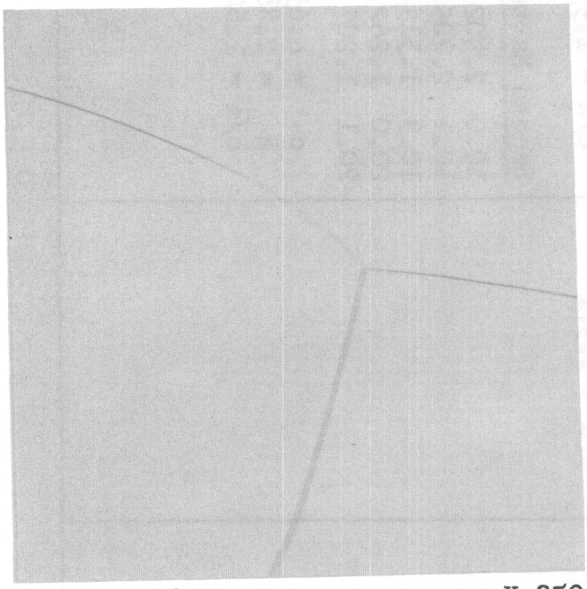

Neg. No. 8320 X 250

Fig. 80

Ti-11% Mo, solution treated 1/2 hour - 1000°C, liquid nitrogen quenched. Completely retained β.

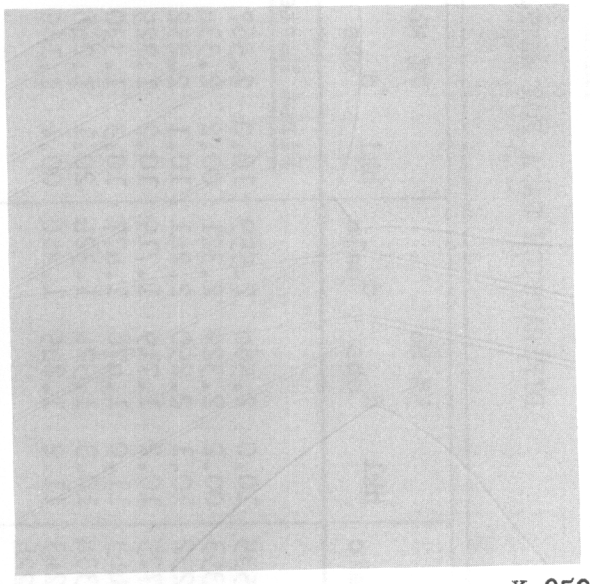

Neg. No. 7746 X 250

Fig. 81

Ti-13% Mo, solution treated 1/2 hour - 1000°C, liquid nitrogen quenched. Completely retained β. The few α' needles were probably developed during metallography. That this is a surface phenomena is obvious since some needles disappear.

Etchant: 60 cc glycerine, 20 cc HNO_3, 20 cc HF

TABLE VII

DIFFRACTION DATA FOR WATER QUENCHED Ti-Mo ALLOYS

3% Mo			5% Mo			7% Mo			9% Mo			11% Mo		13% Mo	
hkl	d_{obs}	d_{calc}	hkl	d_{obs}	d_{calc}	hkl	d_{obs}	d_{calc}	hkl	d_{obs}	d_{calc}	hkl	d_{obs}	hkl	d_{obs}
						First Martensite			First Martensite						
10.0	2.558	2.535	10.0	2.566	2.559	10.0	2.567	2.565	10.0	2.583	2.614	β		β	
00.2	2.345	2.353	00.2	2.329	2.321	00.2	2.334	2.331	00.2	2.312	2.315	110	2.298	110	2.301
10.1	2.245	2.232	10.1	2.250	2.241	10.1	2.252	2.247	10.1	2.263	2.276	200	1.639	200	1.628
10.2	1.724	1.725	10.2	1.719	1.719	10.2	1.725	1.725	10.2	1.725	1.733	211	1.327	211	1.328
11.0	1.476	1.463	11.0	1.478	1.477	10.3	1.330	1.329	11.0	1.513	1.510				
10.3	1.331	1.334	10.3	1.324	1.324	20.1	1.246	1.236	10.3	1.331	1.329				
11.2	1.247	1.243	11.2	1.245	1.246	00.4	1.165	1.165							
20.1	1.232	1.224													
c = 4.707 kX			c = 4.642 kX			c = 4.662 kX			c = 4.630 kX						
a = 2.927 kX			a = 2.954 kX			a = 2.962 kX			a = 3.018 kX						
c/a = 1.608			c/a = 1.571			c/a = 1.574			c/a = 1.534						
						Second Martensite			Second Martensite						
						10.0	2.502	2.501	00.2	2.263	2.275				
						10.1	2.205	2.201	10.1	2.188	2.200				
						10.3	1.315	1.315	10.2	1.693	1.687				
						20.0	1.262		11.0	1.451	1.451				
						20.1	1.207	1.207							
						c = 4.638 kX			c = 4.550 kX						
						a = 2.887 kX			a = 2.902 kX						
						c/a = 1.606			c/a = 1.568						
									β Pattern						
									110	2.294					
									200	1.630					

TABLE VIII

DIFFRACTION DATA FOR LIQUID NITROGEN QUENCHED Ti-Mo ALLOYS

3% Mo			5% Mo			7% Mo			9% Mo			11% Mo		13% Mo	
hkl	d_{obs}	d_{calc}	hkl	d_{obs}	d_{calc}	hkl	d_{obs}	d_{calc}	hkl	d_{obs}	d_{calc}	hkl	d_{obs}	hkl	d_{obs}
						First Martensite			First Martensite						
10.0	2.560	2.553	10.0	2.568	2.550	10.0	2.574	2.584	10.0	2.586	2.580	β		β	
00.2	2.340	2.341	00.2	2.332	2.340	00.2	2.340	2.342	00.2	2.325	2.329	110	2.310	110	2.301
10.1	2.244	2.241	10.1	2.249	2.239	10.1	2.258	2.262	10.1	2.262	2.257	200	1.631	200	1.627
10.2	1.725	1.725	10.2	1.726	1.724	10.2	1.726	1.735	10.2	1.727	1.729	211	1.330	211	1.329
11.0	1.472	1.474	11.0	1.476	1.472	11.0	1.499	1.492	11.0	1.515					
10.3	1.331	1.331	10.3	1.333	1.331	10.3	1.339	1.336	10.3	1.331	1.330				
11.2	1.248	1.247	11.2, 20.1	1.242	1.246	20.1	1.243	1.245	20.1	1.243	1.243				
c = 4.681 kX			c = 4.679 kX			c = 4.685 kX			c = 4.658 kX						
a = 2.948 kX			a = 2.945 kX			a = 2.983 kX			a = 2.979 kX						
c/a = 1.588			c/a = 1.589			c/a = 1.571			c/a = 1.564						
						Second Martensite			Second Martensite						
						10.0	2.508	2.524	10.0	2.490					
						00.2	2.313	2.341	00.2	2.262	2.261				
						10.1	2.213	2.222	10.1	2.195	2.209				
						10.2	1.709	1.716	10.2	1.694	1.686				
						11.0	1.457	1.457	11.0	1.452	1.461				
						10.3	1.331	1.327	10.3	1.292	1.295				
						11.2	1.238	1.237	20.0	1.268	1.266				
									11.2	1.231	1.227				
						c = 4.683 kX			c = 4.522 kX						
						a = 2.914 kX			a = 2.923 kX						
						c/a = 1.607			c/a = 1.547						
									β Pattern						
									200	1.631					
									211	1.331					

TABLE IX

AVERAGE HARDNESS OF TITANIUM-CHROMIUM ALLOYS

	5% Cr	7% Cr
As quenched (liquid nitrogen)	311 DPH	363 DPH
1 hour at 100°C	349 DPH	421 DPH
1 hour at 225°C	390 DPH	554 DPH

Metallographic and diffraction examination of these specimens showed no detectable change after this artificial aging treatment.

3. Titanium-Manganese Alloys

Alloys containing 3% manganese were found to be α' with a small amount of retained β for both the water quenched and liquid nitrogen quenched treatments. The 5% manganese, water quenched alloy was completely retained β. The 5% manganese, liquid nitrogen quenched alloy, however, showed the presence of α' development. All other alloys were found to be completely retained β. The findings described above were verified in all cases by metallographic investigation. Typical microstructures are shown in Figures 84 through 89. As in the Ti-Cr alloys, there apparently is but one martensitic decomposition product.

4. Sand Blast Specimens

Specimens that were retained β on quenching were sand blasted as previously described. The diffraction analysis of these specimens was disappointing. Apparently, the only contribution of the blasting operation was to cold work the specimen. This was obvious from examination of the diffraction patterns which showed broad peaks instead of sharp peaks as in the quenched specimens. Diffraction patterns of the sand blasted 5% manganese and 11% molybdenum alloy showed an indication of the development of the hexagonal α' phase, but the diffraction lines were not strong enough to make a more thorough analysis. The metallographic examination cannot be interpreted as being indicative of the true microstructures since the blasted surface was heavily pitted and had to be removed for microexamination. Figures 88 to 90 may be considered typical of the sand blasted structures.

E. Summary

The preceding investigation yielded the following results:

1. The method of integrated intensities is not a satisfactory method of determining relative amounts of β and α' in titanium alloys.

2. In Ti-Mo alloys, two hexagonal martensitic products are developed on quenching.

Neg. No. 8321 X 250

Fig. 82

Ti-3% Cr, solution treated 1/2 hour - 1000°C, water quenched, α' structure.

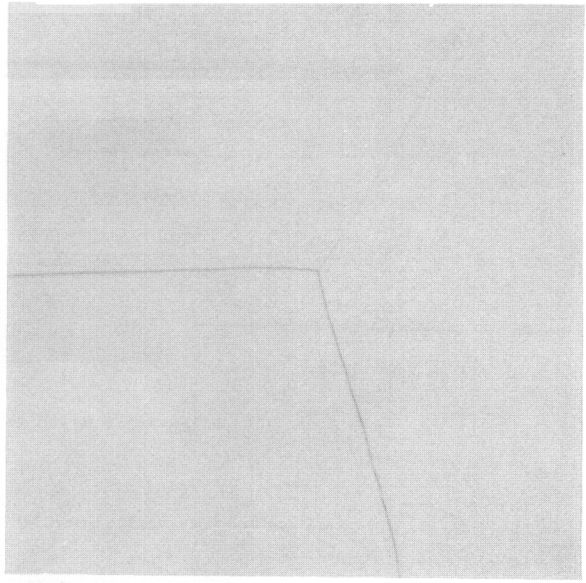

Neg. No. 8317 X 250

Fig. 83

Ti-9% Cr, solution treated 1/2 hour - 1000°C, water quenched. Completely retained β.

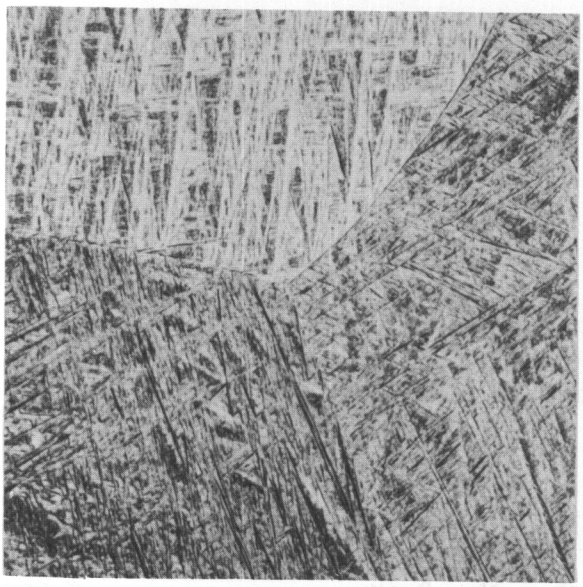

Neg. No. 8342 X 250

Fig. 84

Ti-3% Mn, solution treated 1/2 hour - 1000°C, water quenched. α' structure.

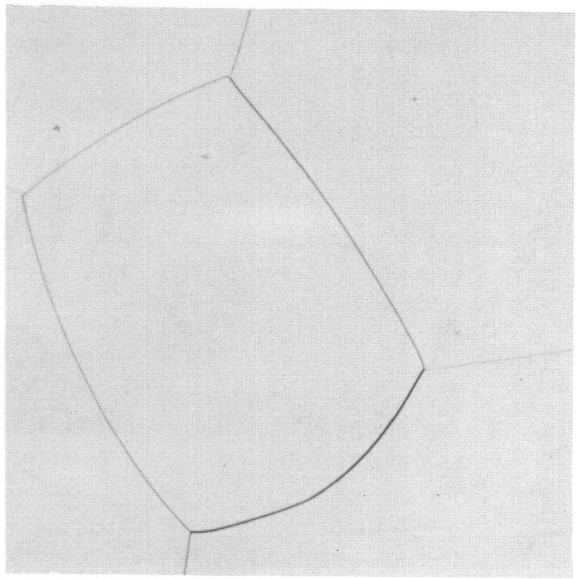

Neg. No. 8343 X 250

Fig. 85

Ti-5% Mn, solution treated 1/2 hour - 1000°C, water quenched. Completely retained β.

Etchant: 60 cc glycerine, 20 cc HNO_3, 20 cc HF

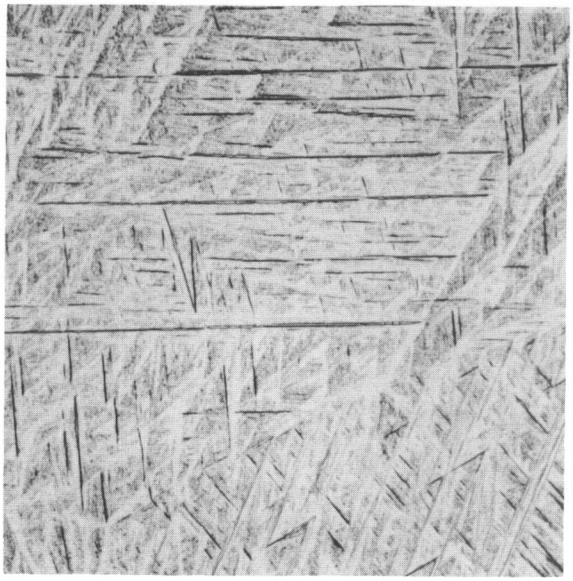

Neg. No. 8344 X 250

Fig. 86

Ti-3% Mn, solution treated 1/2 hour - 1000°C, liquid nitrogen quenched. α' structure.

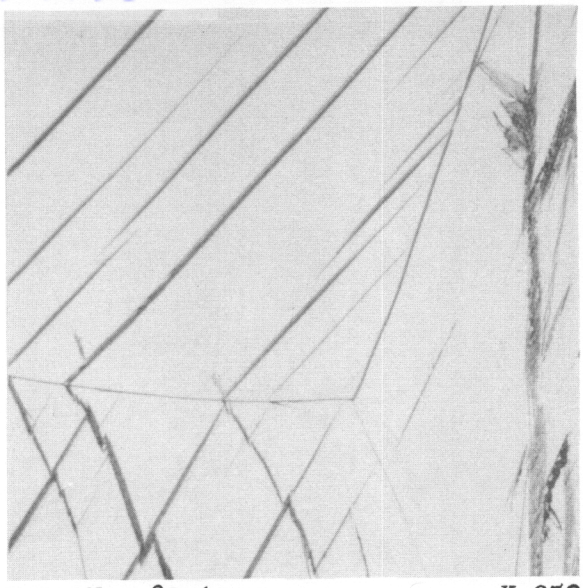

Neg. No. 8346 X 250

Fig. 87

Ti-5% Mn, solution treated 1/2 hour - 1000°C, liquid nitrogen quenched. Retained β with α' needles.

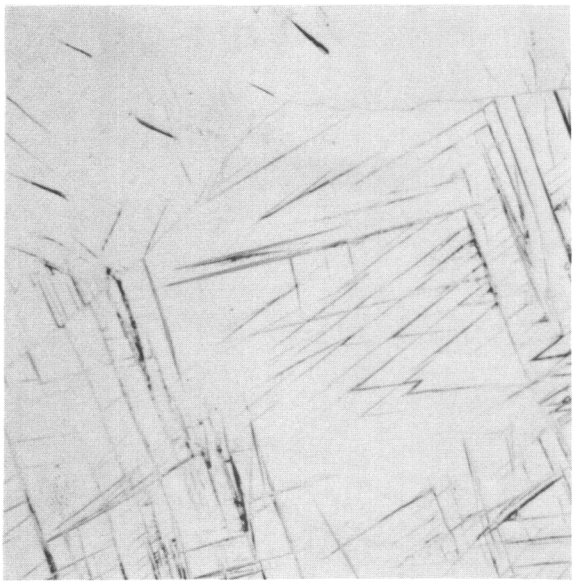

Neg. No. 8464 X 250

Fig. 88

Ti-5% Mn, solution treated 1/2 hour - 1000°C, water quenched. Sandblasted.

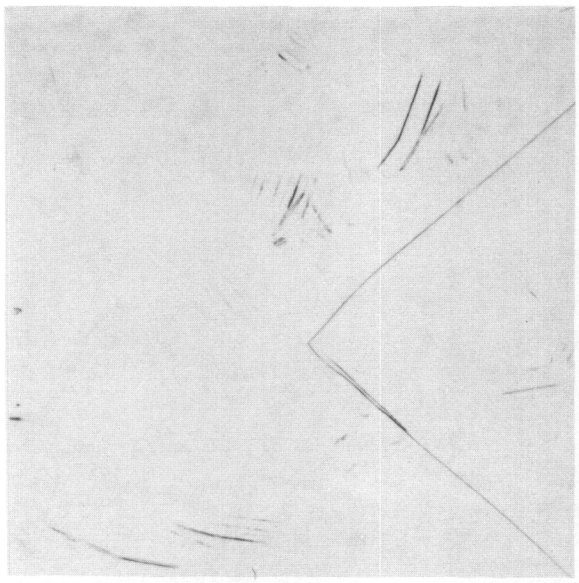

Neg. No. 8465 X 250

Fig. 89

Ti-7% Mn, solution treated 1/2 hour - 1000°C, water quenched. Sandblasted.

Etchant: 60 cc glycerine, 20 cc HNO_3, 20 cc HF

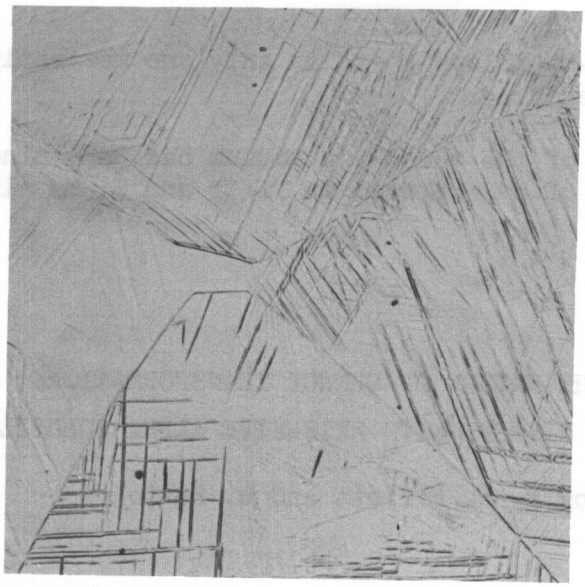

Neg. No. 8466 X 250

Fig. 90

Ti-11% Mo, solution treated 1/2 hour - 1000°C, water quenched. Sandblasted.

Etchant: 60 cc glycerine, 20 cc HNO_3, 20 cc HF

3. The relative proportions of the two hexagonal quench products in Ti-Mo alloys is independent of the quenching temperature. The temperature of quenching does not seem to effect the formation of α'.

4. In Ti-Cr and Ti-Mn alloys there is only one martensitic phase developed on quenching.

5. The temperature of the quenching medium has only minor influence on the quantity of α' produced in Ti-Cr and Ti-Mn alloys.

IX. THE NATURE OF QUENCH TRANSFORMATIONS IN BINARY SYSTEMS WITH EXTENSIVE ALPHA SOLUBILITY

by R. P. Elliott and W. Rostoker

A. Introduction

Binary systems of titanium with aluminum, tantalum and zirconium have extensive solid solubility of the alloying elements in α titanium. By virtue of the forms of phase equilibria, one can quench from a single-phase β field directly to a single-phase α field. Under these conditions, it is potentially possible that the transformation $\beta \rightarrow \alpha$ can occur by atomic movements of the order of only one interatomic distance. This mode of transformation comes within the conventional terms of description of a martensitic-type reaction. On the other hand, microstructures developed by isothermal transformation in the α field which are shown subsequently in the text of the report, indicate configurations quite unlike those normally recognized as characteristically martensitic. An alternate reaction of the type $\beta \rightarrow \alpha + \beta \rightarrow \alpha$ occurring at very high rates by a nucleation and growth mechanism could be operative. The implication of very high reaction rates is deduced from the thermal arrest studies on Ti-Ta and Ti-Zr alloys published by Duwez (25,26). Duwez identified these high speed cooling thermal arrests as representative of Ms temperatures which automatically inferred a mechanism of transformation. The obvious question arises whether the products of transformation at high temperatures but within the α field are identical with the products formed by a direct water quench, especially in view of the differences in the microstructures. One is normally accustomed to regarding the product of a martensitic transformation of an alloy as in a state of metastability with respect to the stable product produced by annealing at elevated temperatures. The attempt was made in this work to identify the occurrence and nature of distinguishable differences in the transformation product produced by two different procedures.

B. Procedure

To this end, two alloys were made. These were Ti-5% Al and Ti-10% Ta. Following arc melting, the alloy ingots were hot forged to cylinders 1-1/8 in. in diameter and then machined to the 1 in. discs required by the spectrometer specimen spinner previously described. Chemical analysis showed the aluminum alloy to contain 5.14% Al and the tantalum alloy to contain 9.35% Ta.

These alloys were sealed in Vycor bulbs and heat treated as follows:

(1) Titanium-Aluminum Alloy

a. Solution treated 1025°C - 1/2 hour, water quenched.

b. Solution treated 1025°C - 1/2 hour, isothermally transformed 800°C - 1/2 hour, water quenched.

c. Following metallographic and x-ray diffraction examination of sample 1-a, this specimen was transformed at 800°C - 1/2 hour.

(2) Titanium-Tantalum Alloy

a. Solution treated 1025°C - 1/2 hour, water quenched.

b. Solution treated 1025°C - 1/2 hour, isothermally transformed 600°C - 1/2 hour, water quenched.

c. Following metallographic and x-ray diffraction examination of sample 2-a, this specimen was transformed at 600°C - 1/2 hour.

After heat treatment, samples were examined on the Norelco Geiger counter spectrometer and then were polished and electrolytically etched. Due caution was observed to prevent any transformation from occurring by cold work during the polishing operations.

In such an experiment as this, it was absolutely necessary to ascertain the reproducibility of lattice parameters and intensities. In order to do this, the diffraction pattern of the water quenched and isothermally transformed specimens were run on one side and then on the other and then repeated. Typical data are shown in Table X below.

TABLE X

COMPARISON OF THE OBSERVED INTERPLANAR SPACINGS
FOR Ti-5% Al ISOTHERMALLY TRANSFORMED

hkl	Side 1			Side 2		
10.0	2.5542	2.5542	2.5549	2.5521	2.5493	2.5507
00.2	2.3654	2.3654	2.3643	2.3571	2.3588	2.3583
10.1	2.2510	2.2510	2.2504	2.2445	2.2435	2.2435

Values of 2 θ could be read from the spectrometer chart within an accuracy of $\pm$ 0.02 degrees of 2 θ for reasonably sharp peaks. For a reading at 2 θ = 40 degrees, such an accuracy is equivalent to an accuracy $\pm$ 0.0003 kX in the interplanar spacing. For the most part, then, for a given sample (same side of a specimen) the accuracy is of the same quality as permitted by the reading errors. From the above table, it can be seen that there is only a small variation of parameter on the two sides of the given sample. Comparison of the peak intensities of this experiment showed that for a given side of a sample, the intensities were reproducible to a high degree of accuracy (an estimated 2%). However, opposite sides of a given sample often were quite dissimilar. It can be concluded that, with the use of the specimen spinner, the Norelco geiger counter spectrometer is capable of reproducing, for one position of a specimen, parameters and intensities to a high degree of accuracy. Because of variation in grain size and orientation distribution, however, line intensities cannot be considered satisfactorily reproducible for variation of position of the specimen.

C. Results and Discussion

Tables XI and XII list the observed diffraction data for the heat treated alloys. From these data the lattice parameters were calculated by the method of least squares. The interplanar spacings and axial ratios were then calculated from these values. The corresponding microstructures of these specimens are shown in Figures 91 through 96.

Metallographic examination shows that there definitely is a difference in the microstructure according to heat treatment. The implication has always been that these differences reflect different modes of transformation.

An examination of the diffraction data in Tables XI and XII show that there is very little difference in the lattice parameters and axial

TABLE XI

TITANIUM-ALUMINUM ALLOYS

hkl	Water Quenched		Isothermally Transformed		Water Quenched and Reheated	
	d_{obs}	d_{calc}	d_{obs}	d_{calc}	d_{obs}	d_{calc}
10.0	2.5571	2.553	2.5500	2.548	2.5521	2.5505
00.2	2.3435	2.345	2.3571	2.353	2.3482	2.3463
10.1	2.2451	2.242	2.2424	2.240	2.2424	2.2409
10.2	1.7278	1.727	1.7309	1.729	1.7272	1.7268
11.0			1.4730	1.471	1.4720	1.4725
10.3	1.3330	1.333	1.3353	1.336	1.3332	1.3334
20.0					1.2757	1.2752
11.2	1.2479	1.248	1.2466	1.247	1.2473	1.2472
20.1	1.2314	1.232	1.2289	1.230	1.2304	1.2306
	c = 4.689 kX a = 2.948 kX c/a = 1.591		c = 4.706 kX a = 2.942 kX c/a = 1.600		c = 4.693 kX a = 2.945 kX c/a = 1.594	

TABLE XII

TITANIUM-TANTALUM ALLOYS

hkl	Water Quenched		Isothermally Transformed		Water Quenched and Reheated	
	d_{obs}	d_{calc}	d_{obs}	d_{calc}	d_{obs}	d_{calc}
10.0	2.5479	2.540	2.5563	2.556	2.5381	2.5380
00.2	2.3341	2.337	2.3411	2.343	2.3612	
10.1	2.2339	2.232	2.2451	2.244	2.2318	2.2304
10.2	1.7194	1.720	1.7282	1.727	1.7185	1.7192
11.0	1.4660	1.466	1.4749	1.475	1.4655	1.4652
10.3	1.3281	1.328	1.3330	1.333	1.3267	1.3278
11.2	1.2424	1.242	1.2481	1.248	1.2413	1.2414
20.1	1.2249	1.225	1.2329	1.233	1.2242	1.2246
	c = 4.674 kX a = 2.932 kX c/a = 1.594		c = 4.687 kX a = 2.951 kX c/a = 1.588		c = 4.674 kX a = 2.930 kX c/a = 1.595	

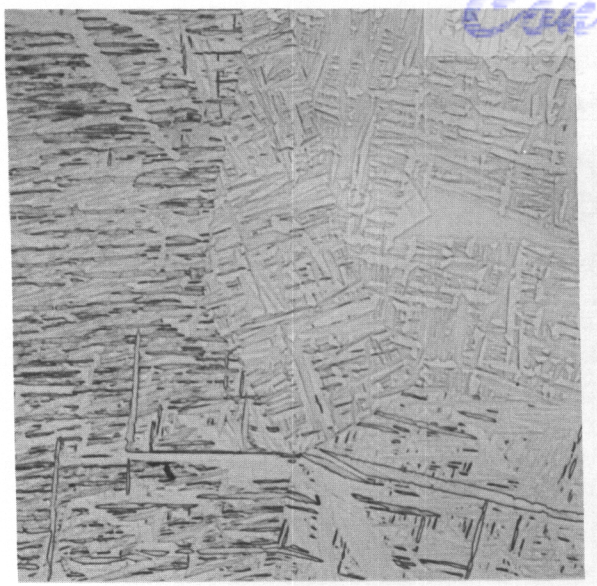

Neg. No. 7978 X 250

Fig. 91

Ti-5% Al, solution treated 1/2 hour - 1025°C, water quenched. α structure formed by an insuppressible transformation mechanism.

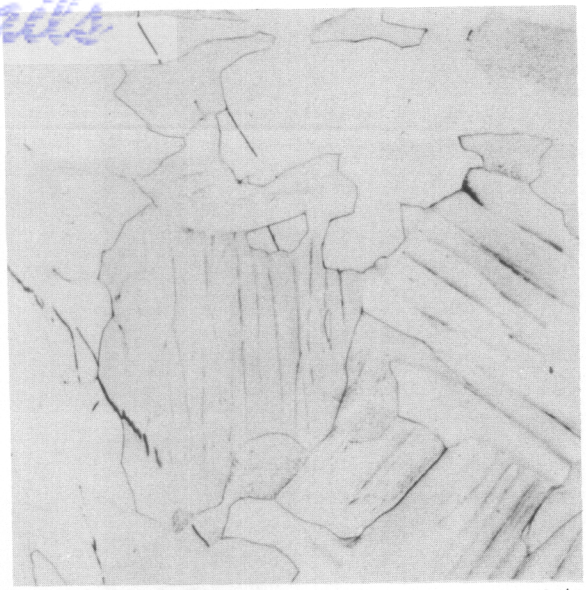

Neg. No. 8595 X 250

Fig. 92

Ti-5% Al, solution treated 1/2 hour - 1025°C, isothermally transformed 1/2 hour - 800°C, water quenched. α structure formed by nucleation and growth.

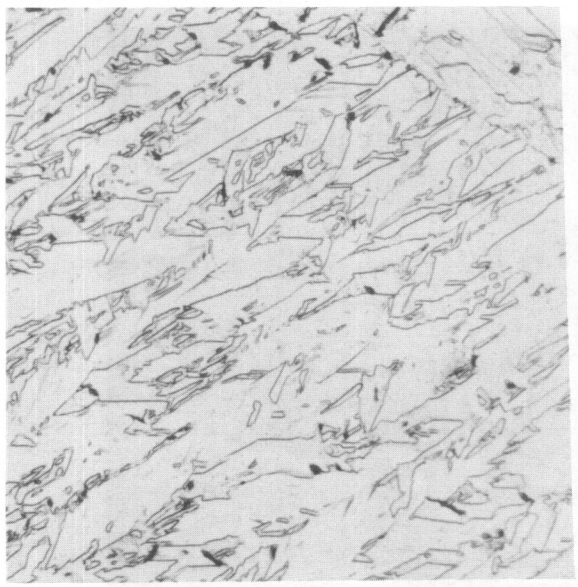

Neg. No. 8594 X 250

Fig. 93

Ti-5% Al, solution treated 1/2 hour - 1025°C, water quenched. Reheated 1/2 hour - 800°C, water quenched. Tempered quench product α. Shows growth of structure presented in Fig. 91.

Etchant: 60 cc glycerine, 20 cc HNO_3, 20 cc HF

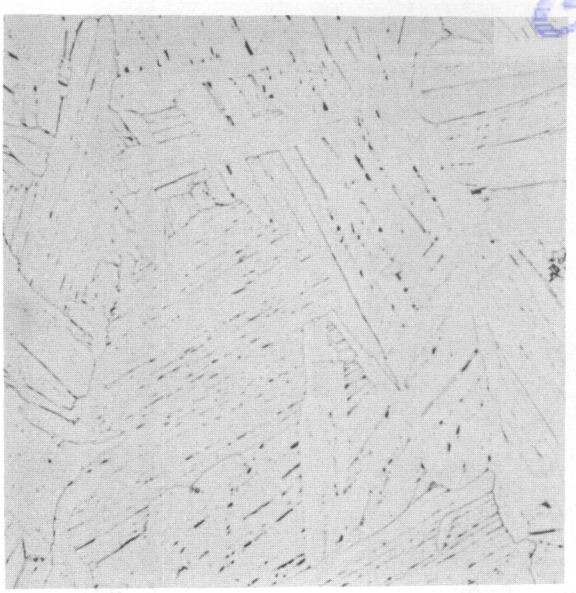

Neg. No. 7976 X 250

Fig. 94

Ti-10% Ta, solution treated 1/2 hour - 1025°C, water quenched. α structure developed by rapid quenching.

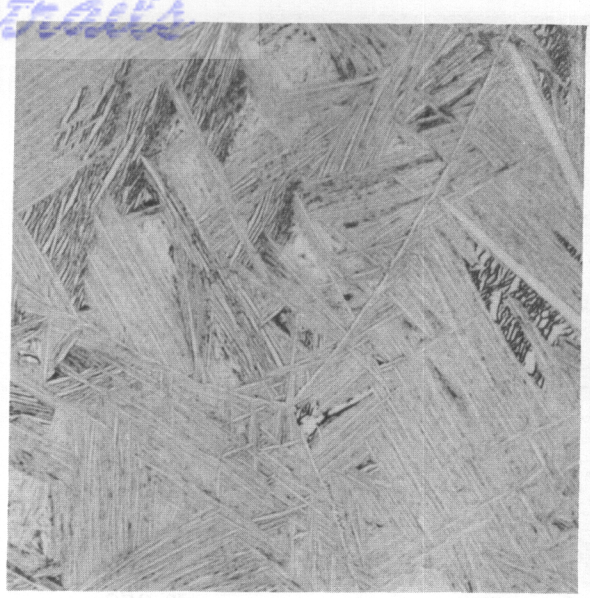

Neg. No. 7977 X 250

Fig. 95

Ti-10% Ta, solution treated 1/2 hour - 1025°C, isothermally transformed 1/2 hour - 600°C, water quenched. α structure developed by nucleation and growth.

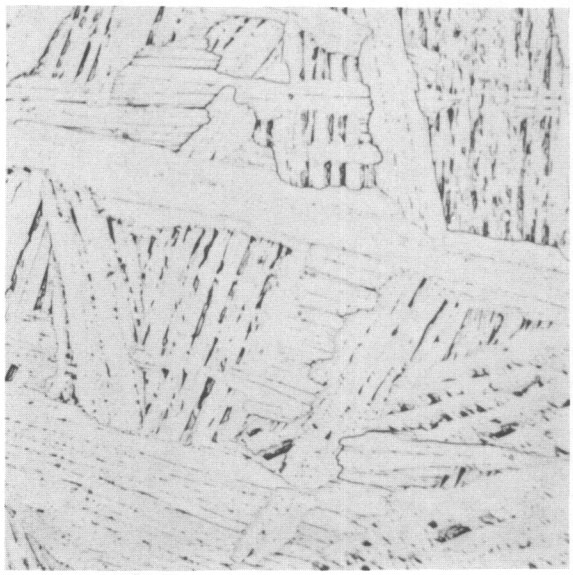

Neg. No. 8593 X 250

Fig. 96

Ti-10% Ta, solution treated 1/2 hour - 1025°C, water quenched. Reheated 1/2 hour - 600°C, water quenched. Tempered quench product α. Apparently no different from Fig. 94.

Etchant: 60 cc glycerine, 20 cc HNO_3, 20 cc HF

ratios for the alloys. If there were metastability, it would be expected that the sample after water quenching would relieve itself of this metastability when subsequently transformed at the elevated temperature. That the parameters and axial ratios of this sample are identical after isothermal transformation to the values of the water quenched treatment is evidence that any metastability is less than the sensitivity of the technique followed in this investigation. Further evidence supporting this conclusion is given by the line shapes of the spectrometer patterns. In alloys of Ti-Cr, Ti-Mn or Ti-Mo in which it is known that the hexagonal structure that is formed on quenching is metastable with respect to the equilibrium b.c.c. β and h.c.p. α of lower alloy content, the only lines that are clearly resolved are the strong triplet 10.0, 00.2, and 10.1. All other lines are broad and diffuse. In the diffraction pattern of the α phase formed by quenching alloys of Ti-Al and Ti-Ta all the lines are clearly resolved.

The evidence obtained in this study gives no support to the hypothesis that the transformation products on quenching of Ti-5% Al and Ti-9% Ta alloys are martensitic.

X. MECHANISM OF TEMPERING OF ALPHA PRIME

by R. F. Domagala and W. Rostoker

A. Experimental Procedures and Materials

The α' phase, recognized as a metastable supersaturated isomorph of the α phase must, on reheating to any given temperature, change in composition to that of the equilibrium α as dictated by the equilibrium phase diagram.

There are at least three possible mechanisms by which solute rich α' can revert to equilibrium α.

(1) Rejection of alloy-rich β, causing depletion of the solute content of the α', or rejection of alloy-poor α leaving β as a final residue.

(2) Diffusion of titanium atoms from the adjacent β matrix into the α' needles, causing a dilution of the alloy content to that of equilibrium α.

(3) Nucleation of equilibrium α at the α'/β interface and subsequent growth of α by a double diffusion process.

In point of significance, mechanism (1), if operative, could have a hardening effect associated with it while mechanisms (2) and (3), if operative, would be unlikely to induce hardening.

Experiments were conducted to attempt to distinguish which is the operative mechanism. Careful metallography of selected α' needles after progressive tempering anneals formed the basis of this work. To permit such studies it was necessary to choose alloys which develop discrete needles of α'. Exploratory work with alloys containing 9, 10, and 11% molybdenum indicated that the fewer needles present, the better the opportunity to observe metallographic changes in any given needle. An alloy containing nominally 13% molybdenum was finally selected as most suitable for the main program of work. Preshaped samples of this alloy were first given a solution treatment at 1000°C, followed by a water quench. The discolored specimens were then cleaned by a dip in a $HF-HNO_3$ mixture. Metallographic preparation consisted of mechanical polishing on successively finer abrasive papers, followed by electrolytic polishing and an acid etch to develop the structure. Samples so prepared had a limited number of discrete α' needles. These needles probably developed as a result of the $HF-HNO_3$ etching bath since α' needles are not normally encountered in alloys of this composition. There was definite evidence in experiments with this alloy in wire form that α' developed during the etching process.

The method of identifying a given needle for study consisted of marking off an area on this prepared specimen surface with micro-hardness indentations and using these indentations as coordinates for re-locating any selected area within. After an area was selected and particular needles photographed the specimen was carefully sealed in vacuo in a Vycor bulb and annealed. At the conclusion of an anneal the bulb was withdrawn from the furnace and air cooled without breaking the bulb. Providing utmost care was taken in handling and sealing the specimen, the selected needles could be examined after annealing without the necessity of repolishing the sample. The specimen was then returned to a new Vycor bulb, evacuated, sealed and heat treated further. Regardless of the care taken, however, no more than four anneals could be completed before the specimen required new metallographic preparation, which invariably cut through the original α' needles. In view of this fact and the mechanism of transformation suggested by the anneals at 700°C, certain of the treatments were carried on without repeated identification of individual α' needles. Instead, the structure of α' needles occurring in many beta grains were observed.

B. Results and Discussion

The initial tempering experiments were carried out at 700°C. Cumulative times at temperatures totaled 0, 0.5, 1.5, 3, 6, 15 and 31 hours. Figure 97 shows a group of α' needles selected for study at this temperature. After 0.5 hour, the selected needles, Figure 98, are seen to be unaffected. After 1.5 hours at 700°C, Figure 99, a slight precipitate may be seen within the matrix of the β grains but the α' needles themselves appear unchanged. This condition persisted after a total annealing time of three hours, as shown in Figure 100. After 6 hours (Figure 101), the α' needles were seen to exhibit a fine precipitate throughout. Figure 102 illustrates another area of the specimen, also after 6 hours at 700°C, which shows greater contrast between

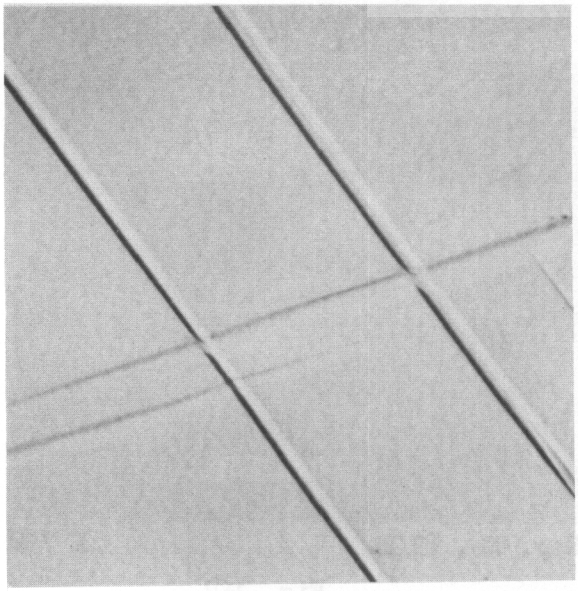

Neg. No. 7779 X 750

Fig. 97

α' needles selected for study at 700°C. Ti-13% Mo alloy, quenched from 1000°C.

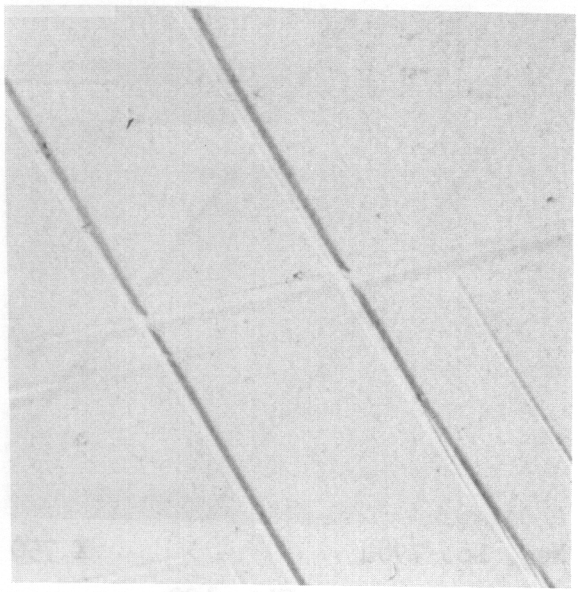

Neg. No. 7899 X 750

Fig. 98

Same as Fig. 97, after 0.5 hours at 700°C.

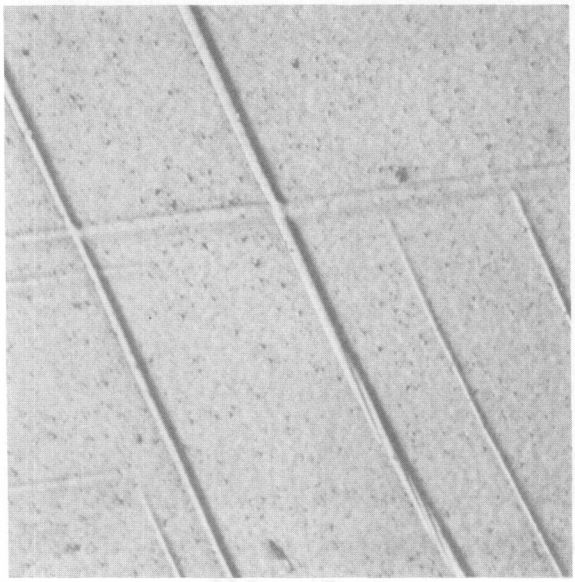

Neg. No. 7938 X 750

Fig. 99

α' needles are unaffected after 1.5 hours at 700°C. Discrete particles of precipitate appear in β matrix.

Etchant: 60 cc glycerine, 20 cc HNO_3, 20 cc HF

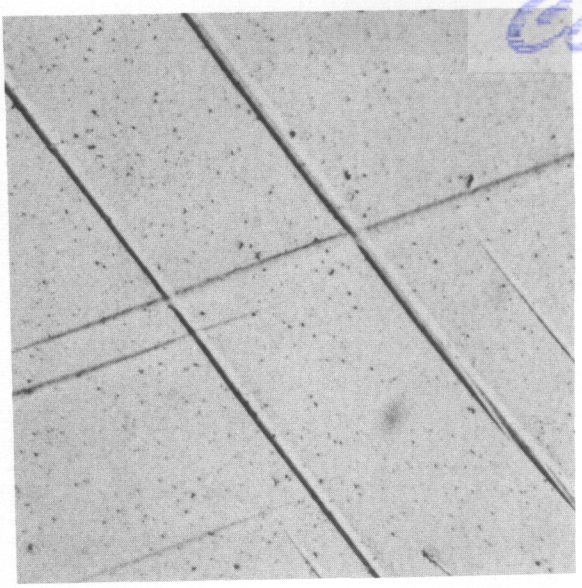

Neg. No. 7984 X 750

Fig. 100

After 3 hours at 700°C, microstructure remains relatively unchanged.

Neg. No. 8104 X 750

Fig. 101

Same α' needles after 6 hours at 700°C. Needles are heavily peppered with very fine particles of precipitate.

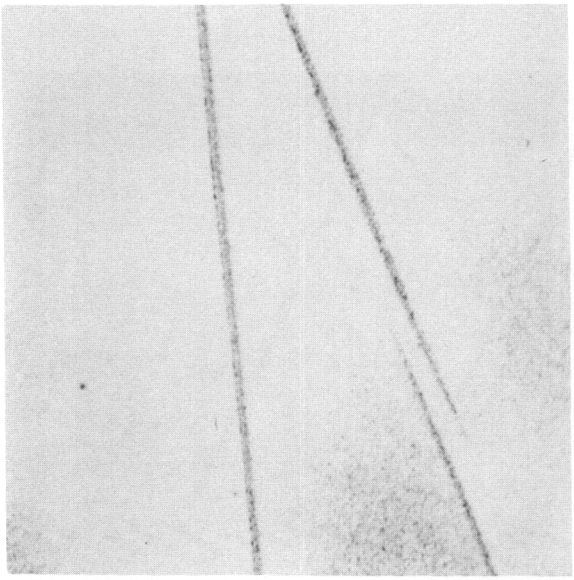

Neg. No. 8106 X 750

Fig. 102

Same as Fig. 101, but another area showing greater contrast between α' needles and β matrix.

Etchant: 60 cc glycerine, 20 cc HNO_3, 20 cc HF

the needles and the matrix. The identity of the precipitate in the α' needles as shown in Figures 101 and 102 is open to some discussion. If the particles are β growing in a matrix of what will ultimately be α, it is difficult to imagine a mechanism whereby the tempered needle ultimately blends into the background of α particles in a β matrix. Mechanisms 2 and 3 listed earlier allow the particles to be α in which case the final structure is a natural consequence. If the particles are α, however, it suggests that more than a single mechanism is operative in the tempering of α', as is further discussed below.

After a total of 15 hours of treatment, the specimen required metallographic reworking so the originally selected needles could not be viewed. Characteristic α' needles in the β grains after tempering for 15 hours are shown in Figure 103. This micrograph showed a new type of temper structure. The α' needles took the form of a duplex or banded configuration. The background showed the normal precipitation of α in β. There was no evidence of those α' needles with the fine dispersion which were observed on shorter reheat times. The duplex needles appeared to have a center midrib of β and bands of α on either side. At more advanced stages of tempering the bands break up into shorter pieces (Figures 104 and 105). This process continues although even after 31 hours at 700°C, fragments of the α bands are still apparent.

The midrib is interpreted as β for two reasons: (1) no reaction to polarized light. This is characteristic of β while α reacts by four sharp changes in reflectivity on a 360 degree rotation. The side bands do react in this fashion. (2) When the side bands break up, the midrib becomes continuous with the β matrix.

It is conceivable that the geometry of an original needle together with the manner of cutting through it might lead to the duplex appearance. However, if this were true such banded needles should be observed in specimens quenched from 1000°C, that is, the non-tempered needles. In no case was this observed.

The occurrence of the β midrib indicates a process of oriented growth which is a rather unusual development. The duplex needles resulting from oriented growth have been observed only in specimens annealed at 750° and 700°C. No such oriented growth phenomenon was observed at either 600° or 500°C. It should be re-emphasized that there were only a very small number of such ribbed needles present in the specimen and the major area of the specimen consisted of fine particles of α in β. A similar type needle may also occur when β grows on either side of the α' needle, since several non-ribbed needles were observed together with the duplex type. The non-ribbed α needles were always observed to be surrounded by an area of isothermal β containing no α precipitate.

At 750°C, the tempering of α' proceeded so rapidly that the intermediate stages of tempering were not observed. Figure 106 shows some needles of α' in the specimen as quenched from 1000°C. After 1 hour at 750°C, the structure of Figure 107 was evident. In the former figure,

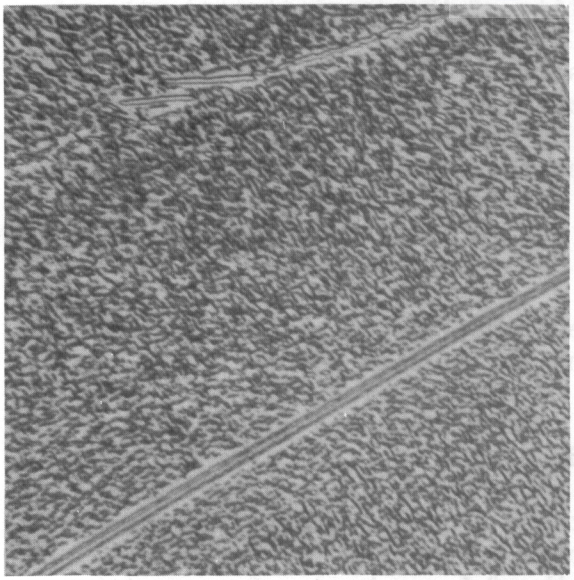

Neg. No. 8203 X 1000

Fig. 103

After 15 hours at 700°C and metallographic repolishing a duplex needle is visible and a second such needle is seen in the process of breaking up.

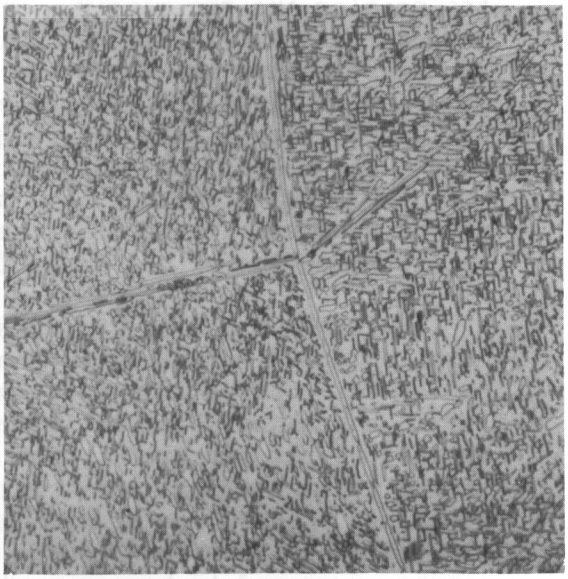

Neg. No. 8215 X 750

Fig. 104

After 31 hours at 700°C, duplex α' needles continue to break up.

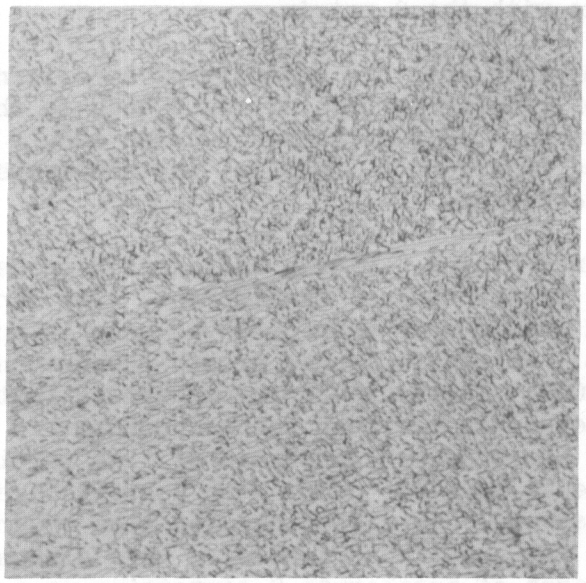

Neg. No. 8216 X 750

Fig. 105

Another area of specimen after 31 hours at 700°C.

Etchant: 60 cc glycerine, 20 cc HNO_3, 20 cc HF

several crossed α' needles are evident while the latter figure shows a pair of the ribbed needles crossed. Once again, as at 700°C, the presence of the duplex tempered needles was observed in a general structure of small α particles in a β matrix. Several such needles were seen in the typical arrangement of two ribs of α with a midrib of β. To illustrate the continuity of the β midrib with the parent β phase, Figure 108 is included. This structure is that of a 10% molybdenum alloy annealed for 1 hour at 750°C after being quenched from 1000°C. The specimen is one that was employed in preliminary studies conducted in this phase of work. Here the β midrib may be seen to blend without interface into the β matrix of the adjoining grain.

Figure 109 shows α' needles in a specimen subsequently annealed at 600°C. After 6 hours, Figure 110, the structure consists of a very fine precipitate, presumably α, through the β grains. No indications were observed of where the former α' needles had been, and no signs of ribbed needles were seen. After 31 hours at 600°C, the structure remains unchanged as shown in Figure 111.

A sequence of photomicrographs showing the tempering of α' needles at 500°C is shown in the following figures. Figure 112 shows the needles selected for study in this specimen. Figure 113 shows the same area after 15 hours at 500°C while Figure 114 illustrates the structure after 35 hours. Neither of these structures shows anything occurring within the α' needles, although indications of a very fine precipitate can be seen in the parent β grains. After 60 hours at temperature, Figure 115, no change in the metallographic appearance of the area was observed. After a total annealing time of 108 hours at 500°C, it was necessary to metallographically rework the sample, and Figure 116 shows the appearance of the alloy at that time. A very fine precipitate throughout the β grain may be seen with no real evidence to show where the former α' needles had been. No duplex type needles were observed in this specimen.

C. Summary

The results of this work may be summarized as follows:

(a) Needles of α' on reheating were observed to change in one of two fashions: (1) development of a finely dispersed precipitate within the needle, (2) development of a duplex structure possessing a midrib and two side bands.

(b) In the duplex type structure, the midrib was identified from reasonable rationalization as β and the side bands as α. It can only be inferred that the finely dispersed precipitate is α.

(c) The duplex tempered structure occurred at 700° and 750°C only. The fine precipitate tempered structure occurred at all temperatures employed.

(d) With prolonged annealing the "fine precipitate" tempered needles blend into the two-phase structure of the matrix. The duplex

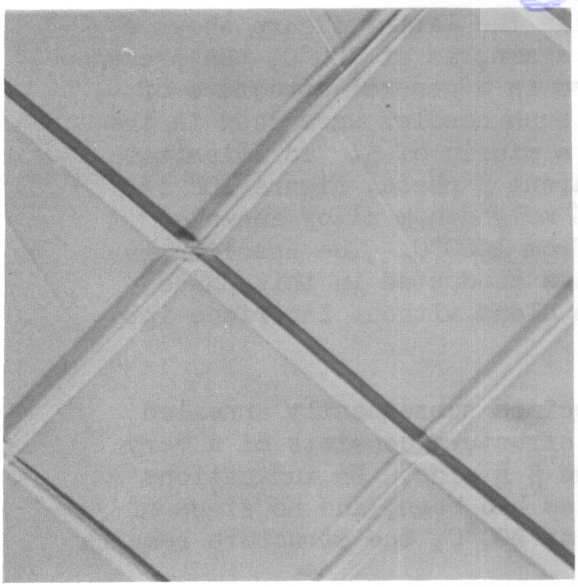

Neg. No. 8244 X 750

Fig. 106

α' needles in Ti-13% Mo alloy quenched from 1000°C.

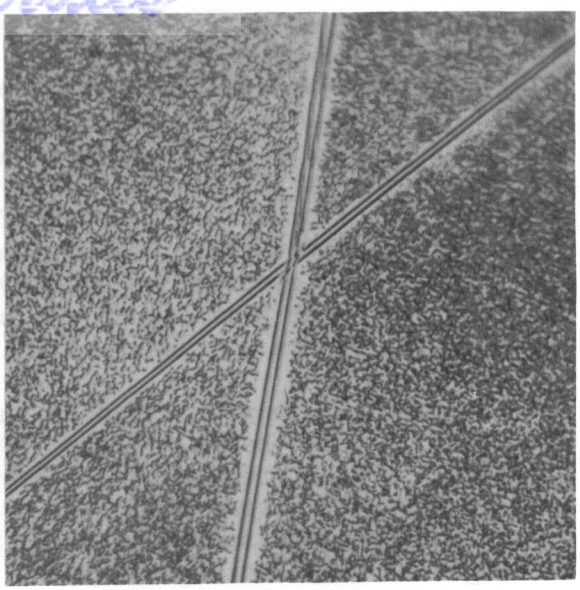

Neg. No. 8258 X 750

Fig. 107

Same specimen as in Fig. 106 after 1 hour at 750°C. A pair of crossed, duplex α' needles may be seen.

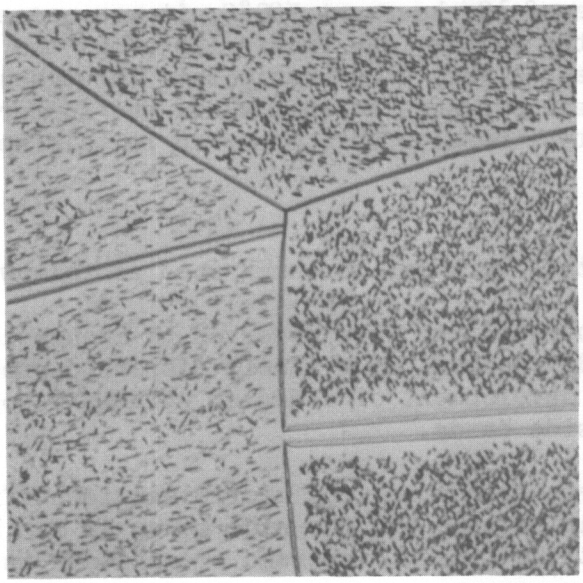

Neg. No. 7531 X 1000

Fig. 108

A Ti-10% Mo alloy solution treated at 1000°C, quenched and heated for 1 hour at 750°C. Continuity between the needle and midrib and adjacent β grain is evident.

Etchant: 60 cc glycerine, 20 cc HNO_3, 20 cc HF

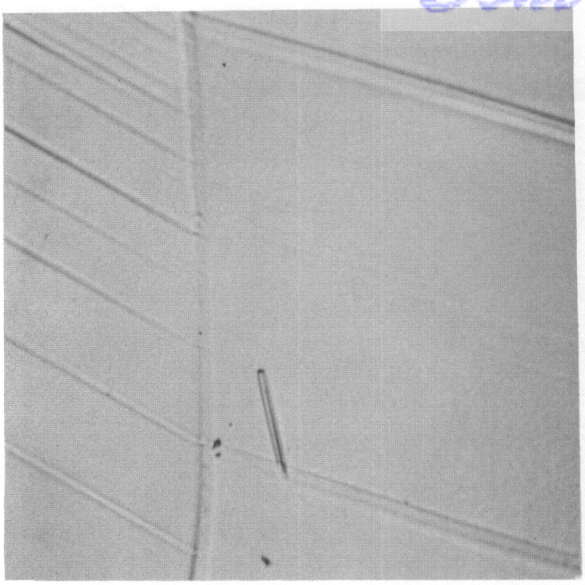

Neg. No. 8111 X 750

Fig. 109

Needles of α' in specimen quenched from 1000°C, scheduled for annealing at 600°C.

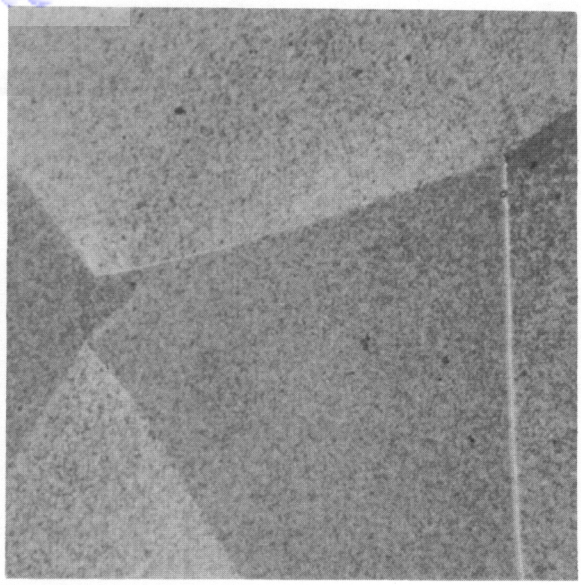

Neg. No. 8207 X 750

Fig. 110

After 6 hours at 600°C no evidence of former α' needles is visible.

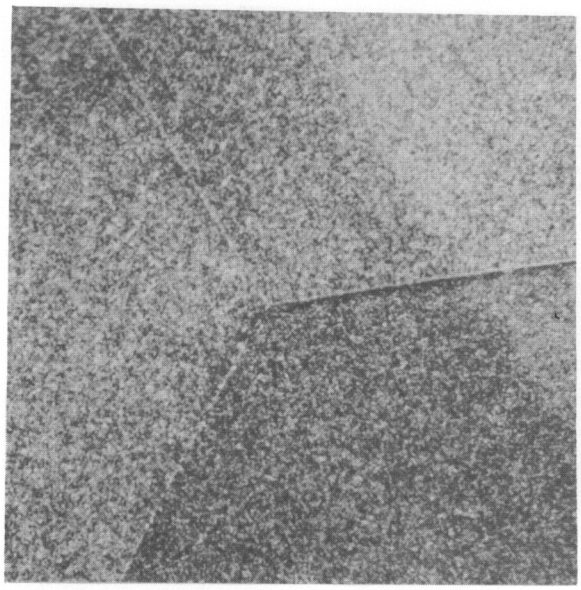

Neg. No. 8248 X 750

Fig. 111

After 31 hours at 600°C a slight coarsening of the very fine precipitate occurs but the structure remains essentially unchanged.

Etchant: 60 cc glycerine, 20 cc HNO_3, 20 cc HF

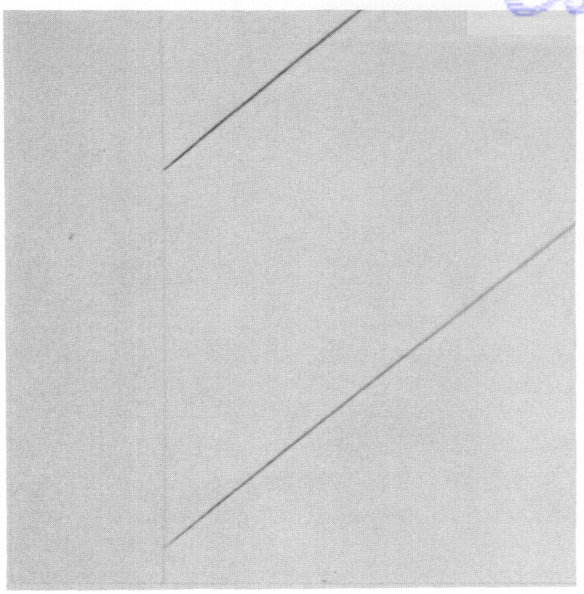

Neg. No. 7936 X 750

Fig. 112

Ti-13% Mo alloy quenched from 1000°C. α' needles selected for study at 500°C.

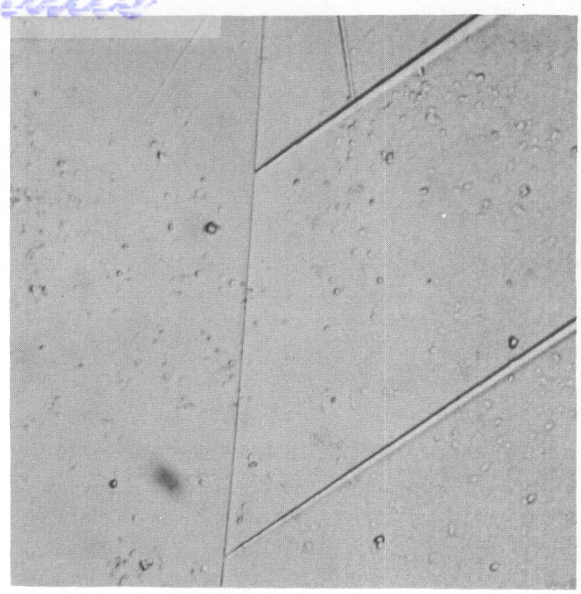

Neg. No. 7981 X 750

Fig. 113

Needles after 15 hours at 500°C are unchanged; particles of precipitate appear in β matrix.

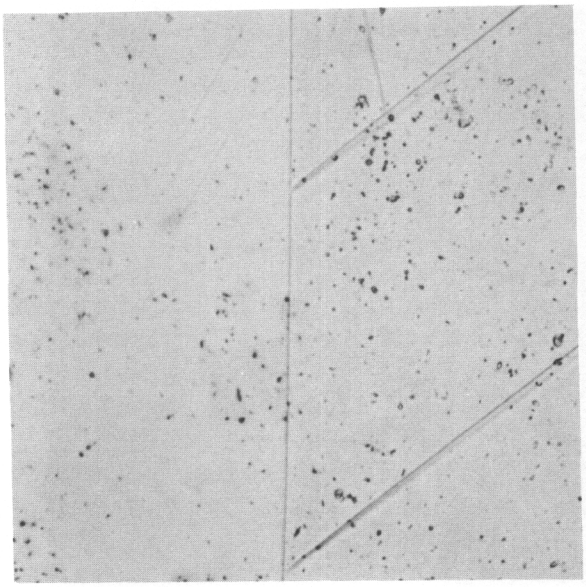

Neg. No. 8108 X 750

Fig. 114

After 35 hours at 500°C, little change in microstructure is evident.

Etchant: 60 cc glycerine, 20 cc HNO_3, 20 cc HF

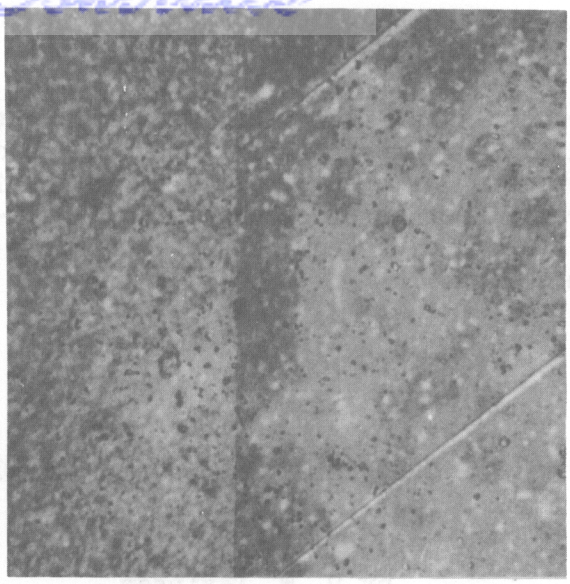

Neg. No. 8202 X 750

Fig. 115

After 60 hours at 500°C, metallographic structure remains unchanged.

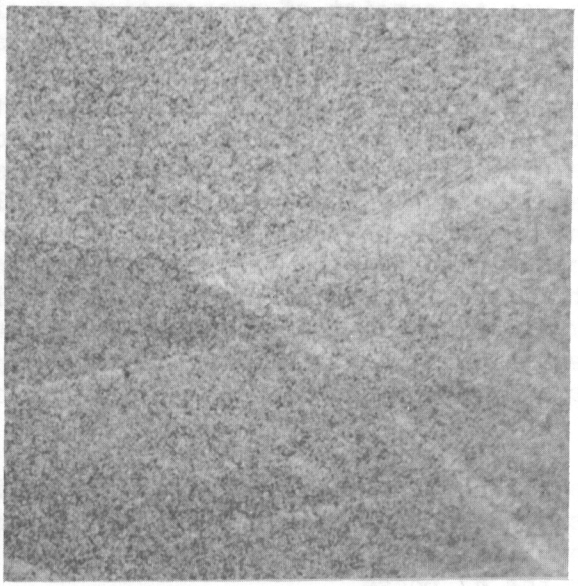

Neg. No. 8246 X 750

Fig. 116

Specimen required metallographic reworking after 108 hours at 500°C. The general appearance of the entire sample is indicated by this area.

Etchant: 60 cc glycerine, 20 cc HNO_3, 20 cc HF

tempered structure changes by fragmentation of the side bands of α. The β midrib blends with the β matrix.

These observations have been confined only to titanium-molybdenum alloys. It is likely in tempering of α' in eutectoid type alloys that an additional phenomenon of precipitation of intermetallic compounds can occur. A parallel series of experiments with Ti-Cr alloys would serve to augment the state of knowledge on tempering of the martensitic phase in titanium alloys.

XI. THE MECHANISM OF THE β→α TRANSFORMATION IN A Ti-12% Mo ALLOY

by D. W. Levinson

Because of the strong progressive reduction in transformation rate at temperatures above and below the nose of the TTT curves in transforming titanium alloys, it was felt that a study of the mode of rejection of the α phase from β was warranted. In order to most effectively study this solid state transformation, single crystal x-ray methods were selected as the most powerful.

The program was to consist of preparation of single β crystals of a Ti-12% Mo alloy and examination of such single crystals in various stages of heat treatment in the α rejection range by transmission Laue and, if necessary, rotating and oscillating crystal techniques. By these methods, it is possible to examine the nature of the precipitate in its earliest stages since the crystal will be infested with many very small particles at relatively few orientations, namely, the multiplicity of the habit plane in the β phase. By suitably orienting the parent β crystal, it is possible to examine the precipitate in the very early stages at which time the individual precipitate particles may be so small in one or two dimensions as to forbid normal coherent diffraction. In this way, data regarding structure and habit of the precipitate can be obtained at times and with precision beyond the capability of the powder camera.

It was hoped to show whether or not the rejection of the hexagonal α phase from β is preceded by any coherent transition structure and whether or not the habit of α at the earliest stages is identical to that observed for the α' phase.

A method was developed to produce single β crystals of proper size for study. This method consisted of annealing for 24 hours at 1100°C a 3/64 in. diameter alloy rod. The heat treatment was carried out in sealed Vycor bulbs under a partial pressure of helium and the specimens were quenched in cold water (the bulbs were broken) at the end of the

anneal to retain the β phase. These rods were centerless ground from hot forged and swaged, arc melted, iodide base material.

Large β grains resulted, many of which occupied the entire cross section of the sample and were up to 1/16 in. long. These were separated from the sample by etching in a mixture consisting of the following:

50 ml HNO_3 conc

50 ml HF conc

This acid mixture attacks grain boundaries much more vigorously than the remainder of the grains and eventually reduces the cross section in the vicinity of the grain boundary to the point where the grains may be easily separated by brittle fracture of the boundary. This is shown in Figures 117 and 118.

The crystals thus obtained were 1/2 to 1 mm on a side. These crystals were heat treated at four temperatures in the α rejection range, specifically, at 500°, 550°, 600° and 700°C.

The heat treatment of the individual crystals was carried out by sealing the individual crystals in small, individual Pyrex bulbs. The crystals were wrapped in 0.001 in. molybdenum foil to prevent contact with the glass wall and were water quenched after appropriate times at temperatures.

The resulting heat treated crystals were oriented in a three-circle goniometer by the back reflection Laue method and transmission Laue photographs were made with the x-ray beam normal to the (100) and (111) crystallographic planes.

This work could not be completed during the contract period. The production of single crystals suitable for study required considerably more time than was at first anticipated. In addition the transformation rate for the single crystals prepared was surprisingly slow and much time was spent in the x-ray examination of the untransformed single crystals without the knowledge that they had not yet transformed. The transformation rates of the single crystal appear to be an order of magnitude slower than polycrystalline material at the same temperature. It is hoped that the progress reported herein will be of assistance in future studies on this important subject.

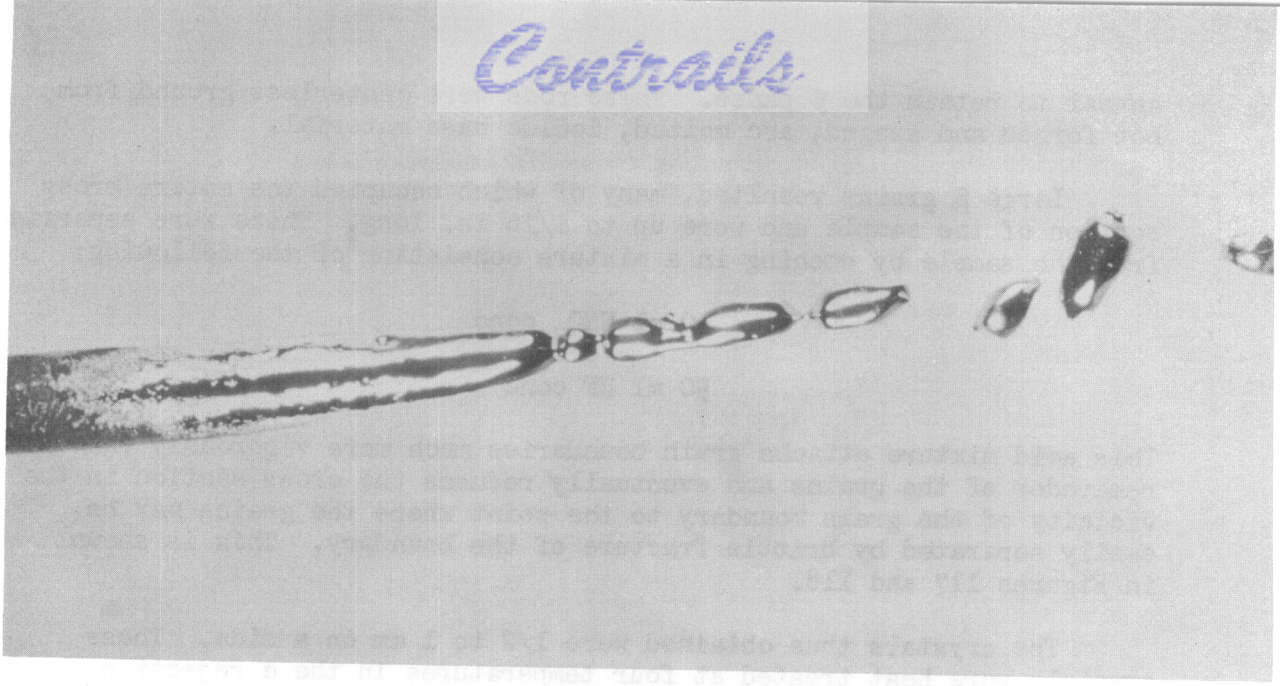

Fig. 117

Macrograph (X 8) showing action of etching reagent on coarse grained wire.

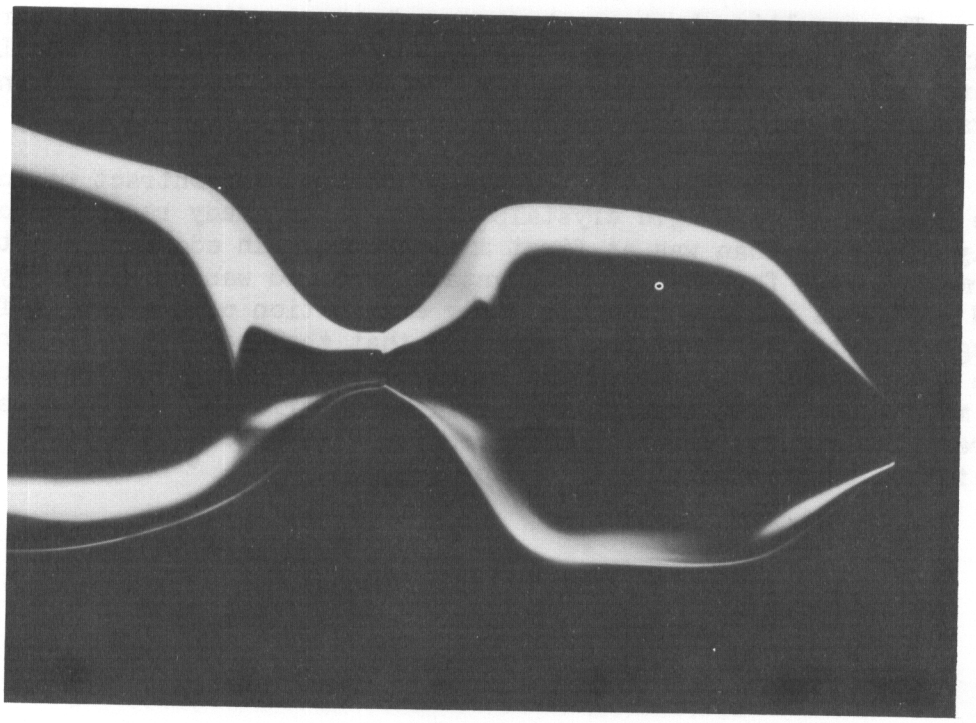

Fig. 118

Micrograph (X 50) showing junction between two β grains. At this stage crystals fracture readily.

BIBLIOGRAPHY

1. M. Hansen, H. D. Kessler and D. J. McPherson, "The Titanium-Silicon System," Trans. ASM 44 (1952) 518.

2. R. J. Van Thyne, D. H. Turner and H. D. Kessler, "Double Melting Produces Homogeneous Alloys," The Iron Age 172 (Aug. 6, 1953) 146.

3. D. W. Levinson and D. J. McPherson, "Structural Changes of Commercial Titanium and Titanium-Base Alloys on Heat Treatment," Armour Research Foundation Quarterly Reports Nos. 10 and 11 to the Aeronautical Research Laboratory under Contract No. AF 33(038)-16437, May 15 to August 15, 1953 and August 15 to November 15, 1953.

4. J. L. Wyatt, "Electrical Resistance of Titanium Metal," Journal of Metals 5, July, 1953, 903.

5. H. D. Kessler and M. Hansen, "Transformation Kinetics and Mechanical Properties of Titanium-Aluminum-Chromium Alloys," ASM Preprint No. 6 (1953).

6. H. D. Kessler and M. Hansen, "Transformation Kinetics and Mechanical Properties of Titanium-Aluminum-Molybdenum Alloys," ASM Preprint No. 7 (1953).

7. W. F. Carew, F. A. Crossley, H. D. Kessler, M. Hansen, "Titanium Alloys for Elevated Temperature Application," Armour Research Foundation Quarterly Report No. 9 to WADC under Contract No. AF 33(038)-22806, June 1 to August 31, 1953; November 18, 1953.

8. J. V. Gluck, J.W. Freeman, "Intermediate Temperature Creep and Rupture Behavior of Titanium and Titanium Alloys," University of Michigan Progress Report No. 4 to WADC under Contract No. AF 33(616)-244, July 14, 1952.

9. W. F. Carew, F. A. Crossley, H. D. Kessler, M. Hansen, "Titanium Alloys for Elevated Temperature Application," WADC Technical Report 52-245, Wright Air Development Center, Wright-Patterson Air Force Base, Ohio, November, 1952.

10. H. M. Meyer, W. Rostoker, "Study of Effects of Alloying Elements on the Weldability of Titanium Sheet," WADC Technical Report 52-230, Wright Air Development Center, Wright-Patterson Air Force Base, Ohio, May 1954.

11. M. Hansen, E. L. Kamen, H. D. Kessler and D. J. McPherson, "Systems Titanium-Molybdenum and Titanium-Columbium," Trans. AIME 191 (1951) 881.

12. H. K. Adenstedt, J. R. Pequignot, J. M. Raymer, "The Titanium-Vanadium System," Trans. ASM 44 (1952) 997.

13. W. M. Parris, L. L. Hirsch, P. D. Frost, "Low Temperature Aging in Titanium Alloys," Journal of Metals, February (1953) 178.

14. W. Rostoker, D. J. McPherson, M. Hansen, "Structural Changes of Commercial Titanium and Titanium-Base Alloys on Heat Treatment," WADC Technical Report 53-62, Wright Air Development Center, Wright-Patterson Air Force Base, Ohio, February, 1953.

15. D. J. DeLazaro, W. Rostoker, "The Influence of Oxygen Contents on Transformations in a Titanium Alloy Containing 11 Per Cent Molybdenum," Acta Metallurgica 1, November, 1953, 674.

16. D. J. DeLazaro, M. Hansen, R. E. Riley, W. Rostoker, "Time-Temperature Transformation Characteristics of Titanium-Molybdenum Alloys," Trans. AIME 194, 1952, 285.

17. D. J. DeLazaro, W. Rostoker, "Correlation Between Heat Treatment, Microstructure, and Mechanical Properties of Titanium-Molybdenum Alloys," ASM Preprint No. 8, 1953.

18. M. Hansen, D. J. McPherson and W. Rostoker, "Constitution of Titanium Alloy Systems," WADC Technical Report 53-41, Wright Air Development Center, Wright-Patterson Air Force Base, Ohio, February, 1953.

19. R. J. Van Thyne and H. D. Kessler, "Influence of Oxygen, Nitrogen and Carbon on the Phase Relationships of the Ti-Al System," Journal of Metals 6 (February, 1954) 193.

20. H. K. Adenstedt and W. A. Freeman, "The Tentative Titanium-Silver System," WADC Technical Report 53-109, Part 1, Wright Air Development Center, Wright-Patterson Air Force Base, Ohio, April, 1953.

21. K. Tamaru and S. Sakita, "On the Quantitative Determination of Retained Austenite in Quenched Steels," Sci. Repts., Tohoku Imperial University 20 (1931) 1.

22. F. S. Fletcher, M. Cohen and D. P. Antia, "Quantitative Determination of Retained Austenite by X-Rays," Trans. AIME 154 (1943) 306.

23. B. L. Averbach and M. Cohen, "X-Ray Determination of Retained Austenite by Integrated Intensities," Trans. AIME 176 (1948) 401.

24. New York University, "Mechanism of Martensitic Transformation of Titanium Alloys," Interim Technical Report No. 1, Contract No. DA-30-069-ORD-823, Watertown Arsenal (1953).

25. P. Duwez, "Allotropic Transformations in Titanium-Zirconium Alloys," Journal, Institute of Metals 80 (1951-2) 525.

26. P. Duwez, "The Martensitic Transformation in Titanium Binary Alloys," Trans. ASM 45 (1953) 934.